Stony Brook University

Role of Fatty Acid Binding Proteins and FAAH-2 in Endocannabinoid Uptake and Inactivation

A Dissertation Presented

by

Martin Kaczocha

to

The Graduate School

in Partial Fulfillment of the

Requirements

for the Degree of

Doctor of Philosophy

in

Molecular and Cellular Biology

Stony Brook University

May 2009

Stony Brook University

The Graduate School

Martin Kaczocha

We, the dissertation committee for the above candidate for the

Doctor of Philosophy degree, hereby recommend

acceptance of this dissertation

Dale G. Deutsch, Ph.D. – Dissertation Advisor
Professor, Department of Biochemistry and Cell Biology
Stony Brook University

Robert S. Haltiwanger, Ph.D. – Chairperson of Defense
Professor, Department of Biochemistry and Cell Biology
Stony Brook University

Deborah A. Brown, Ph.D.
Professor, Department of Biochemistry and Cell Biology
Stony Brook University

Erwin London, Ph.D.
Professor, Department of Biochemistry and Cell Biology
Stony Brook University

Stephen Yazulla, Ph.D., Outside Member of the Dissertation Committee
Professor, Department of Neurobiology and Behavior
Stony Brook University

This dissertation is accepted by the Graduate School

Lawrence Martin
Dean of the Graduate School

Abstract of the Dissertation

Role of Fatty Acid Binding Proteins and FAAH-2 in Endocannabinoid Uptake and Inactivation

by

Martin Kaczocha

Doctor of Philosophy

in

Molecular and Cellular Biology

Stony Brook University

2009

In the central nervous system, the endocannabinoid system regulates numerous physiological processes including analgesia, motor coordination, and memory. The endocannabinoids, including anandamide, are lipophilic signaling molecules that serve as ligands for cannabinoid receptors. Similar to hydrophilic neurotransmitters such as dopamine, anandamide signaling is terminated by cellular uptake and metabolic inactivation. Due to its lipophilicity, anandamide likely requires intracellular carriers to traverse the hydrophilic cytosol and reach its principal catabolic enzyme FAAH, localized on the ER. To date, mechanisms mediating intracellular anandamide trafficking have not been well characterized. In the current study, COS-7 cells stably expressing FAAH-eGFP proteins with localizations restricted to the ER, mitochondria, or the Golgi apparatus were generated. Anandamide was internalized and hydrolyzed with similar rates in cells expressing these spatially-restricted FAAH-eGFP variants, suggesting that intracellular trafficking of anandamide may be mediated by cytosolic carrier proteins.

FABPs were identified as anandamide carriers. Anandamide uptake and hydrolysis were potentiated following overexpression of FABP5 and FABP7 and reduced following their inhibition. These results establish FABPs as the first known intracellular carriers for endocannabinoids and suggest that this family of proteins may comprise the endogenous repertoire of endocannabinoid carriers.

A second FAAH enzyme (termed FAAH-2) was recently identified in human tissues. In contrast to FAAH, FAAH-2 is not found in the genomes of mice and rats and has therefore eluded characterization. In the current study, a thorough biochemical characterization of FAAH-2 was performed. The enzyme hydrolyzed anandamide and PEA with rates ten to thirty times lower than FAAH *in vitro*. Despite its low *in vitro* activity, FAAH-2 hydrolyzed anandamide and PEA with rates approximately one third that of FAAH in intact cells. FAAH-2 localized to cytoplasmic lipid droplets, which are intracellular organelles that serve as sites for lipid storage and liberation. The N-terminus of FAAH-2 was identified as a lipid droplet targeting sequence and was essential for the expression of a catalytically competent FAAH-2 enzyme. Intracellular delivery of anandamide to lipid droplets was similar as to the ER. Collectively, these results demonstrate that FAAH-2 is an efficient NAE hydrolyzing enzyme that localizes to lipid droplets, thereby establishing these organelles as novel intracellular sites of NAE inactivation.

Table of Contents

Abbreviations

ΔTM	Lacking transmembrane region
2-AG	2-arachidonoylglycerol
ADRP	Adipocyte differentiation-related protein
BSA	Bovine serum albumin
CB1	Cannabinoid receptor 1
CB2	Cannabinoid receptor 2
COS7-FAAH-eGFP	COS-7 cells stably expressing FAAH-eGFP
COX-2	Cyclooxygenase 2
eGFP	Enhanced green fluorescent protein
ER	Endoplasmic Reticulum
FAAH	Fatty acid amide hydrolase
FABP	Fatty acid binding protein
GRASP65	Golgi ReAssembly Stacking Protein 65 kDa
HRP	Horseradish peroxidase
K_m	Michaelis constant
KO	Knockout
LOX	Lipoxygenase
NAAA	N-acylethanolamine-hydrolyzing acid amidase
NAE	N-acylethanolamine
OEA	Oleoylethanolamide
PEA	Palmitoylethanolamide
PNGase F	N-Glycosidase F
PPAR	Peroxisome proliferator-activated receptor
rFAAH	Rat fatty acid amide hydrolase
RFP	Red fluorescent protein
RT-PCR	Reverse transcription polymerase chain reaction
SDS-PAGE	Sodium dodecyl sulfate polyacrylamide gel electrophoresis
TM	Transmembrane region
TOM20	Translocase of outer membrane 20 kDa component
TRPV1	Transient receptor potential vanilloid receptor 1
V_{max}	Maximum velocity

List of Figures

Chapter 1

Chapter 2

Acknowledgements

First and foremost, I would like to thank Dr. Dale Deutsch for being a great mentor. Dale is also an incredibly kind, supportive, and easygoing person in and out of the laboratory setting, and for this I am most grateful. Dale also provides his students with the opportunity to devise and execute their own projects with minimal micromanagement. It is this successful mentoring style that I would like to emulate if I am ever given the opportunity to establish a laboratory of my own.

I would like to acknowledge members of my committee: Dr. Robert Haltiwanger, Dr. Erwin London, Dr. Deborah Brown, and Dr. Stephen Yazulla. They have provided me with support and constructive criticisms that helped guide my projects to fruition. I especially thank Dr. Yazulla for being a walking dictionary of word origins and jokes.

I would like to thank my parents, Marian and Zofia, for providing me with constant encouragement and unwavering support throughout my years in school. They are unequivocally the best parents that anyone could hope to have. I am forever indebted to Sherrye for being a fantastic wife, a great collaborator, and for challenging my scientific ideas and political viewpoints. And to my son Eryk, you've brought more joy to my life than you can imagine and as fate would have it, you are already developing a penchant for grasping at biochemistry textbooks.

I must also acknowledge Nadine and Malgosia. Nadine has been a fantastic lab mate for the last few years and has made the Deutsch lab a great place to work. Malgosia taught me everything that I know about molecular biology and is a great drinking partner when times call for it. Lastly, as a scientist I must acknowledge nature for evolving a fascinating and unique signaling system that I've had the opportunity to study.

Publications

Kaczocha M, Glaser ST, and Deutsch DG. Identification of intracellular carriers for the endocannabinoid anandamide. Proc Natl Acad Sci U S A. 2009 Mar 23. [Epub ahead of print]

Hermann A, **Kaczocha M**, and Deutsch DG. 2-Arachidonoylglycerol (2-AG) membrane transport: history and outlook. AAPS J. 2006;8(2):E409-12.

Kaczocha M, Hermann A, Glaser ST, Bojesen IN, and Deutsch DG. Anandamide uptake is consistent with rate-limited diffusion and is regulated by the degree of its hydrolysis by fatty acid amide hydrolase. J Biol Chem. 2006 Apr 7;281(14):9066-75.

Glaser ST, **Kaczocha M**, and Deutsch DG. Anandamide transport: a critical review. Life Sci. 2005 Aug 19;77(14):1584-604.

CHAPTER 1

INTRACELLULAR TRANSPORT OF ANANDAMIDE IS MEDIATED BY FABPs

SUMMARY

The endocannabinoid anandamide is a neuromodulatory lipid that activates cannabinoid and vanilloid receptors on the plasma membrane. Anandamide is hydrolyzed principally by the endoplasmic reticulum (ER)-localized enzyme fatty acid amide hydrolase (FAAH). The transient nature of anandamide signaling requires an efficient mechanism(s) for ligand clearance and inactivation. Due to its lipophilicity, it is likely that anandamide employs intracellular carrier proteins to accelerate its diffusion from the plasma membrane to FAAH-containing membranes. To date, no proteins capable of intracellularly transporting anandamide have been identified.

In the current study, anandamide trafficking was examined in COS-7 expressing FAAH-eGFP variants localized to the ER, mitochondria, or the Golgi apparatus. Anandamide uptake and hydrolysis were indistinguishable between cells expressing these FAAH variants, lending support to the hypothesis that anandamide may use intracellular carriers to reach FAAH. Fatty acid binding proteins (FABPs) are ubiquitously expressed cytosolic carriers for fatty acids and are therefore suitable candidates as putative

intracellular transporters for anandamide. FABP3, FABP5, and FABP7 are the only members of the FABP family expressed in brain. Transfection of neuroblastoma N18TG2 or COS-7 cells expressing FAAH with FABP5 and FABP7, but not FABP3, significantly potentiated the uptake and hydrolysis of anandamide. Treatment of COS-7 or N18TG2 cells with the competitive FABP ligand oleic acid or the reversible FABP inhibitor BMS309403 significantly reduced anandamide uptake and metabolism at time points as early as 3 sec. RT-PCR analysis confirmed that N18TG2 cells express FABP3 and FABP5, confirming that FABPs may function as endogenous anandamide carriers in these cells. Collectively, these results identify the first intracellular transport proteins for the endocannabinoid anandamide and suggest that intracellular endocannabinoid trafficking in mammalian tissues may be coordinated by multiple cytosolic transporters.

INTRODUCTION

A. The Endocannabinoid System

The endocannabinoids are a class of endogenous neuromodulatory lipids. The prototypical members of this family, anandamide and 2-AG, serve as ligands for cannabinoid receptors (CB) (Howlett, *et al.*, 2002). Similar to Δ^9-tetrahydracannabinol, the psychoactive constituent of marijuana, anandamide is a partial agonist at both CB1 and CB2 receptors, and unlike Δ^9-tetrahydracannabinol, also activates vanilloid TRPV1 receptors (de Lago, *et al.*, 2002, Devane, *et al.*, 1988, Matsuda, *et al.*, 1990, Munro, *et al.*, 1993, Zygmunt, *et al.*, 1999). CB1 receptors are expressed throughout the central nervous system in brain, spinal cord, and the eye, and in peripheral tissues including testes, adipose tissue, liver, and pancreas (Garcia-Ovejero, *et al.*, 2009, Herkenham, *et al.*, 1991, Hohmann, *et al.*, 1995, Jeong, *et al.*, 2008, Regard, *et al.*, 2008, Starowicz, *et al.*, 2008, Yazulla, *et al.*, 1999). Within the central nervous system, CB1 receptors localize primarily to axon terminals of neurons (Katona, *et al.*, 1999, Oropeza, *et al.*, 2007).

The expression of CB2 receptors is restricted to cells of immune origin, including the microglia of the central nervous system and peripheral macrophages (Cabral and Marciano-Cabral, 2005, Cabral, *et al.*, 2008, Carlisle, *et al.*, 2002, Facchinetti, *et al.*, 2003, Shiratsuchi, *et al.*, 2008). There is still considerable controversy whether CB2 receptors are expressed in neurons of the central nervous system (Van Sickle, *et al.*, 2005). TRPV1 receptors are primarily expressed by sensory neurons and are activated by endogenous ligands such as anandamide and N-arachidonoyl dopamine, by exogenous ligands such as capsaicin, and by noxious stimuli including pH and heat (Davis, *et al.*,

2000, Ferrer-Montiel, *et al.*, 2004, Huang, *et al.*, 2002, Starowicz, *et al.*, 2007, Zygmunt, *et al.*, 1999).

Upon activation, CB1 and CB2 receptors couple to inhibitory $G_{i/o}$ G-proteins, resulting in the activation of potassium channels, inhibition of calcium channels, and activation of mitogen-activated protein kinase pathways (Lambert and Fowler, 2005, Mackie and Hille, 1992, Mackie, *et al.*, 1993, Mackie, *et al.*, 1995, Sarker, *et al.*, 2003). In neurons of the central nervous system, such changes in cellular permeability to sodium and potassium ions result in hyperpolarization of the cell's membrane potential. The net effect of these alterations is the suppression of neuronal excitability under physiological and pathophysiological conditions. It is therefore not surprising that CB1 receptors mediate depolarization-induced suppression of inhibition, a type of short term plasticity in the brain (Ohno-Shosaku, *et al.*, 2001, Wilson, *et al.*, 2001, Wilson and Nicoll, 2001). Cannabinoid receptors also mediate other physiological processes including analgesia, vasodilation, neuroprotection, cell migration, cancer cell invasion, and the regulation of food intake (for review, see (Howlett, *et al.*, 2002, Lambert and Fowler, 2005)).

The physiological actions of anandamide are tightly controlled through its enzymatic synthesis and degradation (Ahn, *et al.*, 2008). In contrast to classical hydrophilic neurotransmitters that are stored in vesicles and released upon depolarization of presynaptic neurons, lipophilic endocannabinoids utilize "on demand" synthetic mechanisms (for review, see (Bisogno and Di Marzo, 2007, Hashimotodani, *et al.*, 2007)). Specifically, upon neuronal depolarization, the rise in intracellular calcium concentrations induces endocannabinoid synthesis (Di Marzo, *et al.*, 2005, Hashimotodani, *et al.*, 2005, van der Stelt, *et al.*, 2005).

Anandamide is synthesized from its N-arachidonoyl phosphatidylethanolamine precursor by three possible pathways: (1) direct cleavage of N-arachidonoyl phosphatidylethanolamine to anandamide and phosphatidic acid by N-acyl phosphatidylethanolamine phospholipase D (Okamoto*, et al.*, 2004), (2) double de-acylation of N-arachidonoyl phosphatidylethanolamine to glycerophospho-anandamide by alpha-beta hydrolase 4 followed by cleavage to anandamide by glycerophosphodiesterase 1 (Simon and Cravatt, 2006, Simon and Cravatt, 2008), or (3) phospholipase C-mediated cleavage of N-arachidonoyl phosphatidylethanolamine to phospho-anandamide followed by phosphatase-mediated cleavage to anandamide (Liu*, et al.*, 2006). It is currently not known whether all of these pathways coordinate the synthesis of anandamide in the central nervous system or whether one pathway predominates. It was recently demonstrated that similar to CB1, N-acyl phosphatidylethanolamine phospholipase D localizes to presynaptic axons in the mouse brain (Egertova*, et al.*, 2008).

B. FAAH

Following the discovery of anandamide as an endogenous ligand for cannabinoid receptors, our laboratory first demonstrated that an enzymatic activity present in neuronal cells and rat tissues hydrolyzed anandamide to arachidonic acid (Figure 1) (Deutsch and Chin, 1993). This activity was present in several organs including brain, liver, kidney, and lung. The enzyme mediating anandamide hydrolysis was subsequently identified as FAAH (Cravatt*, et al.*, 1996). FAAH displays considerable catalytic promiscuity, hydrolyzing N-acylethanolamines (NAEs) such as anandamide, PEA and OEA, N-acyl

taurines, N-acyl dopamines, N-acyl glycines, 2-AG, and primary fatty acid amines such as oleamide (Figure 2) (Burstein, *et al.*, 2002, Cravatt, *et al.*, 1996, Cravatt, *et al.*, 2001, Goparaju, *et al.*, 1998, Huang, *et al.*, 2002, Rimmerman, *et al.*, 2008, Saghatelian, *et al.*, 2004). In addition to FAAH, a recently discovered FAAH-2 enzyme found in primates but not mice or rats, and NAAA, an acid amidase expressed in macrophages, have been reported to hydrolyze anandamide and PEA *in vitro* (Sun, *et al.*, 2005, Tsuboi, *et al.*, 2005, Wei, *et al.*, 2006). Conversion of anandamide to bioactive prostamides by cyclooxygenase -2 (COX-2) and other metabolites by the lipoxygenase (LOX) and cytochrome P450 pathways have been reported (Figure 1) (Maccarrone, *et al.*, 2000, Snider, *et al.*, 2007, Snider, *et al.*, 2008, Stark, *et al.*, 2008, Yu, *et al.*, 1997).

FAAH is inhibited by various inhibitors including phenylmethylsulfonyl fluoride and the phospholipase A_2 inhibitor methyl arachidonyl fluorophosphonate, typical of a serine hydrolase (De Petrocellis, *et al.*, 1997, Deutsch and Chin, 1993, Deutsch, *et al.*, 1997, Koutek, *et al.*, 1994). Indeed, FAAH is a member of the amidase signature superfamily of serine hydrolases, characterized by a conserved stretch of approximately 160 amino acids (Figure 3A) (Chebrou, *et al.*, 1996, Cravatt, *et al.*, 1996). The enzyme possesses an unusual Serine-Serine-Lysine catalytic triad that is conserved among amidase signature enzymes (Omeir, *et al.*, 1999, Patricelli and Cravatt, 1999). The N-terminal transmembrane segment of FAAH is dispensable for activity since a FAAH variant lacking the N-terminus (ΔTMFAAH) retains its membrane binding capability and is catalytically active (Arreaza and Deutsch, 1999, Patricelli, *et al.*, 1998). FAAH is a dimeric monotopic membrane protein and interacts with membranes through an α-helical membrane binding domain (Figure 3A and B) (Balali-Mood, *et al.*, 2009, Bracey, *et al.*,

2002, Bracey, *et al.*, 2004). FAAH also possesses a polyproline domain predicted to interact with Src homology 3 domain containing proteins. The enzyme localizes to the cytoplasmic face of ER membranes *in vivo* and in cultured cells (Arreaza and Deutsch, 1999, Glaser, *et al.*, 2003, Gulyas, *et al.*, 2004, Patricelli, *et al.*, 1998, Wei, *et al.*, 2006).

FAAH KO mice possess highly elevated levels of NAEs including anandamide, PEA and OEA, and N-acyl taurines (Cravatt, *et al.*, 2001, Cravatt, *et al.*, 2004). The dramatic elevation of anandamide levels in FAAH KO mice suggests that FAAH is the principal anandamide inactivating enzyme *in vivo* (Cravatt, *et al.*, 2001). FAAH KO mice exhibit antinociceptive and anti-inflammatory phenotypes resulting from enhanced signaling via CB1 and peroxisome proliferator-activated receptor alpha (PPARα), suggesting that FAAH may represent a promising therapeutic target (Cravatt, *et al.*, 2001, Cravatt, *et al.*, 2004, Lichtman, *et al.*, 2004, Lo Verme, *et al.*, 2005, Webb, *et al.*, 2008).

C. Membrane Transport of Anandamide

The endogenous anandamide tone is regulated by synthetic and inactivating enzymes. In the rodent brain, CB1 receptors and the putative anandamide synthesizing enzyme N-acyl phosphatidylethanolamine phospholipase D localize to axon terminals of presynaptic neurons, while FAAH localizes to somatodendritic compartments of postsynaptic neurons (Egertova, *et al.*, 1998, Egertova, *et al.*, 2003, Egertova, *et al.*, 2008, Gulyas, *et al.*, 2004). This complementary distribution pattern suggests that anandamide may be synthesized in presynaptic cells and signal in an autocrine fashion (Egertova, *et al.*, 2008), requiring transport into postsynaptic cells for inactivation by FAAH.

The mechanism(s) governing the membrane transport of anandamide is not well understood. It was originally proposed that anandamide may enter cells via a putative membrane transporter based upon saturability, temperature dependency, and competitive inhibitor studies (Beltramo*, et al.*, 1997, Di Marzo*, et al.*, 1994, Hillard*, et al.*, 1997). Despite years of intensive research, a membrane transporter has not been identified. Therefore, an alternative hypothesis that anandamide may cross the plasma membrane unaided was proposed (Patricelli and Cravatt, 2001). Our laboratory was the first to demonstrate that anandamide membrane transport occurred by simple diffusion in cultured neuroblastoma and astrocytoma cells (Glaser*, et al.*, 2003). These studies were subsequently confirmed in non-neuronal cells, including RBL-2H3, rabbit platelets, and erythrocyte ghosts (Bojesen and Hansen, 2005, Fasia*, et al.*, 2003, Kaczocha*, et al.*, 2006). These data are consistent with the ability of all cell-types, including those lacking a functional endocannabinoid system, to take up and hydrolyze anandamide when transfected with FAAH (for review, see (Glaser*, et al.*, 2005, Hillard and Jarrahian, 2000)).

D. Anandamide uptake is coupled to its hydrolysis by FAAH

Exogenously applied anandamide is rapidly taken up by cells and inactivated by FAAH (Glaser*, et al.*, 2003, Kaczocha*, et al.*, 2006). By hydrolyzing internalized anandamide, FAAH reduces its intracellular concentration and maintains an inward concentration gradient, thereby enhancing anandamide accumulation in the steady-state (Figure 4A) (Day*, et al.*, 2001, Deutsch*, et al.*, 2001). This concept is best exemplified by data from a recent publication (Kaczocha*, et al.*, 2006). In RBL-2H3 cells, which express

FAAH (Bisogno*, et al.*, 1997), anandamide is promptly taken up and hydrolyzed (Figure 4B). Over the time course tested, these cells continue to internalize anandamide in a non-saturable manner. In contrast, anandamide uptake approaches equilibrium when FAAH activity is abolished by the inhibitor CAY10400. Note that the ability of FAAH activity to enhance anandamide uptake is temporally-dependent and is not readily observable at very early time points (< 25 sec) in the cultured cell system employed. Importantly, anandamide uptake in the absence of FAAH is significantly lower than in cells with function enzyme at longer time points (90 sec and 5 min). It is the FAAH-driven component of anandamide uptake that can be modulated by FAAH inhibitors, compounds that interfere with anandamide delivery to FAAH, or proteins that enhance anandamide trafficking to FAAH.

In the absence of FAAH activity, intact anandamide is internalized and accumulates in cells in concentrations exceeding those in the extracellular media, giving rise to the idea of an intracellular anandamide "sink" (Hillard and Jarrahian, 2000, Hillard and Jarrahian, 2003). This "sink" may represent anandamide that is either dissolved in intracellular lipid membranes and therefore not in equilibrium with extracellular anandamide, or anandamide bound to an intracellular binding protein(s) (Glaser*, et al.*, 2005, Hillard and Jarrahian, 2003).

E. Intracellular transport of anandamide: role of FABPs

Anandamide is a lipophilic molecule with a predicted octanol/water partition coefficient (Log P) value of 5.1 (Fezza*, et al.*, 2008), suggesting that its hydrophobic character may limit its solubility and diffusion through the aqueous cytosol. Since FAAH

localizes to ER membranes, it is likely that efficient delivery of anandamide to FAAH requires intracellular binding proteins (Deutsch*, et al.*, 2001, Glaser*, et al.*, 2003, Hillard and Jarrahian, 2003, Kaczocha*, et al.*, 2006, Patricelli and Cravatt, 2001). To date, no intracellular anandamide carriers have been identified.

Indirect support for the carrier hypothesis was provided in a study from our laboratory (Kaczocha*, et al.*, 2006). We found that compounds described by others to be anandamide transmembrane transporter inhibitors (OMDM2 and AM1172), which were devoid of FAAH inhibitory activity (Fegley*, et al.*, 2004, Ortar*, et al.*, 2003), reduced anandamide accumulation in a temporally-dependent manner (Figure 5). As expected, these compounds were only effective upon the FAAH-dependent component of anandamide uptake (Kaczocha*, et al.*, 2006). Since these inhibitors are structural analogs of anandamide, their efficacy may stem from competition with anandamide for binding to intracellular carriers.

Since anandamide is efficiently delivered to FAAH in FAAH-transfected cells normally devoid of a functional endocannabinoid system (for review, see (Glaser*, et al.*, 2005, Hillard and Jarrahian, 2000, Hillard and Jarrahian, 2003)), candidate intracellular trafficking proteins should be widely expressed and bind a variety of ligands. As such, it is unlikely that anandamide possesses dedicated trafficking machinery. Rather, it is likely that anandamide may utilize translocation machinery used by other lipophilic molecules.

The structural similarity of endocannabinoids with fatty acids suggests that both families of molecules may share a common trafficking mechanism. There are a number of proteins reported to carry lipophilic compounds, including cellular retinoic acid-binding protein, sterol carrier protein-2, and FABPs (Furuhashi and Hotamisligil, 2008,

Schroeder, *et al.*, 2007, Sessler and Noy, 2005). Of these, only the FABP family displays considerable affinity for free fatty acids (see below) and other ligands such as retinoic acid (Hanhoff, *et al.*, 2002, Richieri, *et al.*, 2000, Schug, *et al.*, 2007, Xu, *et al.*, 1996, Zimmerman, *et al.*, 2001).

FABPs are small (~15 kDa), soluble proteins that bind fatty acids and mediate their cytoplasmic and nuclear transport (Furuhashi and Hotamisligil, 2008, Schug, *et al.*, 2007). There are ten known mammalian members of the FABP family. These include FABP1 (Liver FABP), FABP2 (Intestinal FABP), FABP3 (Heart FABP), FABP4 (Adipocyte FABP), FABP5 (Epidermal FABP), FABP6 (Ileal FABP), FABP7 (Brain FABP), FABP8 (Myelin FABP), FABP9 (Testis FABP), and FABP12 (Testis/Retinal FABP) (for review, see (Furuhashi and Hotamisligil, 2008, Liu, *et al.*, 2008)). While the expression of certain FABPs is restricted to a few tissues (e.g., FABP2), others are widely expressed. FABP3 and FABP5 are found in numerous tissues including heart, skin, brain, kidney, lung, liver, and retina (Furuhashi and Hotamisligil, 2008). Importantly, FABP3, FABP5, and FABP7 are expressed throughout the brain (Murphy, *et al.*, 2004, Owada, *et al.*, 1996, Owada, *et al.*, 2002, Owada, *et al.*, 2002, Pelsers, *et al.*, 2004). FABP3 and FABP5 are found in neuronal populations while FABP7 expression is restricted to cells of glial origin (Owada, *et al.*, 1996).

FABPs bind fatty acids with high affinity, with reported K_d values ranging from 2 to 2500 nM depending on the study and method used (Hanhoff, *et al.*, 2002, Richieri, *et al.*, 2000, Xu, *et al.*, 1996, Zimmerman, *et al.*, 2001). FABPs bind saturated, monounsaturated, and polyunsaturated fatty acids with similar affinities (Hanhoff, *et al.*, 2002, Richieri, *et al.*, 2000, Xu, *et al.*, 1996, Zimmerman, *et al.*, 2001). This binding

promiscuity of FABPs suggests that they may also interact with fatty acid derivatives such as the endocannabinoids. Indeed, binding of endocannabinoids to FABPs was very recently reported in a symposium abstract (Sun*, et al.*, 2008). In this study, anandamide and arachidonic acid both interacted with FABP7 with a three-fold higher affinity than FABP3, establishing a possible role for FABPs as intracellular carriers for anandamide (Sun*, et al.*, 2008).

FABP3, FABP5, and FABP7 KO mice have been generated (Murphy*, et al.*, 2004, Murphy*, et al.*, 2005, Owada*, et al.*, 2002, Owada*, et al.*, 2002, Owada*, et al.*, 2006). Uptake of fatty acids, including arachidonic acid, was significantly reduced in the hearts and brains of FABP3 KO mice (Murphy*, et al.*, 2004, Murphy*, et al.*, 2005). Fatty acid uptake studies were not performed with FABP5 and FABP7 KO mice.

Understanding endocannabinoid uptake and inactivation is important from a basic science and therapeutic standpoint. Inhibition of anandamide degradation by FAAH produces antinociceptive and anti-inflammatory phenotypes (Cravatt*, et al.*, 2001, Cravatt*, et al.*, 2004), suggesting that pharmacological blockade of anandamide inactivation may present a promising therapeutic strategy for ailments associated with pain and other disorders (Koutek*, et al.*, 1994). While it has been shown that anandamide transmembrane transport is consistent with passive diffusion (Kaczocha*, et al.*, 2006), it is currently not known how cells ferry endocannabinoids within the cell. The goal of the present study was to examine the rate of anandamide delivery to intracellular FAAH and determine whether (1) anandamide intracellular trafficking is rapid and independent of FAAH's subcellular localization and (2) determine whether FABPs mediate anandamide intracellular transport.

Figure 1. Metabolism of anandamide. In cultured cells and tissues, anandamide is hydrolyzed into arachidonic acid and ethanolamine principally by FAAH. FAAH-2 and NAAA also hydrolyze anandamide. Anandamide is also converted into bioactive prostamides by COX-2. LOX- and cytochrome P450-mediated conversion of anandamide respectively into hydro(pero)xides and epoxyeicosatrienoic acid ethanolamides has also been observed.

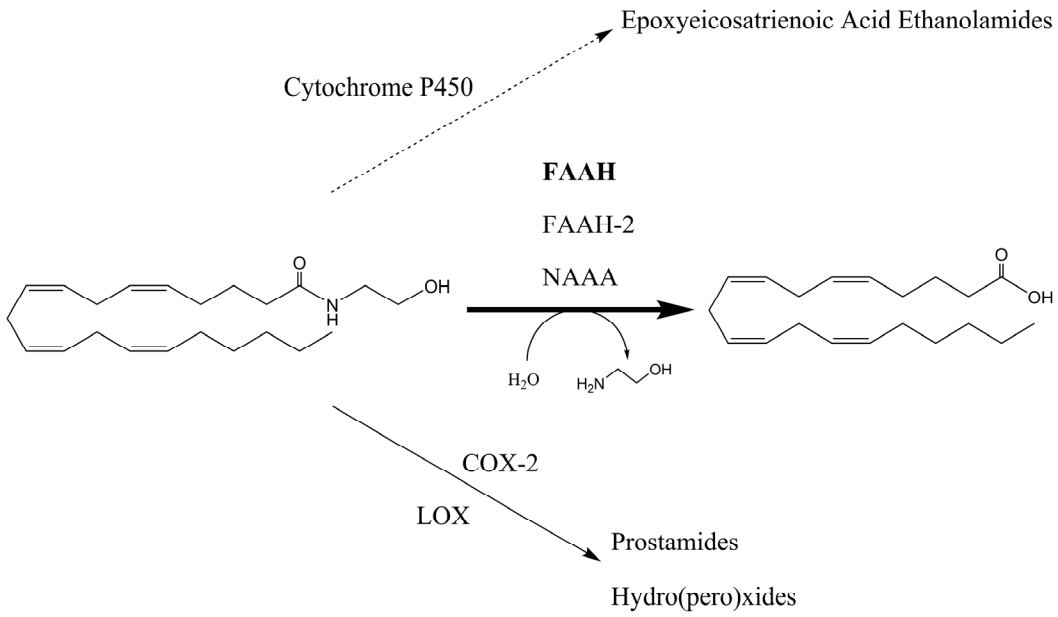
Epoxyeicosatrienoic Acid Ethanolamides
Cytochrome P450
FAAH
FAAH-2
NAAA
O
N
H
OH
H2O
H2N
OH
O
OH
COX-2
LOX
Prostamides
Hydro(pero)xides

Figure 2. Diversity of FAAH substrates. FAAH substrates include NAEs such as anandamide, PEA and OEA, primary fatty acid amines such as oleamide, N-arachidonoyl dopamine, and N-arachidonoyl taurines.

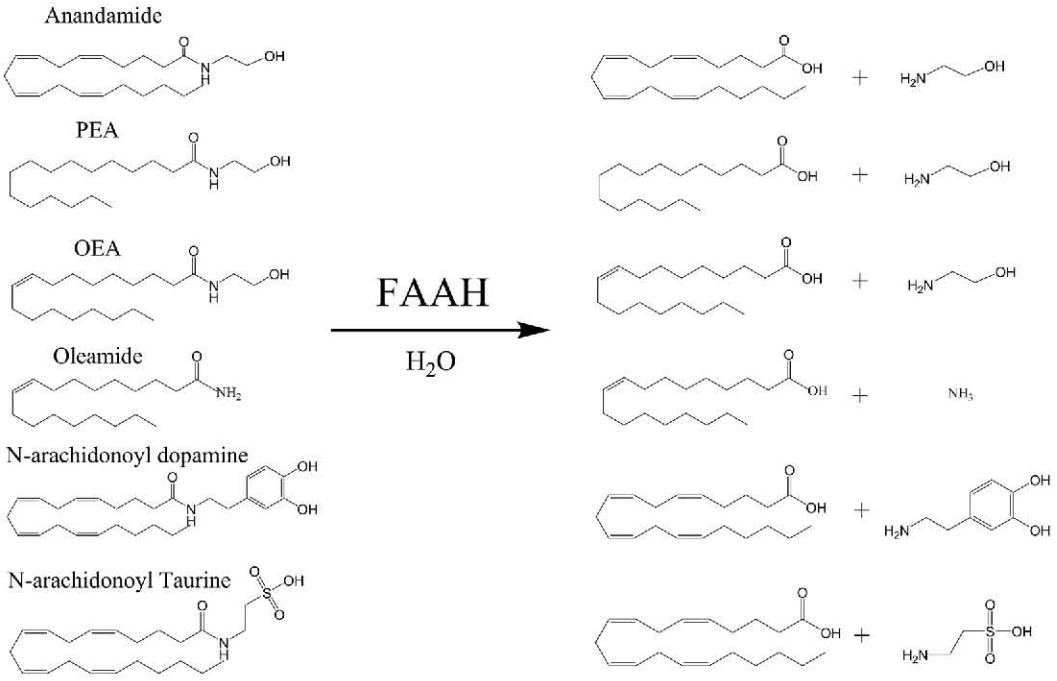
Anandamide
PEA
OEA
Oleamide
N-arachidonoyl dopamine
N-arachidonoyl Taurine
FAAH
H2O
NH3

Figure 3. Structural features of FAAH. (A) FAAH possesses several domains including a predicted N-terminal transmembrane helix that is dispensable for activity, an amidase signature sequence bearing the Serine-Serine-Lysine catalytic triad, a polyproline sequence, and a membrane binding domain. (B) Crystal structure of dimeric rat ΔTMFAAH with bound inhibitor (MAP) in the enzyme's active site. The active site of FAAH faces the lipid bilayer and is in proximity to the α18/19 membrane binding domain through which its lipid substrates are believed to enter the active site. Figure adapted from (Ahn*, et al.*, 2008, McKinney and Cravatt, 2005).

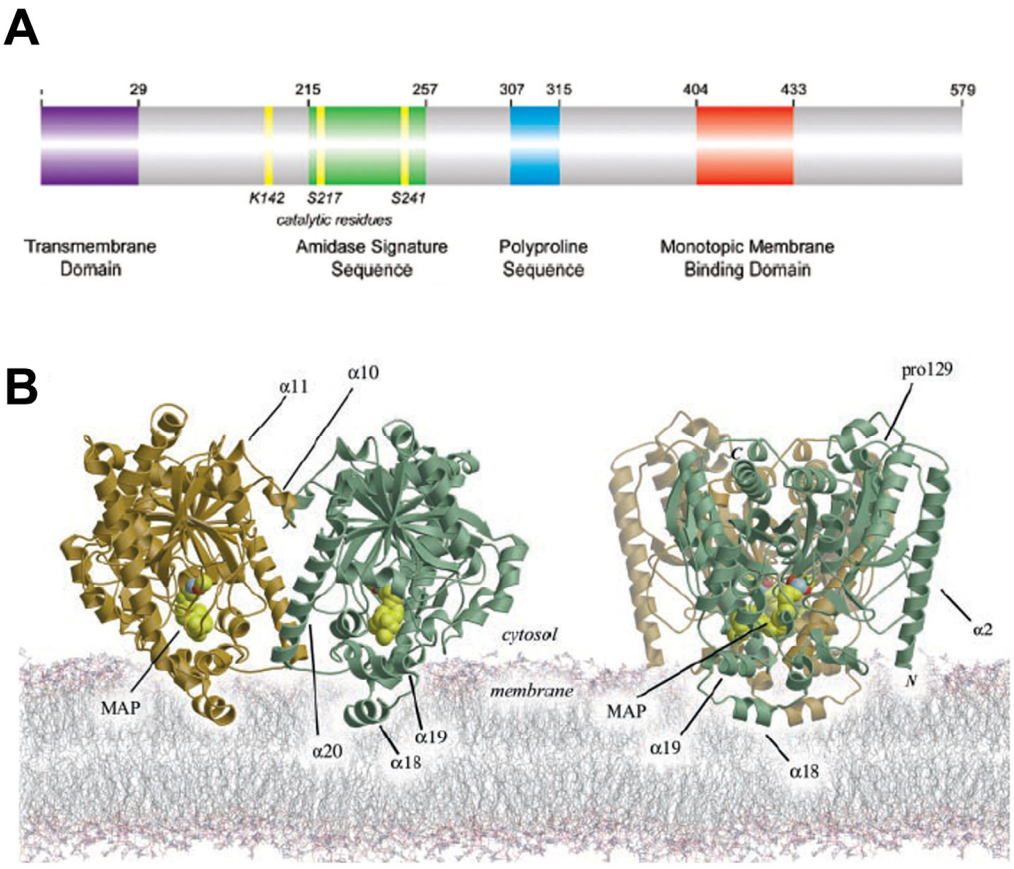
A
29
215
257
307
315
404
433
579
K142
S217
S241
catalytic residues
Transmembrane Domain
Amidase Signature Sequence
Polyproline Sequence
Monotopic Membrane Binding Domain
B
α11
α10
pro129
C
α2
N
cytosol
membrane
MAP
α20
α19
α18
MAP
α19
α18

Figure 4. Hydrolysis of anandamide maintains an inward concentration gradient. (A) Exogenously applied anandamide is rapidly taken up by cells and hydrolyzed by ER-localized FAAH into arachidonic acid. Anandamide hydrolysis by FAAH reduces its intracellular concentration and maintains an inward concentration gradient that promotes continued non-saturable uptake of anandamide into the cell. (B) Time course of [^{14}C]anandamide uptake and hydrolysis in RBL-2H3 cells. Over a 5 min time course, [^{14}C]anandamide uptake and metabolism increase proportionally. Anandamide hydrolysis is significantly reduced in cells treated with the FAAH inhibitor CAY10400. This triggers a collapse of the anandamide gradient maintained by FAAH, resulting in accumulation of intact anandamide inside cells and the onset of equilibrium. Note that at the earlier time points (25 and 45 sec), FAAH activity does not have a significant impact upon anandamide uptake due to the initial influx of exogenous [^{14}C]anandamide. Figure taken from (Kaczocha*, et al.*, 2006).

A

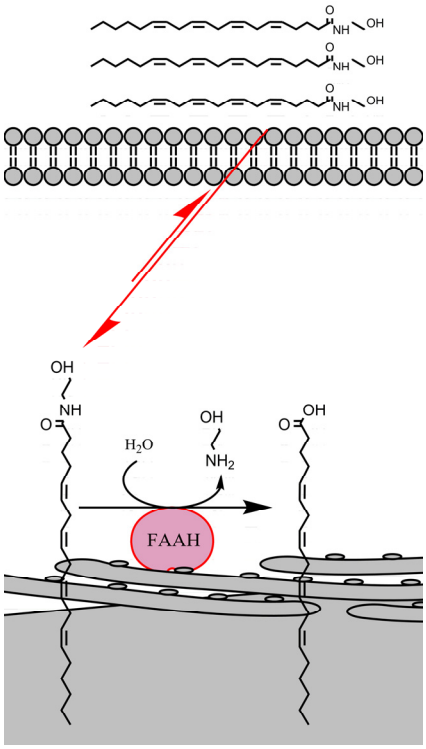
OH
NH
O
H2O
OH
NH2
OH
O
FAAH

B

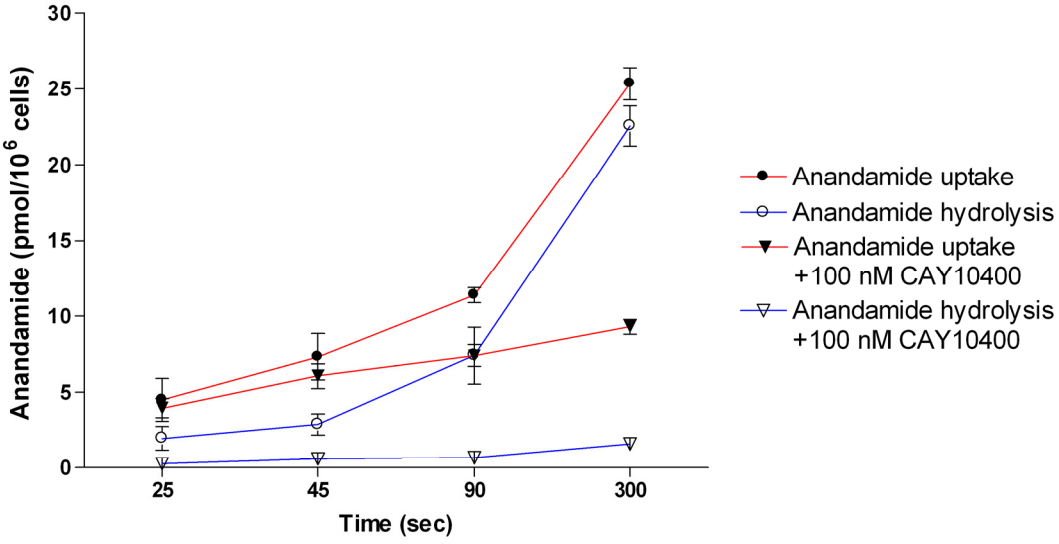
Anandamide (pmol/10^6 cells)
30
25
20
15
10
5
0
25
45
90
300
Time (sec)
Anandamide uptake
Anandamide hydrolysis
Anandamide uptake
+100 nM CAY10400
Anandamide hydrolysis
+100 nM CAY10400

Figure 5. Inhibition of anandamide uptake by "transport" inhibitors. RBL-2H3 cells were incubated with [^{14}C]anandamide for 25 sec, 90 sec, or 5 min in the presence of (A) 100 nM CAY10400, (B) 10 μM OMDM2, or (C) 10 μM AM1172. Anandamide uptake was quantified and compared to accumulation in vehicle treated cells. *, $p < 0.05$ and **, $p < 0.01$. Figure taken from (Kaczocha*, et al.*, 2006).

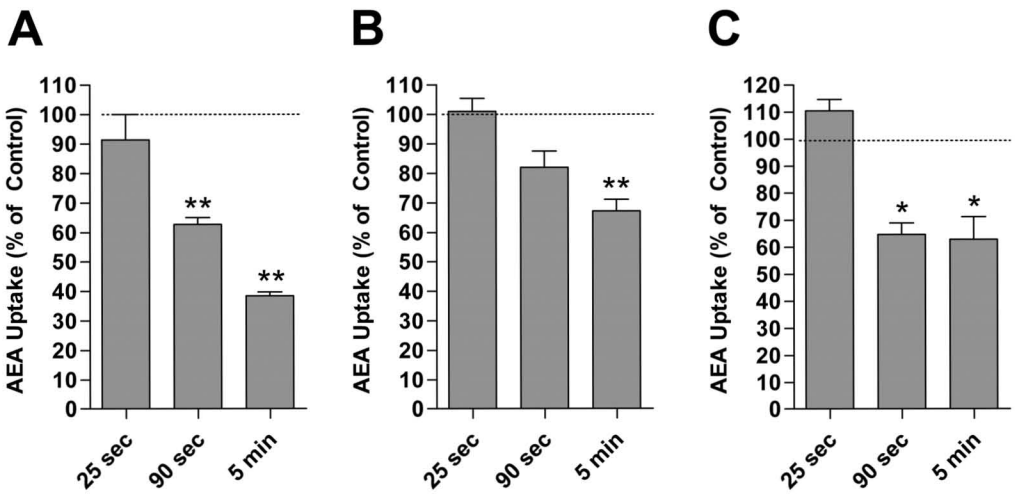
A
B
C
AEA Uptake (% of Control)
110
100
90
80
70
60
50
40
30
20
10
0
120
**
*
25 sec
90 sec
5 min

MATERIALS AND METHODS

Chemicals. Anandamide, oleic acid, and URB597 ([3-(3-carbamoylphenyl)phenyl] N-cyclohexylcarbamate) were from Cayman Chemical (Ann Arbor, MI). BMS309403 (((2′-(5-Ethyl-3,4-diphenyl-1H-pyrazol-1-yl)(1,1′-biphenyl)-3-yl)oxy)-acetic acid) was from Calbiochem (San Diego, CA). Fatty acid-free BSA and PMSF were from Sigma. [^{14}C]anandamide (arachidonoyl [1-^{14}C]ethanolamide, 53 mCi/mmol) was provided by the Drug Supply Program at the National Institute on Drug Abuse.

Cell Culture and Generation of Stable Cell-lines. COS-7 and N18TG2 cells were grown in DMEM supplemented with 10% fetal bovine serum, 100 U/ml penicillin/streptomycin, 2 mM L-glutamine, and 1 mM sodium pyruvate in a humidified incubator containing 95% air and 5% CO_2. Transfections were carried out using Lipofectamine 2000 (Invitrogen, Carlsbad, CA) according to the manufacturer's instructions. For stable cell selection, forty eight hours after transfection, cells were expanded in medium containing 750 μg/ml geneticin (Invitrogen, Carlsbad, CA). Following four weeks in selection media, stable cells expressing identical levels of the indicated FAAH-eGFP fusion proteins were obtained by flow cytometry at the Flow Cytometry Core Facility in Stony Brook University and expanded.

Cloning of Spatially Restricted FAAH Variants and FABPs. Rat FAAH was PCR amplified and subcloned into the eGFP-N1 plasmid (Clonetech) using XhoI and KpnI and the following primers: forward 5'-TATACTCGAG**GCCACC**ATGGTGCTGAGCGAAGTGTG-3' and reverse 5'-TATATGGTACCGACGATGGCTGCTTTTGAGG-3'. Underlined nucleotides represent restriction sites while those in bold represent a Kozak consensus sequence. ΔTMFAAH

was subcloned into eGFP-N1 using XhoI and KpnI and the following primers: forward 5'-TATATCTCGAGCGATGGACCGGGCGCCAG-3' and reverse 5'-GATATATGGTACCGACGATGGCTGCTTTTGAGG-3'. To localize FAAH to mitochondrial outer membranes, TOM20 (residues 1-33) was fused to the N-terminus of ΔTMFAAH-eGFP using NheI and XhoI and the following primers: forward 5'-GATATAGCTAGC**GCCACC**ATGGTGGGCCGGAACAGC-3' and reverse 5'-GATATACTCGAGGTTGGGGTCACTCCGCCTTT-3'. To localize FAAH to the outer membranes of the Golgi apparatus, Grasp65 was fused to the N-terminus of ΔTMFAAH-eGFP using NheI and EcoRI. The following primers were used: forward 5'-GATATAGCTAGC**GCCACC**ATGGGGCTAGGGGCAAGC-3' and reverse 5'-GATATAGAATTCCAGCCCAGGCTCTGGATCTGG-3'. FABP3, FABP5, and FABP7 were cloned from mouse brain RNA using PCR and the following primers: FABP3 forward 5'-GATATAAAGCTT**GCCACC**ATGGCGGACGCCTTTGTC-3' and reverse 5'- GATATACTCGAGTCACGCCTCCTTCTCATAAGTC-3', FABP5 forward 5'-GATATAAAGCTT**GCCACC**ATGGCCAGCCTTAAGGATC-3' and reverse 5'-GATATACTCGAGTCATTGCACCTTCTCATAGAC-3', and FABP7 forward 5'-GATAGGTACC**GCCACC**ATGGTAGATGCTTTCTGCGCAA-3' and reverse 5'-GATATACTCGAGCTATGCCTTTTCATAACAGCGAAC-3'. FABP3 and FABP5 were digested with HindIII and XhoI while FABP7 was digested with XhoI and KpnI and inserted into pcDNA4. All constructs were verified by DNA sequencing.

Immunolocalization of Fusion Proteins. COS-7 cells stably expressing FAAH-eGFP fusion proteins were plated unto coverslips. To assess mitochondrial localization, the cells were treated with 175 nM Mitotracker Red CM-H_2XRos (Molecular Probes,

Eugene, OR) in DMEM + 10% fetal bovine serum for 25 min at 37°C, followed by fixation in 3% paraformaldehyde for 15 minutes. The cells were subsequently permeabilized with 0.2% Triton X-100 for 5 min at 4°C and treated with rabbit anti-calreticulin antibodies (1:200) (Affinity Bioreagents, Golden, CO) or mouse anti-GM130 antibodies (1:100) (BD Transduction Labs, San Jose, CA) in 5% normal goat serum followed by donkey anti-rabbit or donkey anti-mouse IgG Alexa Fluor 594 antibodies (1:800) (Molecular Probes, Eugene, OR). All images were acquired using a Zeiss LSM 510 META NLO Two-Photon Laser Scanning Microscope.

Western Blotting. All samples were run on a 10% SDS-PAGE gel. Following transfer to a nitrocellulose membrane at 100V for 25 min, the blots were blocked for one hour in 5% non-fat dry milk in PBST. The blots were probed with rabbit anti-eGFP (1:2000) (Molecular Probes, Eugene, OR), mouse anti-β actin (1:30000) or mouse anti-FABP3 (1:100) (Abcam, Cambridge, MA), rabbit anti-FABP5 (1:100) or rabbit anti-FABP7 (1:100) (Santa Cruz Biotechnology, Santa Cruz, CA) antibodies for 1 hour with shaking. The blots were rinsed three times with PBST followed by incubation with goat anti-mouse or goat anti-rabbit IgG HRP-conjugated antibodies (1:8000) (Molecular Probes, Eugene, OR) for 1 hour. The blots were rinsed three times with PBST, developed using the Immun-Star HRP substrate (Bio-Rad, Hercules, CA) and exposed to film.

Proteinase K Protection Analysis. COS-7 cells were homogenized by passage through a 26 gauge needle in buffer A (10mM HEPES-NaOH, pH 7.5, containing 1mM EDTA, 1.5mM $MgCl_2$, 10mM KCl and 250 mM sucrose). Unbroken cells and nuclei were pelleted by centrifugation at 1000g for 10 min and the resulting supernatant was subjected to centrifugation at 100,000g for 60 min at 4°C. The pellet containing

membranes was resuspended in buffer B (50 mM Tris pH 8, 3 mM $CaCl_2$, 1.5 mM $MgCl_2$, 10 mM KCl, 100mM NaCl, 250mM sucrose) and treated with 500 μg/ml proteinase K for 30 min at 37°C in the presence or absence of 1% Triton X-100, or left untreated. The reactions were quenched by the addition of 20 mM PMSF. The samples were separated by SDS-PAGE and visualized by immunoblotting with anti-eGFP and anti-calreticulin antibodies (1:2000) (Affinity Bioreagents, Golden, CO).

FAAH Enzyme Assays. Cell homogenates were incubated with 100 μM anandamide + 0.1 μCi [^{14}C]anandamide in Tris-HCl (pH 9) containing 0.1% BSA. For activity analyses, the time and total protein concentration were adjusted to maintain substrate conversion at approximately 10%. For inhibitor studies, 50 μg of COS-7 or 100 μg N18TG2 cell homogenates were pre-treated with 100 μM oleic acid, 100 μM BMS309403, or vehicle (DMSO) control for 15 min followed by incubation with [^{14}C]anandamide (100 μM) for 1 or 30 min, respectively. Reactions were stopped by the addition of two volumes of 1:1 chloroform:methanol and the phases separated by centrifugation. The methanol phase (containing [^{14}C]ethanolamine) was sampled and quantified using a Beckman LS 6500 scintillation counter.

Determination and Inhibition of anandamide Cellular Uptake and Hydrolysis. Cells were plated at ~90% confluency in 35mm dishes, washed twice in DMEM and preincubated with the desired pharmacological compounds or vehicle controls (EtOH or DMSO). The cells were washed twice in DMEM and subsequently incubated for 10 min, 5 min, 10 sec, or 3 sec with 750 μl [^{14}C]anandamide + unlabeled anandamide (100 nM or 10 μM) that was pre-equilibrated for 75 min in medium containing 0.15% BSA. The equilibration step is necessary to avoid uneven distribution of the radiotracer and to

ensure that it is stable in solution pre-bound to BSA. Less than 1% of anandamide was hydrolyzed during this pre-equilibration step. Following the incubation, 750 µl of ice-cold DMEM + 0.15% BSA was added to the plates, the media separated from cells, which were then washed with DMEM + 0.15% BSA to remove non-specifically bound anandamide. The cells were scraped three times with 400 µl of ice-cold 2 mM EDTA in PBS and two volumes of chloroform:methanol (1:1) added to the media and cells, and the phases separated by centrifugation. The resulting aqueous (containing [^{14}C]ethanolamine) and organic (containing intact [^{14}C]anandamide) phases were counted by liquid scintillation counting. [^{14}C]anandamide uptake was determined by summing the production of [^{14}C]ethanolamine in the media and cells with intact cellular [^{14}C]anandamide. Hydrolysis of [^{14}C]anandamide was quantified by production of [^{14}C]ethanolamine in the media and cells. Blanks consisting of either untransfected COS-7 cells or N18TG2 cells treated with 100 nM URB597 were subtracted from all conditions except the 3 sec time point.

RT-PCR Analysis of Endogenous FABP Expression. One microgram of RNA extracted from mouse brain or N18TG2 cells using the RNeasy mini kit (Qiagen, Valencia, CA) was subjected to cDNA synthesis using the Superscript III first strand synthesis kit (Invitrogen, Carlsbad, CA). The resulting cDNAs were subjected to PCR using primers specific for FABP3, FABP5, FABP7, or β-actin. The following primers were used. For FABP3, forward 5'-CATCGAGAAGAACGGGGATA-3' and reverse 5'-TGCCATGAGTGAGAGTCAGG-3'; FABP5 forward 5'-CAAAACCGAGAGCACAGTGA-3' and reverse 5'-CACGATCATCTTCCCATCCT-3'; FABP7 forward 5'-AGTGGGAAACGTGACCAAAC-3' and 5'-

TTTCTTTGCCATCCCACTTC-3'; and β-actin forward 5'-AGATGACCCAGATCATGTTTGA-3' and reverse 5'-CACAGCTTCTCCTTAATGTCA-3'. The following cycling conditions were used: denaturation at 94^{o}C for 30 sec, annealing at 58^{o}C for 30 sec, and extension at 72^{o}C for 30 sec for a total of 30 cycles. The resulting products were visualized on an agarose gel.

Statistical Analyses. Results are expressed as means ± standard error. Statistical significance was evaluated using two tailed unpaired t-tests against vector transfected or vehicle treated controls.

RESULTS

A. Generation of FAAH-eGFP variants with distinct subcellular localizations.

FAAH variants with discrete intracellular localizations were designed to explore putative intracellular trafficking mechanisms for anandamide. It is expected that if the intracellular delivery of anandamide to FAAH is mediated by cytosolic binding proteins, then its rate of hydrolysis by FAAH will be unaffected if FAAH is re-localized to distinct subcellular organelles. FAAH was first tagged with eGFP at its C-terminus (FAAH-eGFP) (Figure 6). To localize FAAH to mitochondrial outer membranes, the mitochondrial localization sequence of TOM20 (residues 1-33) (Kanaji*, et al.*, 2000) was fused to the N-terminus of ΔTMFAAH-eGFP, generating TOM-ΔTMFAAH-eGFP. To localize FAAH to the Golgi apparatus, ΔTMFAAH-eGFP was fused to the Golgi apparatus resident protein GRASP65 (Barr*, et al.*, 1997), yielding GRASP-ΔTMFAAH-eGFP.

Stable cell-lines expressing these fusion proteins were generated in COS-7 cells, which do not natively express FAAH (Wei*, et al.*, 2006). Similar levels of protein expression and activity were confirmed by western blotting and enzymatic analysis (Figure 7A and B), respectively. FAAH-eGFP localized to the endoplasmic reticulum and mostly co-localized with an ER marker, as previously reported (Figure 8A) (Oddi*, et al.*, 2005). FAAH-eGFP did not localize to the Golgi apparatus as judged by lack of co-localization with the Golgi apparatus marker GM130. TOM-ΔTMFAAH-eGFP co-localized with the mitochondrial dye, Mitotracker CM-H2Xros (Figure 8A). There was no co-localization with the ER marker calreticulin. GRASP-ΔTMFAAH-eGFP was confined to the Golgi apparatus as judged by co-localization with GM130.

Protease protection analysis revealed that FAAH-eGFP, TOM-ΔTMFAAH-eGFP, and GRASP-ΔTMFAAH-eGFP proteins were cleaved following treatment of COS-7 membranes with proteinase K in the absence of Triton X-100 (Figure 8B). In contrast, calreticulin, a luminal ER membrane protein, was cleaved by proteinase K only in the presence of detergent. These data confirm that all three FAAH variants localized to the cytoplasmic face of membranes. Therefore, in cells expressing these spatially restricted FAAH variants, the cytosol presents the sole barrier for anandamide delivery from the plasma membrane to FAAH.

B. Anandamide uptake and hydrolysis by spatially-restricted FAAH-eGFP variants.

Anandamide uptake and hydrolysis assays were carried out to determine whether re-localization of FAAH to the mitochondria or the Golgi apparatus affected the rate of anandamide delivery to FAAH. As shown in Figure 9A, anandamide uptake and hydrolysis were similar in cells expressing FAAH-eGFP, TOM-ΔTMFAAH-eGFP, and GRASP-ΔTMFAAH-eGFP following a 5 min incubation with [^{14}C]anandamide. Since this time point may allow for anandamide to be taken up by one mechanism and potentially redistributed intracellularly, these experiments were repeated using shorter time points. Similar results were obtained following a 10 sec incubation with [^{14}C]anandamide (Figure 9B). Identical results were also found when intracellular anandamide hydrolysis following uptake was examined at 3 sec, with similar rates of anandamide metabolism in cells expressing the three FAAH variants and significantly lower hydrolysis in cells lacking FAAH (Figure 9C). Collectively, these data suggest that

anandamide transport through the plasma membrane and its subsequent intracellular delivery to FAAH occurs by a rapid and organelle non-specific mechanism.

C. Anandamide uptake and hydrolysis are enhanced by FABPs.

The present results suggest that anandamide may utilize intracellular carriers for its cytosolic transport. Since FABPs are widely expressed and three FABP members are expressed in the brain including FABP3, FABP5, and FABP7 (Furuhashi and Hotamisligil, 2008, Owada*, et al.*, 1996, Owada, 2008), these proteins were examined as putative anandamide carriers.

To determine whether brain FABPs can potentiate anandamide uptake and hydrolysis, COS-7 cells expressing FAAH-eGFP were transfected with each FABP and anandamide uptake and metabolism analyzed. Overexpression of FABP5 and FABP7, but not FABP3, enhanced [^{14}C]anandamide uptake by 32% and 35%, respectively (Figure 10). Anandamide hydrolysis was respectively elevated by 31% and 36% in FABP5 and FABP7 overexpressing cells. Western blotting confirmed that all three FABPs were successfully expressed in COS-7 cells (Figure 11). Since FAAH-eGFP and FABPs utilize a common promoter for expression, it was imperative to confirm that overexpression of FABPs did not artifactually affect anandamide uptake by modulating FAAH expression and/or activity. As shown in Figure 12, [^{14}C]anandamide hydrolysis was similar in homogenates of FAAH-eGFP expressing cells transfected with FABPs or vector controls.

To confirm that the ability of FABPs to potentiate anandamide uptake is independent of cell-type, these experiments were repeated in mouse neuroblastoma N18TG2 cells. These cells express CB1 receptors, FAAH, and they take up and

hydrolyze anandamide (Glaser*, et al.*, 2003, Howlett, 1985, Maurelli*, et al.*, 1995). In N18TG2 cells, overexpression of FABP5 and FABP7 significantly enhanced the uptake of [^{14}C]anandamide by 36% and 42%, respectively (Figure 13). Anandamide hydrolysis was respectively elevated by 44% and 53% in FABP5 and FABP7 transfected cells. FABP3 overexpression did not potentiate anandamide uptake or hydrolysis. Western blotting confirmed that similar to COS-7 cells, all three FABPs were successfully overexpressed in N18TG2 (Figure 11). To confirm the endogenous expression of these FABPs in untransfected N18TG2 cells, RT-PCR analysis was performed in N18TG2 cells and mouse brain as a control. As expected, FABP3, FABP5 and FABP7 were expressed in brain while FABP3 and FABP5, but not FABP7, were expressed in N18TG2 cells (Figure 14). Collectively, these data provide evidence that FABPs act as intracellular carriers for anandamide.

D. Inhibition of FABPs reduces anandamide uptake and hydrolysis.

Competitive FABP ligands were employed to examine the contributions of endogenous FABPs towards anandamide uptake and inactivation by FAAH. Initially, COS7-FAAH-eGFP and N18TG2 cells were incubated with the FABP ligand oleic acid (Hanhoff*, et al.*, 2002) and [^{14}C]anandamide uptake and hydrolysis measured following a 5 min incubation. Oleic acid reduced [^{14}C]anandamide uptake in both COS7-FAAH-eGFP cells and in N18TG2 cells by 25% and 53%, respectively (Figure 15). These inhibition studies were repeated using the novel FABP inhibitor BMS309403 (Sulsky*, et al.*, 2007). BMS309403 is a competitive inhibitor of FABPs with reported IC_{50} values of 250 and 350 nM for FABP3 and FABP5, respectively (Furuhashi and Hotamisligil, 2008,

Sulsky*, et al.*, 2007). Treatment of COS7-FAAH-eGFP cells or N18TG2 cells with 20-100 μM BMS309403 resulted in dose-dependent reductions in [^{14}C]anandamide uptake and hydrolysis (Figure. 16). Significant effects in N18TG2 cells were only observed in cells treated with 50 μM and 100 μM BMS309403. The maximal inhibition of anandamide uptake was 48% in COS7-FAAH-eGFP cells and 57% in N18TG2 cells. Anandamide hydrolysis was also significantly reduced. The efficacy of BMS309403 was preserved when cells were pretreated with this inhibitor but subsequently incubated with [^{14}C]anandamide alone (Figure 17). This suggests that BMS309403 did not artifactually reduce anandamide uptake by competing with anandamide for binding to BSA.

Similar to the results at 5 min, BMS309403 also reduced intracellular [^{14}C]anandamide hydrolysis following uptake at 3 sec in COS7-FAAH-eGFP and N18TG2 cells (Figure 18). At the highest concentration tested (100 μM), BMS309403 inhibited [^{14}C]anandamide hydrolysis by ~42% in COS7-FAAH-eGFP cells and ~68% in N18TG2 cells. Oleic acid and BMS309403 did not inhibit FAAH activity over the concentration range used in the current study (Figure 19), suggesting that their effects upon [^{14}C]anandamide uptake stem from inhibition of intracellular transport rather than FAAH.

Figure 6. Constructs used in this study. FAAH-eGFP is shown with its N-terminal transmembrane helix (residues 1-29) in red, residues 30-579 in black, and eGFP in green. This N-terminal helix was replaced with TOM20 (residues 1-33, shown in blue) in TOM-ΔTMFAAH-eGFP. In GRASP-ΔTMFAAH-eGFP, the Golgi resident protein grasp65 (grey) was fused to the N-terminus of ΔTMFAAH-eGFP.

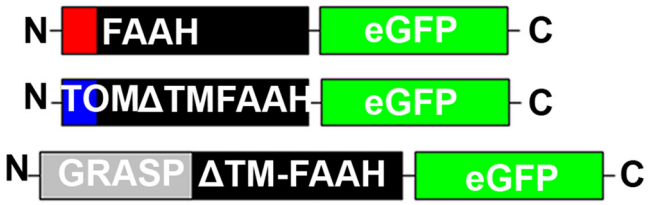
N
FAAH
eGFP
C
N
TOMΔTMFAAH
eGFP
C
N
GRASP
ΔTM-FAAH
eGFP
C

Figure 7. Expression of FAAH variants in COS-7 cells. (A) Western blot analysis indicates similar expression levels of FAAH-eGFP variants in COS-7 cells stably expressing FAAH-eGFP, TOM-ΔTMFAAH-eGFP or GRASP-ΔTMFAAH-eGFP. Blots were probed with eGFP antibodies with β-actin serving as a loading control. (B) Similar rates of [^{14}C]anandamide hydrolysis ($p > 0.05$) by FAAH-eGFP, TOM-ΔTMFAAH-eGFP and GRASP-ΔTMFAAH-eGFP expressing COS-7 homogenates (n=3).

A

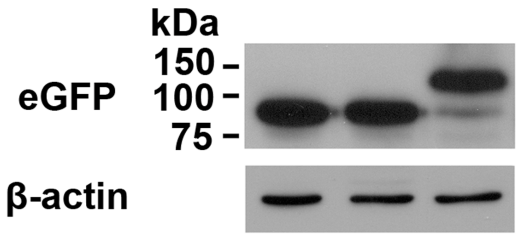
kDa
150
100
75
eGFP
β-actin

B

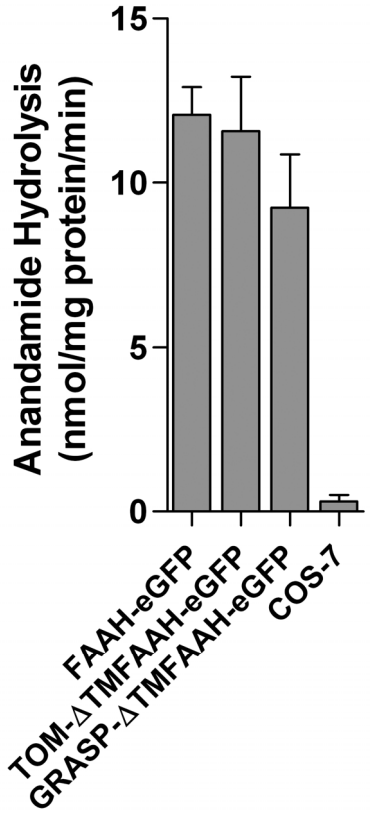
Anandamide Hydrolysis
(nmol/mg protein/min)
15
10
5
0
FAAH-eGFP
TOM-ΔTMFAAH-eGFP
GRASP-ΔTMFAAH-eGFP
COS-7

Figure 8. Subcellular localization and membrane orientation of FAAH variants. (A) FAAH variants localize to specific organelles. Top panel shows FAAH-eGFP fusion proteins (green), middle panel depicts the marker of interest (red), and the bottom panel is the merged image (yellow). FAAH-eGFP localized to the ER and mostly overlapped with the ER marker calreticulin. TOM-ΔTMFAAH-eGFP co-localized with the mitochondrial dye Mitotracker CM-H2Xros and was excluded from the ER. GRASP-ΔTMFAAH-eGFP localized to the Golgi apparatus as judged by co-localization with GM130. Note that overexpression of GRASP-ΔTMFAAH-eGFP resulted in an enlargement of the Golgi apparatus. (B) Proteinase K protection analysis of FAAH-eGFP, TOM-ΔTMFAAH-eGFP and GRASP-ΔTMFAAH-eGFP proteins in membrane fractions of COS-7 cells. Membranes were either left untreated or were incubated with 500 μg/ml proteinase K in the presence or absence of 1% Triton X-100. Samples were resolved by SDS-PAGE and probed with eGFP and calreticulin antibodies.

A

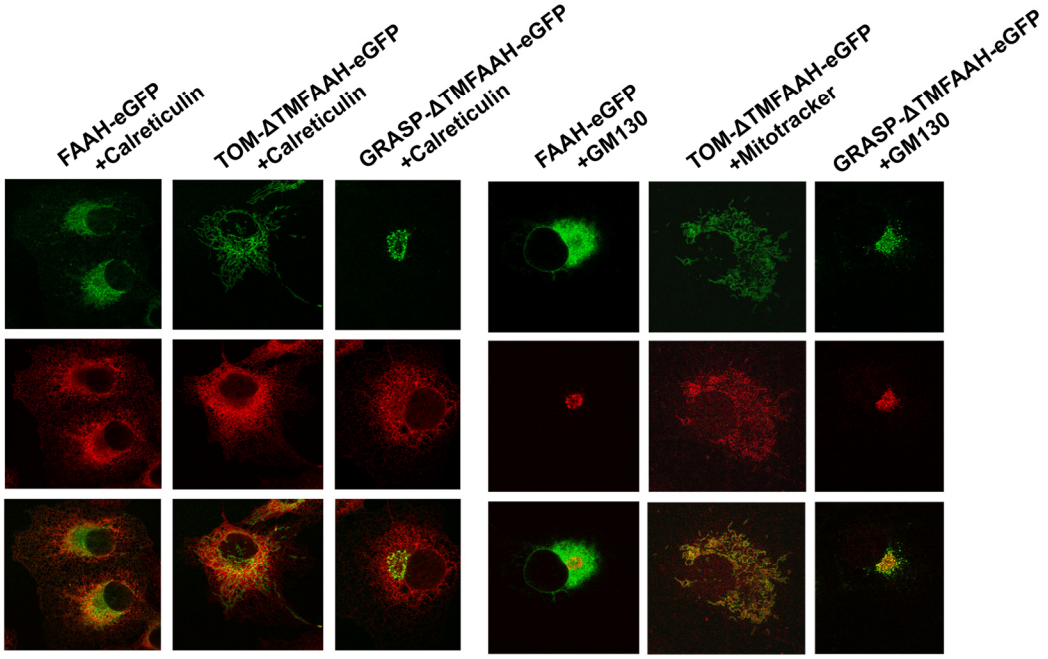
FAAH-eGFP +Calreticulin
TOM-ΔTMFAAH-eGFP +Calreticulin
GRASP-ΔTMFAAH-eGFP +Calreticulin
FAAH-eGFP +GM130
TOM-ΔTMFAAH-eGFP +Mitotracker
GRASP-ΔTMFAAH-eGFP +GM130

B

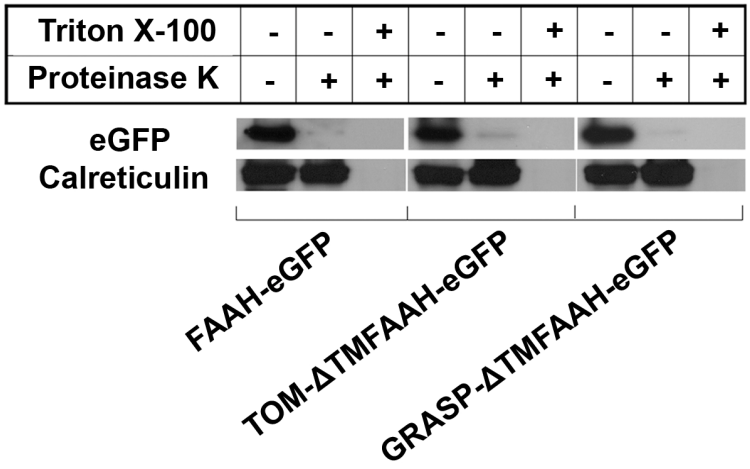
Triton X-100 - - + - - + - - +
Proteinase K - + + - + + - + +
eGFP
Calreticulin
FAAH-eGFP
TOM-ΔTMFAAH-eGFP
GRASP-ΔTMFAAH-eGFP

Figure 9. Anandamide inactivation in COS-7 cells expressing spatially restricted FAAH variants. [^{14}C]anandamide uptake (black bars) and hydrolysis (grey bars) were similar ($P > 0.05$) in COS7-FAAH-eGFP, TOM-ΔTMFAAH-eGFP or GRASP-ΔTMFAAH-eGFP cells following (A) 5 min or (B) 10 sec incubations ($n = 3$). (C) Similar levels ($p > 0.05$) of intracellular [^{14}C]anandamide hydrolysis following uptake at 3 sec in COS7-FAAH-eGFP, TOM-ΔTMFAAH-eGFP or GRASP-ΔTMFAAH-eGFP. Hydrolysis of [^{14}C]anandamide in untransfected COS-7 cells was significantly lower than in FAAH-eGFP controls. **, $p < 0.01$ ($n = 3$).

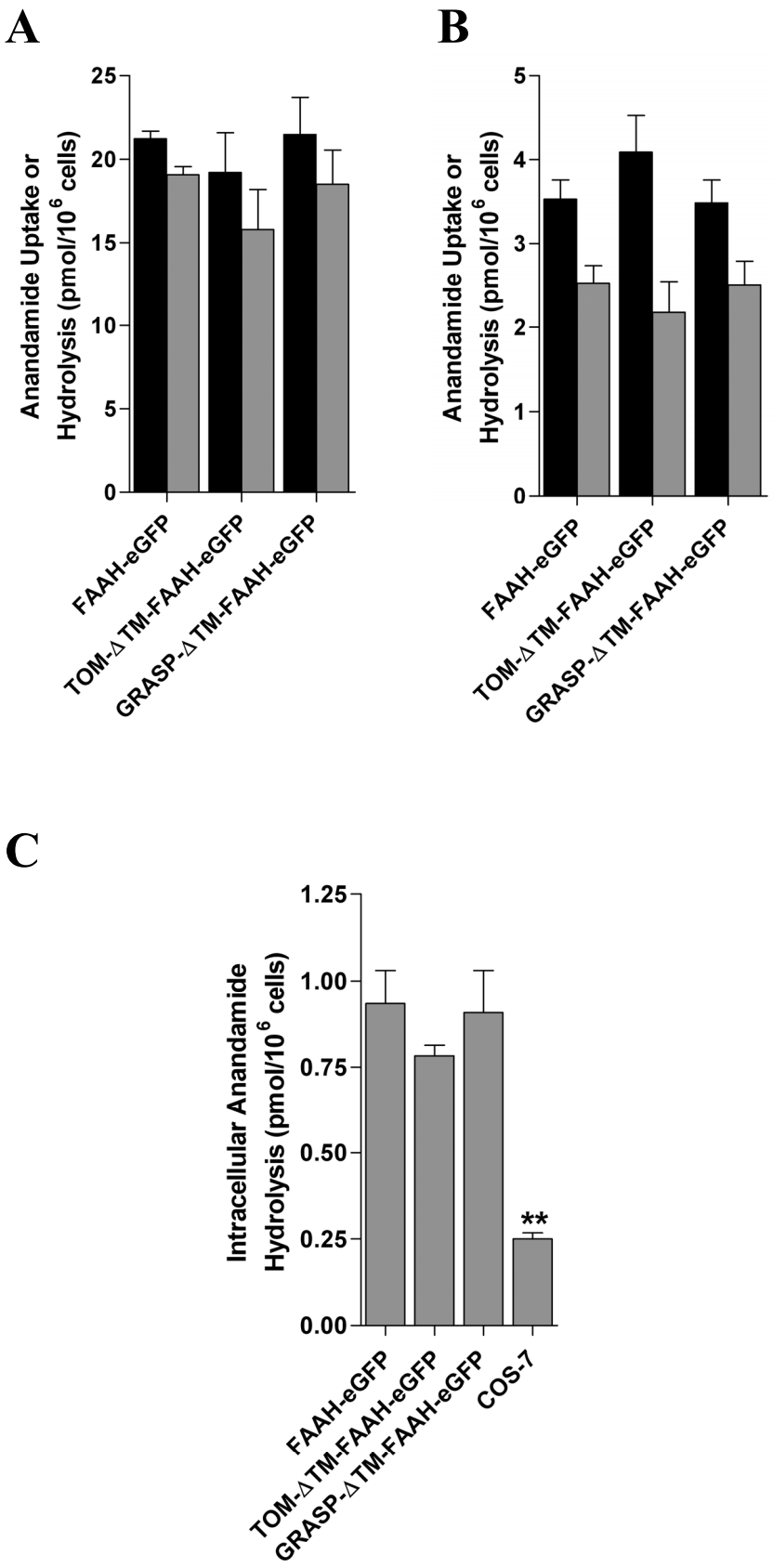
A
B
C
Anandamide Uptake or Hydrolysis (pmol/10^6 cells)
Intracellular Anandamide Hydrolysis (pmol/10^6 cells)
FAAH-eGFP
TOM-ΔTM-FAAH-eGFP
GRASP-ΔTM-FAAH-eGFP
COS-7
**

Figure 10. Effect of FABP overexpression upon anandamide uptake and hydrolysis. Following a 10 minute incubation, [^{14}C]anandamide uptake (black bars) and hydrolysis (grey bars) were significantly elevated in COS7-FAAH-eGFP cells following FABP5 or FABP7, but not FABP3, transfection. **, $p < 0.01$ compared to vector transfected controls (n = 3-5).

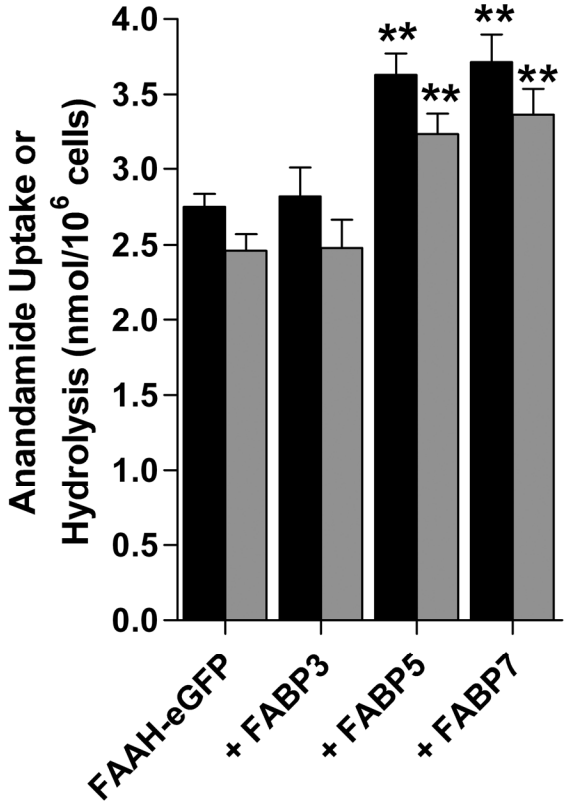
Anandamide Uptake or
Hydrolysis (nmol/10^6 cells)
4.0
3.5
3.0
2.5
2.0
1.5
1.0
0.5
0.0
**
**
**
**
FAAH-eGFP
+ FABP3
+ FABP5
+ FABP7

Figure 11. Overexpression of FABPs in COS7-FAAH-eGFP and N18TG2 cells. Western blot analysis of overexpressed FABP3, FABP5 or FABP7 in COS7-FAAH-eGFP and N18TG2 cells. Blots were probed with the respective antibodies. B-actin serves as a loading control.

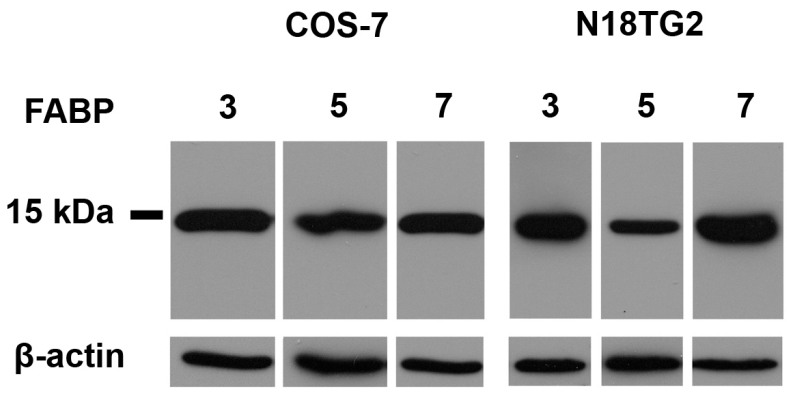
COS-7
N18TG2
FABP
3
5
7
3
5
7
15 kDa
β-actin

Figure 12. Effect of FABP overexpression upon FAAH activity in COS7-FAAH-eGFP cells. Overexpression of FABP3, FABP5, or FABP7 had no effect upon [^{14}C]anandamide hydrolysis by COS7-FAAH-eGFP homogenates ($p > 0.05$).

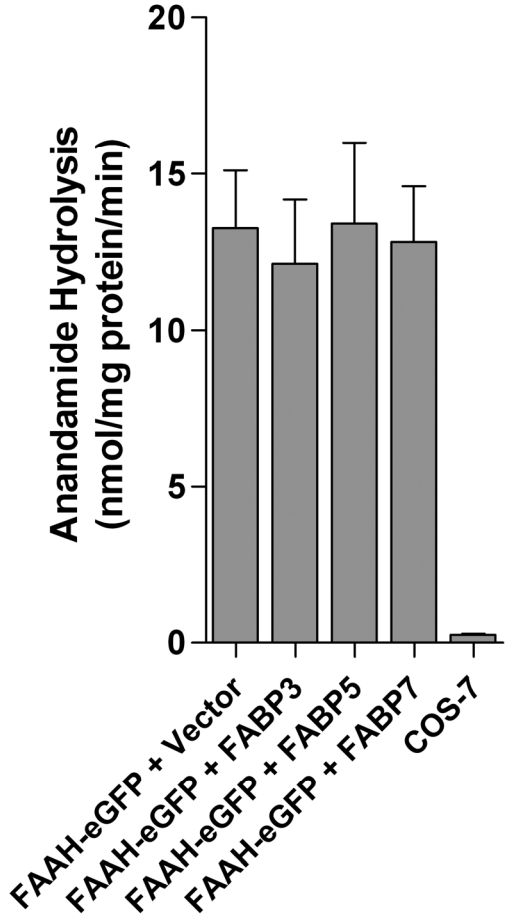
Anandamide Hydrolysis
(nmol/mg protein/min)
20
15
10
5
0
FAAH-eGFP + Vector
FAAH-eGFP + FABP3
FAAH-eGFP + FABP5
FAAH-eGFP + FABP7
COS-7

Figure 13. Effect of FABP overexpression upon anandamide uptake and hydrolysis in N18TG2 cells. [^{14}C]anandamide uptake (black bars) and metabolism (grey bars) by N18TG2 cells were enhanced following transfection with FABP5 and FABP7, but not FABP3. *, $p < 0.05$ and **, $p < 0.01$ compared to vector transfected controls (n = 3-5).

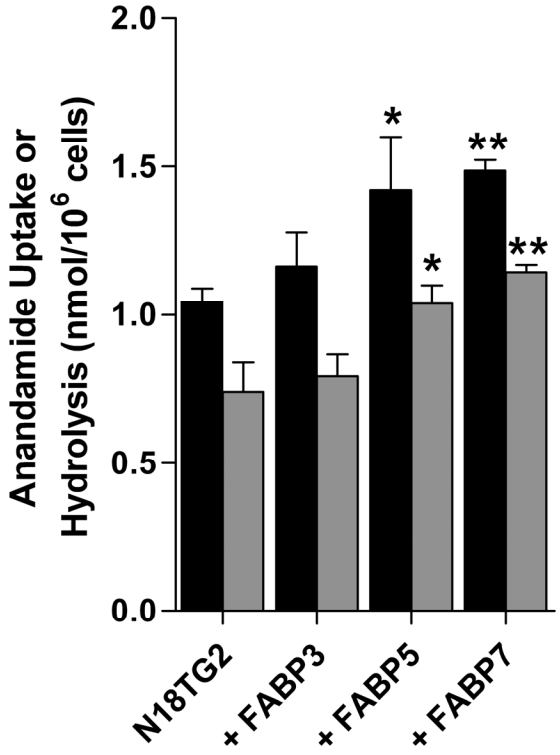
Anandamide Uptake or Hydrolysis (nmol/10^6 cells)
2.0
1.5
1.0
0.5
0.0
*
**
*
**
N18TG2
+ FABP3
+ FABP5
+ FABP7

Figure 14. Expression of FABPs in N18TG2 cells and mouse brain. RT-PCR analysis confirmed the endogenous expression of FABP3, FABP5, and FABP7 in mouse brain and FABP3 and FABP5 in N18TG2 cells. β-actin serves as a loading control.

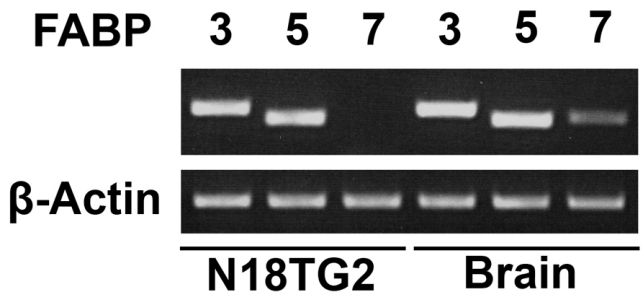
FABP
3
5
7
3
5
7
β-Actin
N18TG2
Brain

Figure 15. Effect of oleic acid upon anandamide uptake and hydrolysis. Treatment of COS7-FAAH-eGFP and N18TG2 cells with 100 μM oleic acid significantly reduced [^{14}C]anandamide uptake (black bars) and hydrolysis (grey bars) at 5 min. *, $p < 0.05$ compared to vehicle-treated controls (n = 3-5)

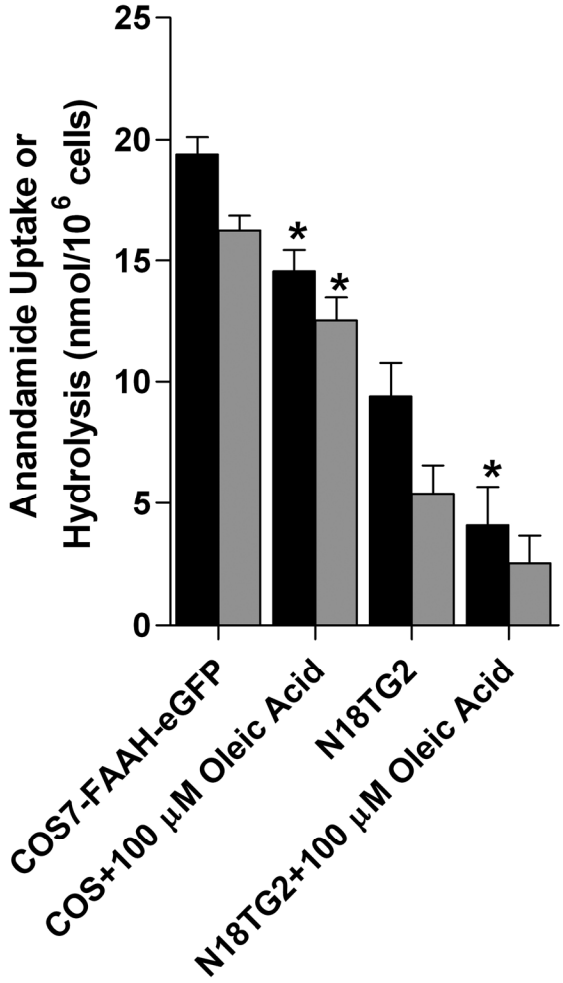
Anandamide Uptake or Hydrolysis (nmol/10^6 cells)
25
20
15
10
5
0
*
*
*
COS7-FAAH-eGFP
COS+100 μM Oleic Acid
N18TG2
N18TG2+100 μM Oleic Acid

Figure 16. Effect of BMS309403 upon anandamide uptake and hydrolysis. [^{14}C]anandamide uptake (black bars) and hydrolysis (grey bars) at 5 min were significantly reduced following treatment of (A) COS7-FAAH-eGFP or (B) N18TG2 cells with 20-100 μM BMS309403. *, $p < 0.05$ and **, $p < 0.01$ compared to vehicle controls (n = 3-5).

A

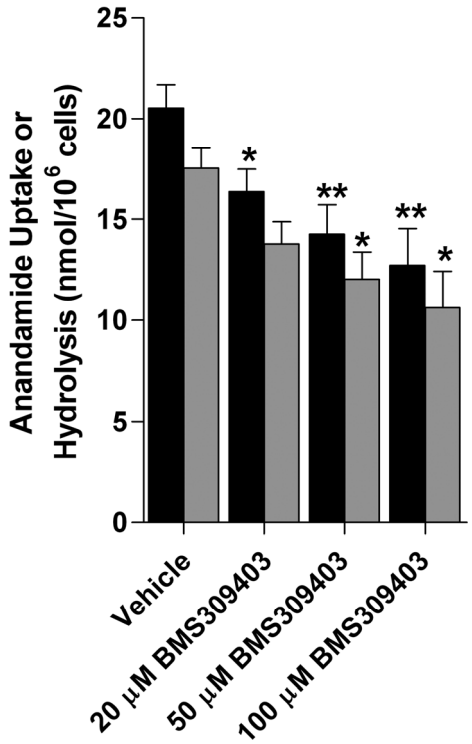
Anandamide Uptake or Hydrolysis (nmol/10^6 cells)
25
20
15
10
5
0
*
**
*
**
*
Vehicle
20 μM BMS309403
50 μM BMS309403
100 μM BMS309403

B

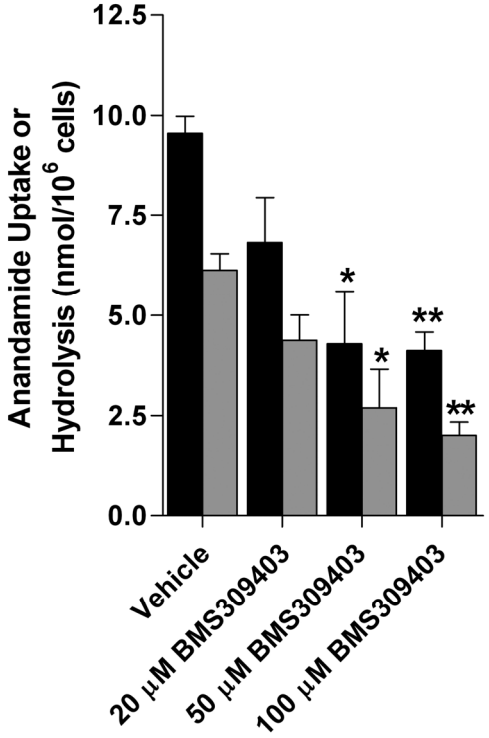
Anandamide Uptake or Hydrolysis (nmol/10^6 cells)
12.5
10.0
7.5
5.0
2.5
0.0
*
*
**
**
Vehicle
20 μM BMS309403
50 μM BMS309403
100 μM BMS309403

Figure 17. Inhibition of anandamide uptake and inactivation by BMS309403 is preserved in pretreated cells. [^{14}C]anandamide uptake (black bars) and hydrolysis (grey bars) at 5 min were significantly reduced in COS7-FAAH-eGFP cells following pre-incubation and co-incubation with 50 μM BMS309403 as well as in cells following a pre-incubation only. **, $p < 0.01$ compared to vehicle controls ($n = 3$).

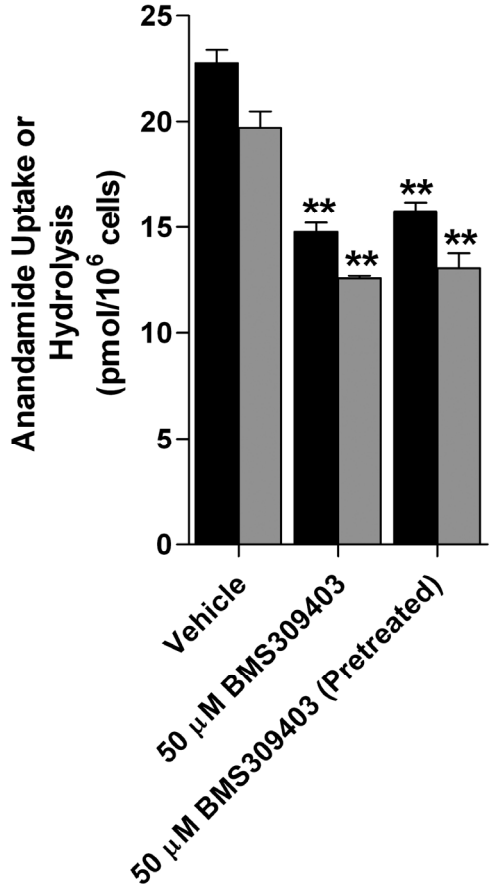
Anandamide Uptake or Hydrolysis (pmol/10^6 cells)
25
20
15
10
5
0
**
**
**
**
Vehicle
50 μM BMS309403
50 μM BMS309403 (Pretreated)

Figure 18. Effect of BMS309403 upon intracellular anandamide hydrolysis at 3 sec. BMS309403 (20-100 μM) reduced the hydrolysis of [^{14}C]anandamide following uptake in (A) COS7-FAAH-eGFP or (B) N18TG2 cells. *, $p < 0.05$ and **, $p < 0.01$ compared to vehicle treated controls (n = 3-5).

A

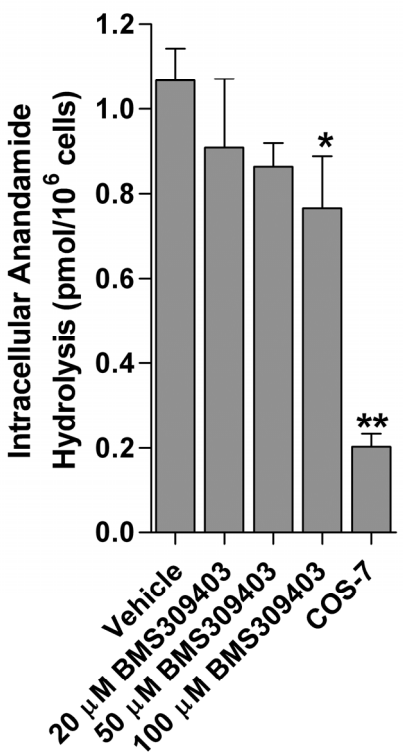
Intracellular Anandamide Hydrolysis (pmol/10^6 cells)
1.2
1.0
0.8
0.6
0.4
0.2
0.0
*
**
Vehicle
20 μM BMS309403
50 μM BMS309403
100 μM BMS309403
COS-7

B

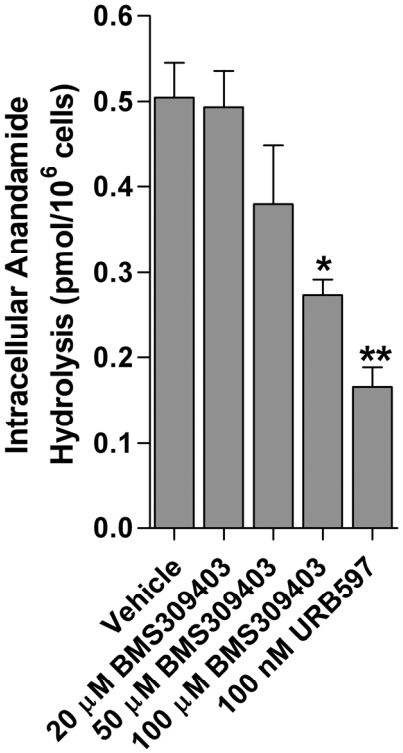
Intracellular Anandamide Hydrolysis (pmol/10^6 cells)
0.6
0.5
0.4
0.3
0.2
0.1
0.0
*
**
Vehicle
20 μM BMS309403
50 μM BMS309403
100 μM BMS309403
100 nM URB597

Figure 19. Effect of BMS309403 and oleic acid upon FAAH activity *in vitro*. [^{14}C]anandamide hydrolysis by (A) COS7-FAAH-eGFP or (B) N18TG2 homogenates was not inhibited ($p>0.05$) by 100 μM oleic acid or BMS309403 ($n = 3$).

A

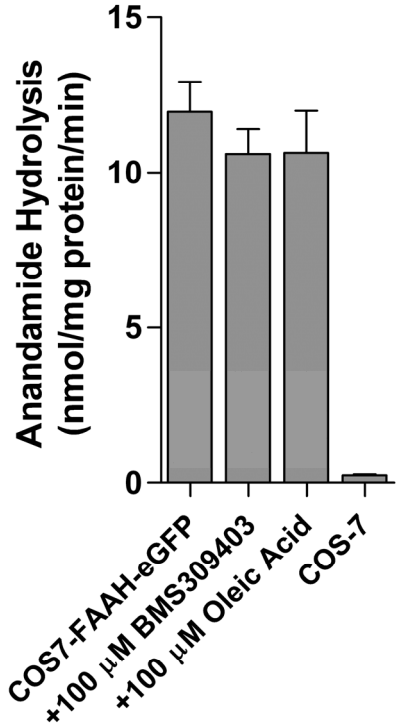
Anandamide Hydrolysis
(nmol/mg protein/min)
15
10
5
0
COS7-FAAH-eGFP
+100 μM BMS309403
+100 μM Oleic Acid
COS-7

B

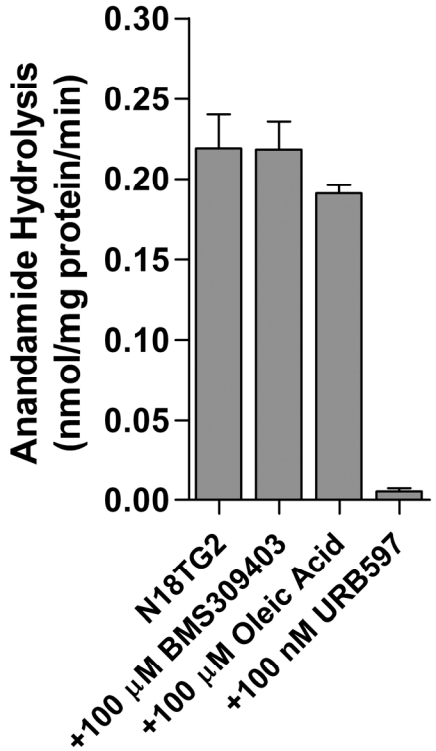
Anandamide Hydrolysis
(nmol/mg protein/min)
0.30
0.25
0.20
0.15
0.10
0.05
0.00
N18TG2
+100 μM BMS309403
+100 μM Oleic Acid
+100 nM URB597

DISCUSSION

Regulation of lipid neurotransmitter signaling poses unique challenges to mammalian systems. In contrast to hydrophilic neurotransmitters, endocannabinoids are hydrophobic and are not stored in synaptic vesicles. Instead, they are generated when needed through a process known as "on demand" synthesis (Hashimotodani*, et al.*, 2007). The transient nature of endocannabinoid signaling requires efficient synthetic enzymes and a mechanism(s) for rapid ligand clearance and inactivation. The presence of cannabinoid receptors on the plasma membrane and FAAH on the ER ensures that sites of anandamide signaling are spatially separated from its site of catabolism. The low solubility of anandamide in the hydrophilic cytosol presents a diffusional barrier and suggests that intracellular proteins may facilitate its trafficking from the plasma membrane to FAAH (Deutsch*, et al.*, 2001, Patricelli and Cravatt, 2001). Despite years of intense effort, proteins mediating anandamide trafficking have not been identified. Herein, FABPs are identified as the first proteins capable of intracellularly transporting anandamide.

The hydrophilic cytoplasm also presents a diffusional barrier to the transport of free fatty acids. To obviate this, intracellular proteins such as FABPs orchestrate the movement of fatty acids inside cells (Furuhashi and Hotamisligil, 2008, Stremmel*, et al.*, 2001). The wide distribution of FABPs throughout the mammalian brain and peripheral tissues (Liu*, et al.*, 2008, Owada*, et al.*, 1996, Pelsers*, et al.*, 2004) suggests that these proteins may represent the primary repertoire of intracellular fatty acid and endocannabinoid carriers.

The data presented herein are in line with the hypothesis that binding proteins such as FABPs act as intracellular anandamide transporters. The rapid and organelle non-specific delivery of anandamide to FAAH is consistent with trafficking via FABPs. Overexpression of FABP5 and FABP7, but not FABP3, enhanced the uptake and hydrolysis of anandamide, suggesting that these proteins may bind anandamide with greater affinity than FABP3. This is consistent with a recent report demonstrating that anandamide binds FABP7 with a three-fold higher affinity than FABP3 (IC_{50} values of 5 vs. 15 μM, respectively), as judged by displacement of a fluorescent probe (Sun*, et al.*, 2008). Similar displacement values were observed for arachidonic acid. The inability of FABP3 to potentiate anandamide inactivation is somewhat surprising given that brain uptake of arachidonic acid was significantly reduced in FABP3 KO mice (Murphy*, et al.*, 2005). This suggests that intracellular transport of arachidonic acid and endocannabinoids may be functionally uncoupled or that FABP3 may serve as a lower affinity auxiliary carrier for the endocannabinoids.

The importance of FABPs as anandamide carriers was further demonstrated through inhibition studies. Both oleic acid and the selective FABP inhibitor BMS309403 significantly reduced anandamide uptake and hydrolysis in COS7-FAAH-eGFP and N18TG2 cells. Neither oleic acid nor BMS309403 completely blocked anandamide uptake, reflecting incomplete FABP inhibition, non-specific binding to BSA or other cellular proteins, or other unknown inhibitor-insensitive anandamide carriers.

The involvement of FABPs as intracellular anandamide carriers may resolve several unexplained phenomena of anandamide uptake. For example, all cells, including those devoid of a functional endocannabinoid system, possess the ability to internalize

anandamide and deliver it to FAAH following transfection with FAAH. Therefore, it is likely that the capability of many cell-types to take up anandamide may coincide with the expression of FABPs. Another unresolved phenomenon involves the efficacy of anandamide "transport" inhibitors, which were designed as inhibitors of a putative anandamide membrane transporter. Since most of these compounds are structural analogs of anandamide (Alexander and Cravatt, 2006, Dickason-Chesterfield*, et al.*, 2006, Fegley*, et al.*, 2004, Ortar*, et al.*, 2003), it is likely that their efficacy may reflect inhibition of FABPs and/or other unidentified intracellular anandamide carriers (Glaser*, et al.*, 2003, Hillard and Jarrahian, 2003, Kaczocha*, et al.*, 2006, Ortega-Gutierrez*, et al.*, 2004).

The binding promiscuity of FABPs suggests that they may also serve as carriers for other NAEs such as PEA and OEA, and the endocannabinoid 2-AG. In addition, FABPs may also shuttle these lipids to the nucleus. A recent report revealed that FABP5 mediates the nuclear translocation of retinoic acid and enhances its activation of nuclear PPAR receptors (Schug*, et al.*, 2007). This finding is intriguing since endocannabinoids and related NAEs have all been shown to varying extents to activate PPAR receptors (Bouaboula*, et al.*, 2005, Fu*, et al.*, 2003, Lo Verme*, et al.*, 2005, Rockwell*, et al.*, 2006). Indeed, it was recently reported that FABPs may potentiate NAE-mediated activation of nuclear PPARs (Sun*, et al.*, 2008).

In conclusion, the results presented herein represent a major advance in our understanding of endocannabinoid inactivation. Prior to these findings, it was not known how hydrophobic endocannabinoids traverse the aqueous cytosol for their inactivation. In addition to providing a mechanism for anandamide uptake, FABPs may also represent

attractive therapeutic targets. For example, inhibition of FABPs abrogates diet-induced insulin resistance and diabetes, and ameliorates atherosclerosis (Furuhashi*, et al.*, 2007, Furuhashi*, et al.*, 2008, Hotamisligil*, et al.*, 1996, Maeda*, et al.*, 2005). These favorable outcomes coupled with the anti-inflammatory and analgesic phenotypes of FAAH KO mice suggest that a therapeutic strategy targeting both of these systems may be desirable.

CHAPTER 2

BIOCHEMICAL CHARACTERIZATION OF FAAH-2

SUMMARY

NAEs constitute a functionally diverse family of signaling molecules that includes anandamide. Spatiotemporal regulation of NAE signaling relies upon the expression, localization, and activity of synthetic and catabolic enzymes. FAAH is the principal enzyme that mediates NAE inactivation *in vivo* since FAAH KO mice possess highly elevated NAE levels and are hypersensitive to NAE administration. Recently, a novel FAAH enzyme (FAAH-2) was discovered in higher mammals that is not found in murid genomes, suggesting that NAE inactivation in higher mammals may be coordinated by both FAAH enzymes. Similar to FAAH, FAAH-2 is a membrane protein of the amidase signature family of serine hydrolases and hydrolyzed numerous NAE substrates *in vitro*. FAAH-2 was proposed by others to reside on the luminal surface of ER membranes. Its role in NAE inactivation in intact cells and its subcellular localization were not examined.

To explore the role of FAAH-2 in NAE inactivation, a thorough biochemical analysis of the enzyme was performed. FAAH-2 catalyzed anandamide and PEA hydrolysis with rates approximately 10 to 30 fold lower than FAAH *in vitro*. However, FAAH-2 hydrolyzed anandamide and PEA with rates approximately one third that of

FAAH in intact cells, indicating its physiological relevance. The novel observation was made that FAAH-2 localized primarily to cytoplasmic lipid droplets. FAAH-2 chimeras attaining cytoplasmic or luminal membrane orientations lacked activity, suggesting that FAAH-2 is adapted to enzymatic catalysis on lipid droplet membranes. The N-terminus of FAAH-2 was identified as a lipid droplet targeting sequence and was both necessary and sufficient to mediate lipid droplet localization. Lastly, a FAAH chimera localizing to lipid droplets hydrolyzed anandamide in intact cells with rates comparable to wild-type FAAH, suggesting that NAEs are readily delivered to lipid droplets for catabolism. Collectively, these data support a model in which FAAH and FAAH-2 both mediate NAE inactivation and suggest that sites of NAE catabolism are spatially separated in cells of higher mammals.

INTRODUCTION

A. NAE Inactivation by FAAH.

NAEs constitute a family of signaling lipids that activate distinct receptor systems. The endocannabinoid anandamide serves as a ligand for plasma membrane CB1 and TRPV1 receptors (Felder*, et al.*, 1993, Zygmunt*, et al.*, 1999) while PEA and OEA activate nuclear PPARα receptors (Fu*, et al.*, 2003, Lo Verme*, et al.*, 2005). Despite their distinct molecular targets, NAEs share a common catabolic enzyme, FAAH. FAAH is expressed in most mammalian tissues, including brain, spinal cord, liver, retina, small intestine, ovary, spleen, but not in heart or muscle (Deutsch and Chin, 1993; Cravatt*, et al.*, 2001, Cravatt*, et al.*, 2004, El-Talatini*, et al.*, 2009, Fu*, et al.*, 2007, Glaser*, et al.*, 2005, Wei*, et al.*, 2006, Yazulla*, et al.*, 1999). The wide distribution of FAAH suggests a primary role for this enzyme in NAE inactivation. FAAH KO mice possess significantly elevated levels of NAEs including anandamide and PEA, and display CB1-mediated antinociceptive and PPAR-dependent anti-inflammatory phenotypes (Cravatt*, et al.*, 2001, Cravatt*, et al.*, 2004, Lo Verme*, et al.*, 2005). These results establish FAAH as the principal NAE catabolizing enzyme *in vivo*.

B. FAAH-2 as a Second NAE Hydrolyzing Amidase Signature Enzyme.

A novel amidase signature serine hydrolase capable of metabolizing NAEs was recently cloned from human cells (Wei*, et al.*, 2006). This enzyme, termed FAAH-2, only shares ~20% sequence identity along its primary structure with FAAH, with high conservation around the catalytic triad (Figure 20). Both enzymes possess a predicted N-terminal transmembrane helix, an amidase signature sequence, and a Ser-Ser-Lys

catalytic triad (Figure 20). Similar to FAAH, FAAH-2 is a membrane protein with a pH optimum of 9, and it hydrolyzes numerous NAEs including anandamide and PEA (Wei*, et al.*, 2006). However, FAAH-2 metabolizes these lipids with lower rates than FAAH *in vitro*, hydrolyzing anandamide and PEA respectively with a V_{max} of 0.46 and 0.2 nmol/mg/min compared to 17 and 2.1 nmol/mg/min for FAAH (Wei*, et al.*, 2006). In contrast to the cytoplasmically-facing FAAH, FAAH-2 appears to reside in luminal membrane compartments and is not subject to N-linked glycosylation. RT-PCR analysis revealed that FAAH-2 is expressed in human heart, kidney, liver, lung, prostate, and ovary. Finally, FAAH-2 is found in the genomes of humans and other primates, and in other species including opossum, frog, zebrafish, pufferfish, and chicken. The FAAH-2 gene resides on the pericentromeric region of the short arm of the X-chromosome, a region prone to rearrangements and deletions, possibly explaining the absence of this enzyme in murid genomes (Wei*, et al.*, 2006).

Apart from this preliminary characterization of FAAH-2, nothing is known about other features of this enzyme, including its subcellular localization and its ability to inactivate NAEs in intact cells. The goal of this project was to perform a full biochemical investigation of FAAH-2.

Figure 20. Sequence comparison of FAAH and FAAH-2. The amidase signature sequences of both enzymes are underlined, the predicted N-terminal transmembrane helices are marked with dashed lines, and the Ser-Ser-Lys catalytic triads are marked with asterisks. Conserved residues are shown in black color. Figure adapted from (Wei*, et al.*, 2006).

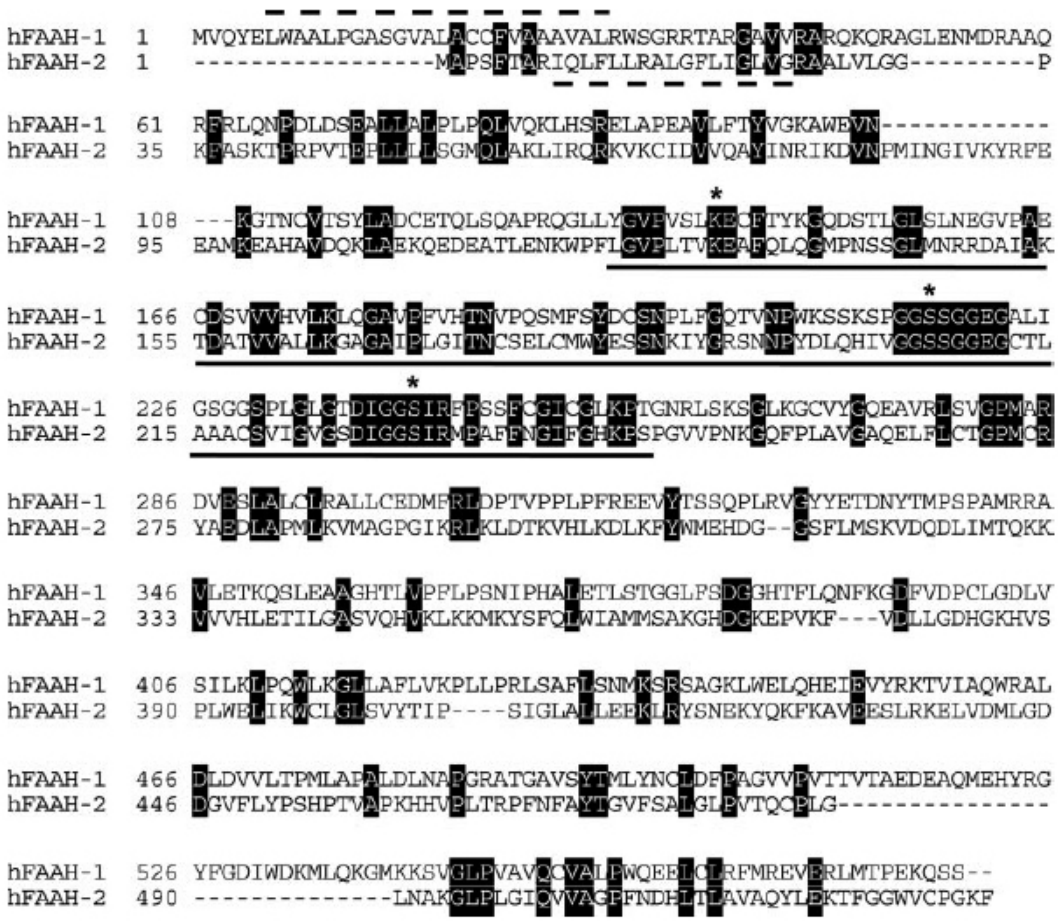

MATERIALS AND METHODS

Materials. Anandamide and PEA were from Cayman Chemical (Ann Arbor, MI). URB597 (cyclohexylcarbamic acid 3'-carbamoyl-biphenyl-3-yl ester) was from Biomol International. [^{14}C]anandamide [ethanolamine-1-^{14}C] (53 mCi/mmol) and [^{14}C]PEA [ethanolamine-1-^{14}C] (53 mCi/mmol) were from the National Institute on Drug Abuse Drug Supply Program. BSA was from Sigma. BODIPY 493/503 was from Molecular Probes (Carlsbad, CA).

Cloning. FAAH-2 cDNA was kindly provided by Benjamin F. Cravatt (The Scripps Research Institute). The FAAH-2 cDNA provided to us differed from the published sequence in three positions as follows: T99C, G1077A, and C1404T. These changes did not alter the corresponding amino acid sequence of FAAH-2. To generate FLAG-tagged FAAH-2, a FLAG epitope was incorporated into the C-terminus of FAAH-2 using PCR and the appropriate primers and was subcloned into pcDNA4 using *XhoI* and *KpnI*. To generate Myc-tagged FAAH-2, the FAAH-2 cDNA (lacking a stop codon) was inserted into the pcDNA4/TO/myc-HisA plasmid (Clontech) using *XhoI* and *KpnI*. To generate CAL-ΔTMFAAH2-FLAG, the N-terminus of FAAH-2 was replaced by the mouse calreticulin signal sequence (1-26). CAL-ΔTMFAAH-FLAG was generated by fusion of the calreticulin signal sequence to the N-terminus of ΔTMFAAH-FLAG. FAAH(N)-ΔTMFAAH2-FLAG contains the N-terminus of human FAAH (residues 1-32). MΔTMFAAH2-FLAG contains residues 35-532 of FAAH-2 and an N-terminal methionine. CAL-ΔTMFAAH2(2-532)-FLAG was produced by replacing the first methionine of FAAH2-FLAG with the calreticulin signal sequence. FAAH2(N)-RFP and FAAH2(N)-rΔTMFAAH-FLAG contain the N-terminus of FAAH-2 (residues 1-35)

fused to the N-terminus of DsRed2 or rat ΔTMFAAH (residues 30-579), respectively. To generate a secreted form of FABP3, the FABP3 cDNA was subcloned into the pSecTag2/Hygro C plasmid using *HindIII* and *XhoI*. The expression plasmid for ADRP was a kind gift from Deborah A. Brown (Stony Brook University). All constructs were confirmed by sequencing.

Immunofluorescence. Immunolocalization experiments were performed as in Chapter 1. The antibodies used were as follows: rabbit anti-calreticulin (1:200) (Affinity Bioreagents, Golden, CO), mouse anti-FLAG M2 (1:500) (Sigma), and mouse anti-Myc (1:500) (provided by Jen-Chih Hsieh, Stony Brook University). To visualize neutral lipids, COS-7 or HeLa cells were respectively incubated with 1 or 2 μg/ml BODIPY 493/503 during secondary antibody incubations.

Western blotting. Western blot analysis was performed as in Chapter 1. The following antibodies were used: mouse anti-FLAG M2 (1:2000), mouse anti-β actin (1:20000) (Abcam, Cambridge, MA), mouse anti-FABP3 (1:100) (Abcam, Cambridge, MA) and mouse anti-Myc (1:5000). The blots were subsequently probed with goat anti-mouse IgG HRP-conjugated antibodies (1:8000) (Molecular Probes, Eugene, OR) and visualized on film.

Enzyme assays. COS-7 or HeLa homogenates, transfected with the indicated construct, were incubated with [^{14}C]anandamide or [^{14}C]PEA (0.1-100 μM) in 100 mM Tris (pH 9) supplemented with 0.1% BSA at 37^{o}C. Incubation times and protein concentrations were adjusted to allow approximately 10-15% substrate conversion. For pH studies, incubations were performed in 50 mM Bis-Tris Propane, 50 mM CAPS, 50 mM citrate, 150 mM NaCl (pH range 5 to 9). The reactions were terminated by addition of two

volumes of 1:1 chloroform:methanol and the phases separated by centrifugation. The methanol phase containing [^{14}C]ethanolamine was counted in a Beckman LS 6500 scintillation counter.

PNGase F treatment of cells. COS-7 cells transfected with the indicated plasmids were homogenized with a 26-guage needle and the resulting homogenates centrifuged for 10 min at 1000g to pellet unbroken cells. The supernatants were denatured by heating for 10 min at 100^{o}C and subsequently treated with PNGase F for 1 hour at 37^{o}C in the presence of 1% NP-40 (New England Biolabs, Ipswich, MA). The samples were then separated by SDS-PAGE and visualized with mouse anti-FLAG or mouse anti-β actin antibodies.

Protein secretion into the media. HeLa cells were transfected with the indicated plasmids. Twenty four hours later, the media were replaced with serum-free OptiMEM media (Invitrogen, Carlsbad, CA) for 12 hours. The media were subsequently collected and centrifuged for 10 min at 1000g to pellet cellular debris. Proteins in the media were precipitated with acetone. Following incubation with 80% acetone for 60 min at -20^{o}C, the media were centrifuged at 13,000g for 10 min and the pellets containing precipitated proteins dried and resuspended in water. The samples were subsequently denatured with SDS-loading buffer and resolved by SDS-PAGE.

Lipid droplet isolation. HeLa cells grown in 10 cm dishes were co-transfected with the indicated plasmids and ADRP using Lipofectamine 2000. Five hours later, the media were replaced with DMEM supplemented with 10% fetal bovine serum and 400 μM oleic acid complexed to BSA (oleic acid to BSA ratio of 6.6:1) and incubated overnight as described (Listenberger*, et al.*, 2007). Cells fed overnight with oleic acid accumulate neutral lipids and possess enlarged lipid droplets. Three plates of FAAH2-FLAG, one

plate of FAAH-FLAG and two plates of FAAH2(N)-rΔTMFAAH-FLAG transfected cells were homogenized in 10 mM Hepes/5 mM EDTA containing 10% sucrose and protease inhibitor cocktail (Roche Applied Science), and centrifuged at 1000g to pellet unbroken cells. The resulting supernatant (700 µl) was overlaid with ~ 4.3 ml of 10 mM Hepes/5 mM EDTA and spun in a Beckman L8-55 centrifuge at 280,000g for 3 hrs at 4^{o}C. Fractions (~700 µl) were collected from the top and the pellet was resuspended in Hepes buffer. The samples were separated by SDS-PAGE and immunoblotted with rabbit anti-calnexin (1:5000) (Novus Biologicals, Littleton, CO), mouse anti-FLAG (1:2000), or guinea pig anti-ADRP antibodies (1:400) (RDI Division of Fitzgerald Industries, Concord, MA). The blots were subsequently incubated with goat anti-mouse, goat anti-rabbit, or rabbit anti-guinea pig IgG HRP-conjugated antibodies (1:8000) (Molecular Probes, Eugene, OR) and visualized on film.

Statistical analysis. All results represent means ± standard error of at least three independent experiments. Statistical analyses were performed using two tailed unpaired Student's *t* tests with Graphpad Prism.

RESULTS

A. Kinetic analysis of FAAH-2.

The enzyme kinetics of FAAH-2 were examined in homogenates of HeLa cells expressing FAAH-2 using [^{14}C]anandamide or [^{14}C]PEA as substrates. The V_{max} and K_m for anandamide were 0.71 ± 0.04 nmol/mg/min and 7.9 ± 1.5 μM, respectively. For PEA, the V_{max} and K_m values were 1.21 ± 0.1 nmol/mg/min and 4.3 ± 1.4 μM, respectively (Figure 21). FAAH-2 attained maximum activity at a pH of 9 (Figure 22), confirming previous results (Wei*, et al.*, 2006).

B. Uptake and hydrolysis of anandamide and PEA by FAAH-2 in cultured cells.

Uptake and hydrolysis assays determined the contribution of FAAH-2 towards anandamide and PEA inactivation in cells. A time course of [^{14}C]anandamide uptake and hydrolysis revealed that HeLa cells expressing FAAH hydrolyzed ~74% of the [^{14}C]anandamide taken up by cells at 1 min and ~85% at 5 min (Figure 23A). FAAH-2 transfected cells hydrolyzed ~29% of the [^{14}C]anandamide taken up by cells at 1 min and ~61% at 5 min. [^{14}C]anandamide uptake was significantly reduced in FAAH-2 transfected cells at 5 min. Mock transfected cells hydrolyzed ~7% and ~8% of the anandamide taken up by cells at 1 and 5 min, respectively. To examine anandamide hydrolysis using more physiologically relevant time points, these experiments were repeated at 3 sec. Similar to the results above, intracellular anandamide hydrolysis in FAAH-2 expressing cells was significantly lower compared to cells transfected with FAAH (Figure 23B). Following subtraction of mock transfected cells, the data revealed that FAAH-2 hydrolyzed anandamide with a rate approximately one third that of FAAH.

PEA hydrolysis by FAAH and FAAH-2 followed a similar trend. FAAH-2 hydrolyzed ~29% and ~59% of the [^{14}C]PEA take up by cells at 1 and 5 min, respectively (Figure 24A). As expected, [^{14}C]PEA metabolism was greater in cells transfected with FAAH, with ~60% and ~77% hydrolysis at 1 and 5 min, respectively. [^{14}C]PEA hydrolysis in mock transfected cells was lower, reaching ~7% and 11% at 1 and 5 min, respectively. It is noteworthy that in contrast to anandamide, PEA uptake does not appear to be coupled to its hydrolysis by FAAH (Jacobsson and Fowler, 2001). Similar results were obtained in this study (Figure 24A). One possible explanation is that PEA is sequestered intracellularly and is not in equilibrium with extracellular PEA. Similar to anandamide, [^{14}C]PEA hydrolysis at 3 sec was significantly lower in cells expressing FAAH-2 compared to FAAH (Figure 24B). Following subtraction of [^{14}C]PEA metabolism in mock transfected cells, FAAH-2 hydrolyzed [^{14}C]PEA with a rate ~40% that of FAAH. Collectively, these data provide evidence that FAAH-2 is an efficient NAE hydrolyzing enzyme in intact cells.

C. Subcellular localization of FAAH-2.

The subcellular localization of FAAH-2 was examined by immunofluorescence. In COS-7 and HeLa cells, FAAH2-FLAG localized to ring-like, hollow cytoplasmic structures that did not overlap with the ER marker calreticulin (Figure 25). In addition, a small pool of ER-localized FAAH2-FLAG was also observed in COS-7 cells but rarely seen in HeLa cells. Typically, there were two distinct populations of COS-7 cells, with ~40% of cells expressing FAAH-2 solely in the cytoplasmic structures and the remaining ~60% in these structures and ER membranes.

These cytoplasmic structures are morphologically similar to lipid droplets/adiposomes (Smirnova*, et al.*, 2006), which possess a core of neutral lipids surrounded by a phospholipid monolayer, and serve as sites of triglyceride and cholesteryl ester storage and mobilization (Thiele and Spandl, 2008). The neutral lipid/lipid droplet-specific dye BODIPY 493/503 was employed to determine whether FAAH-2 localized to adiposomes (Listenberger*, et al.*, 2007). In COS-7 and HeLa cells, FAAH2-FLAG and FAAH2-Myc co-localized with BODIPY 493/503 (Figure 26A). These results confirm that FAAH-2 is present on lipid droplets and that its subcellular distribution is independent of the epitope tag and cell-type used. In accordance with the lipid droplet hypothesis, FAAH-2 was present solely on the ring-like surface of adiposomes (presumably phospholipid monolayers) and was excluded from BODIPY493/503-positive neutral lipid cores (Figure 26B) (Tauchi-Sato*, et al.*, 2002). In contrast to FAAH-2, FAAH-FLAG did not localize to lipid droplets (Figure 27).

The presence of FAAH-2 on lipid droplets was confirmed by subcellular fractionation. HeLa cells were co-transfected with either FAAH-FLAG or FAAH2-FLAG and the lipid droplet-localized protein ADRP, cultured in media supplemented with oleic acid, and subsequently fractionated by ultracentrifugation (Listenberger*, et al.*, 2007). Following ultracentrifugation, fractions were collected from the top. The separation of lipid droplets from ER membranes was confirmed by the distribution of ADRP to fraction 1 and the ER marker calnexin to fraction 7 and the pellet (Figure 28). FAAH2-FLAG was found primarily in the ADRP-positive fraction 1 but not in calnexin-positive fractions, suggesting that the minor ER-localized pool of FAAH-2 present under normal conditions may have redistributed to lipid droplets following oleate feeding of cells. As

expected, FAAH-FLAG distributed solely to the calnexin-positive pellet and was excluded from lipid droplets. Taken together, the fractionation and immunofluorescence results confirm that FAAH-2 localizes primarily to lipid droplets.

D. Generation of cytoplasmically- and luminally-facing FAAH-2 variants.

The localization of FAAH-2 to the lipid droplet surface suggests that this monotopic enzyme faces the cytosol and is not localized in the ER. FAAH-2 does not undergo N-linked glycosylation despite possessing a consensus N-linked glycosylation site, suggesting that it may not reside in luminal membrane compartments (Figure 29). However, it was previously proposed that FAAH-2 attains a luminal membrane orientation (Wei*, et al.*, 2006). To resolve these seemingly contradictory results, cytoplasmically- and luminally/ER-facing FAAH-2 variants were generated and their subcellular localizations and *in vitro* activities examined. FAAH-2 is predicted to possess an N-terminal signal sequence for insertion into the ER lumen (Wei*, et al.*, 2006). To localize FAAH-2 to the cytoplasmic face of membranes, the putative signal sequence of FAAH-2 (residues 1-34) was removed and either replaced with the N-terminus (residues 1-32) of FAAH (generating FAAH(N)-ΔTMFAAH2-FLAG) or left without an N-terminal transmembrane sequence (generating MΔTMFAAH2-FLAG) (see Appendix). To localize FAAH-2 to the ER lumen, the signal sequence from mouse calreticulin (Fliegel*, et al.*, 1989) was fused to the N-terminus of ΔTMFAAH2-FLAG, generating CAL-ΔTMFAAH2-FLAG.

Protease protection analysis of membrane fractions revealed that FAAH(N)-ΔTMFAAH2-FLAG and MΔTMFAAH2-FLAG were present on the cytoplasmic face of

membranes while CAL-ΔTMFAAH2-FLAG was luminally facing (Figure 30). The membrane (non-lipid droplet) associated fraction of FAAH2-FLAG also displayed a luminally facing orientation, possibly reflecting the minor ER-localized pool of FAAH-2 observed by immunofluorescence.

Western blotting confirmed the successful expression of all constructs (Figure 31A), except CAL-ΔTMFAAH2-FLAG, which was only visible upon significant overexposure of film (compare Figures 30 and 31A). The expression level of FAAH(N)-ΔTMFAAH2-FLAG was similar to FAAH2-FLAG while that of MΔTMFAAH2-FLAG was significantly reduced. This suggests that FAAH-2, unlike FAAH (Patricelli*, et al.*, 1998), requires an N-terminal transmembrane helix for expression. Therefore, the significantly reduced expression of CAL-ΔTMFAAH2-FLAG may have resulted from instability of ΔTMFAAH2-FLAG following cleavage of the calreticulin signal sequence in the ER lumen. However, CAL-ΔTMFAAH2(2-532)-FLAG, a fusion protein that retains the N-terminus of FAAH-2 was also not successfully expressed, excluding instability as a factor for the reduced expression (Figure 31C). The lack of significant expression of CAL-ΔTMFAAH2-FLAG was also not due to secretion of the protein into the media (Figure 32). These data suggest that FAAH-2 does not natively localize to the ER lumen. Enzymatic analysis revealed that FAAH(N)-ΔTMFAAH2-FLAG, MΔTMFAAH2-FLAG, and CAL-ΔTMFAAH2-FLAG were catalytically inactive (Figure 31B), suggesting that FAAH-2 does not normally reside on the cytoplasmic face of ER membranes.

The re-localization of FAAH from the cytoplasmic to luminal face of membranes (CAL-ΔTMFAAH-FLAG), which was confirmed by proteinase K and PNGase F

analysis, did not abrogate its activity (Figures 29, 30 and 31). The reduced enzymatic activity of CAL-ΔTMFAAH-FLAG relative to FAAH mirrored its decline in expression, suggesting that FAAH retains its activity in the ER lumen. These data suggest that some amidase signature serine hydrolases are versatile enzymes, capable of functioning in reducing (cytosol) and oxidizing (ER lumen) environments. Importantly, immunofluorescence revealed that CAL-ΔTMFAAH2-FLAG, CAL-ΔTMFAAH-FLAG, and FAAH(N)-ΔTMFAAH2-FLAG were distributed in perinuclear compartments that did not co-localize with BODIPY493/503 (Figure 33). Collectively, these data suggest that FAAH-2 does not natively reside on the cytoplasmic or luminal faces of the ER and that the N-terminus of FAAH-2 is necessary for productive expression of functional enzyme. Therefore, the subpopulation of luminal FAAH-2 (Figure 30) may represent an intermediate in the translocation of FAAH-2 to cytoplasmic lipid droplets. In this respect, the presence of ER-localized FAAH-2 may reflect inefficient targeting of the overexpressed enzyme to lipid droplets in COS-7 cells.

E. The N-terminus of FAAH-2 is a lipid droplet targeting sequence.

Removal of the N-terminus of FAAH-2 abrogated its activity and lipid droplet localization (Figures 31B and 33), suggesting that it is required for adiposome targeting and the generation of a catalytically competent enzyme. To determine whether the N-terminus of FAAH-2 mediates lipid droplet localization, this sequence was fused to RFP (generating FAAH2(N)-RFP) (see Appendix). In transfected cells, RFP localized to the cytoplasm and nucleus and did not co-localize with BODIPY 493/503 (Figure 34A). In contrast, FAAH2(N)-RFP co-localized with BODIPY 493/503, confirming that the N-

terminus of FAAH-2 is sufficient to mediate lipid droplet localization (Figure 34A). The N-terminus of FAAH-2 was subsequently fused to FAAH (generating FAAH2(N)-rΔTMFAAH-FLAG), resulting in re-localization of this enzyme to lipid droplets in COS-7 and HeLa cells (Figure 34B). Note that rat, rather than human FAAH, was used in these studies since problems were encountered expressing this human FAAH variant. The intracellular distribution of FAAH2(N)-rΔTMFAAH-FLAG to lipid droplets was confirmed by subcellular fractionation (Figure 28). Protease protection analysis revealed that similar to FAAH-2, the membrane associated (non-lipid droplet) pool of FAAH2(N)-rΔTMFAAH-FLAG attained a luminal membrane orientation (Figure 35). Collectively, these results demonstrate that the N-terminus of FAAH-2 serves as a lipid droplet targeting sequence.

F. Anandamide readily diffuses to lipid droplets.

It is currently unclear whether the lower hydrolytic activity of FAAH-2 towards NAEs in intact cells reflects the relatively low expression and activity of the enzyme or reduced delivery of anandamide to lipid droplets. Since anandamide trafficking to lipid droplets likely employs FABPs and/or other cytosolic carriers, it is expected that it is delivered to lipid droplets with similar kinetics as to the ER. To examine this experimentally, HeLa cells were transfected with rFAAH-FLAG or FAAH2(N)-rΔTMFAAH-FLAG. Since rFAAH-FLAG is expressed at a higher level than FAAH2(N)-rΔTMFAAH-FLAG (Figure 36A), its expression was titered down yielding rFAAH-FLAG(low). Western blotting and enzymatic assays confirmed that rFAAH-FLAG(low) and FAAH2(N)-rΔTMFAAH-FLAG were expressed at similar levels (Figure

36A and B). Transport and hydrolysis assays revealed similar rates of anandamide uptake and inactivation between cells expressing rFAAH-FLAG(low) and FAAH2(N)-rΔTMFAAH-FLAG at 1 and 5 min (Figure 37A). Intracellular anandamide hydrolysis following uptake at 3 sec was also similar between cells expressing rFAAH-FLAG(low) and FAAH2(N)-rΔTMFAAH-FLAG (Figure 37B). In contrast, anandamide hydrolysis was significantly reduced in cells expressing FAAH2-FLAG. Taken together, these data confirm that anandamide is delivered to lipid droplets with similar efficiency as the ER, thereby establishing lipid droplets as functional sites of NAE catabolism.

Figure 21. Enzyme kinetics of FAAH-2. HeLa homogenates expressing FAAH-2 were reacted with [^{14}C]anandamide or [^{14}C]PEA (0.1-100 μM). Anandamide was hydrolyzed with a V_{max} and K_m of 0.71 ± 0.04 nmol/mg/min and 7.9 ± 1.5 μM, respectively. PEA was hydrolyzed with a V_{max} and K_m of 1.21 ± 0.1 nmol/mg/min and 4.3 ± 1.4 μM, respectively (n = 7).

A

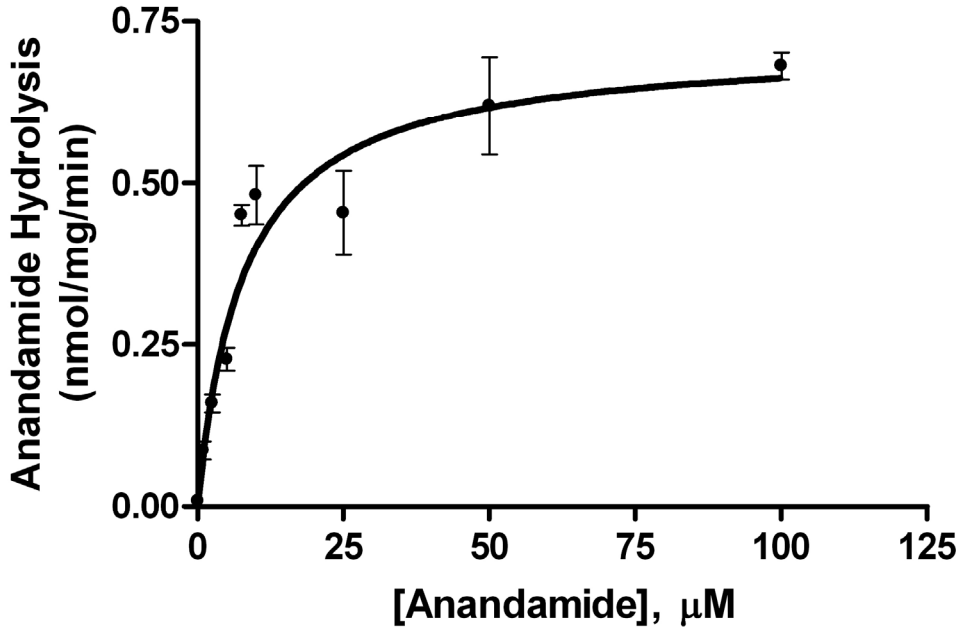
Anandamide Hydrolysis
(nmol/mg/min)
0.75
0.50
0.25
0.00
0
25
50
75
100
125
[Anandamide], μM

B

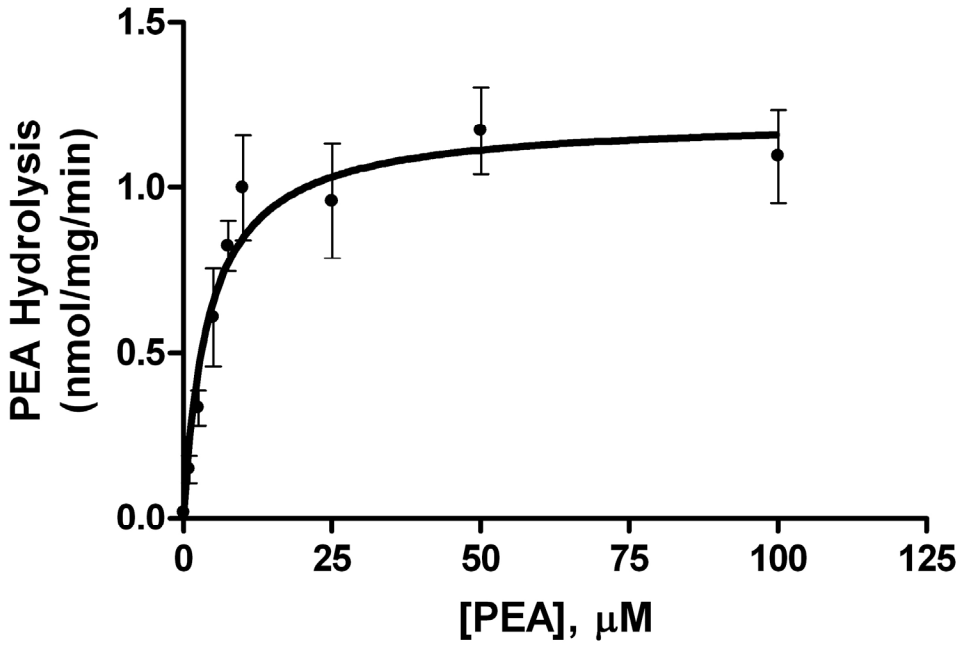
PEA Hydrolysis
(nmol/mg/min)
1.5
1.0
0.5
0.0
0
25
50
75
100
125
[PEA], μM

Figure 22. pH profile of FAAH-2. [^{14}C]anandamide was reacted with homogenates of HeLa cells expressing FAAH-2 in buffers with pH values ranging from 5 to 9. Hydrolysis of [^{14}C]anandamide at different pH values was normalized to activity at pH 9 (n = 3-5).

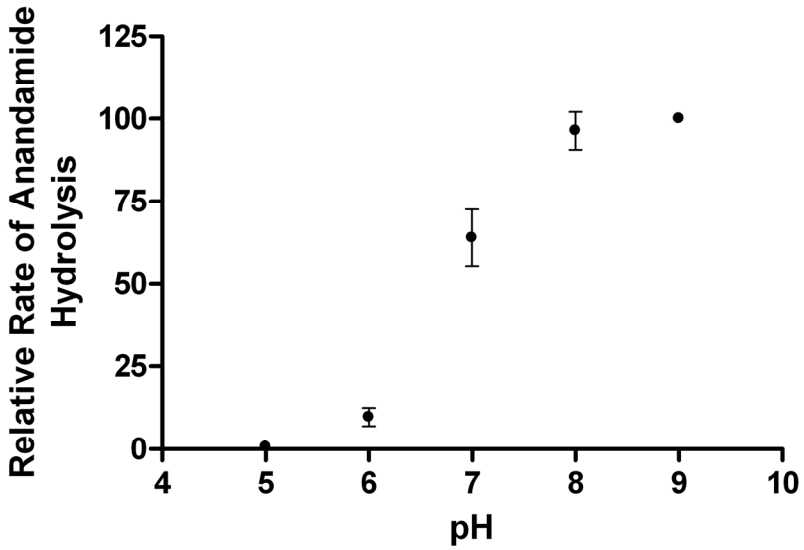
Relative Rate of Anandamide Hydrolysis
125
100
75
50
25
0
4
5
6
7
8
9
10
pH

Figure 23. Uptake and hydrolysis of anandamide in HeLa cells expressing FAAH-2. (A) HeLa cells transfected with FAAH, FAAH-2, or mock controls were incubated with 100 nM [^{14}C]anandamide for 1 or 5 min and uptake (black bars) and hydrolysis (grey bars) determined. *, $p < 0.05$; **, $p < 0.01$; ***, $p < 0.001$ ($n = 3$). (B) Intracellular hydrolysis of [^{14}C]anandamide following uptake at 3 sec. **, $p < 0.01$ ($n = 3$).

A

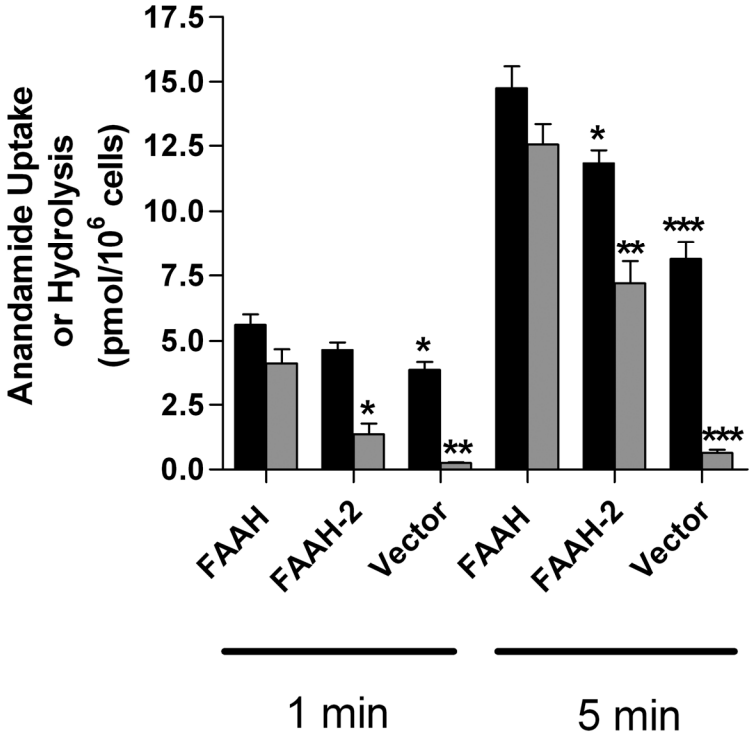
Anandamide Uptake or Hydrolysis (pmol/10^6 cells)
17.5
15.0
12.5
10.0
7.5
5.0
2.5
0.0
*
*
**
*
**
***
***
FAAH
FAAH-2
Vector
FAAH
FAAH-2
Vector
1 min
5 min

B

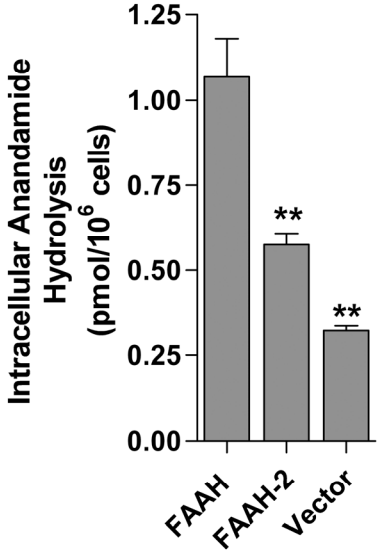
Intracellular Anandamide Hydrolysis (pmol/10^6 cells)
1.25
1.00
0.75
0.50
0.25
0.00
**
**
FAAH
FAAH-2
Vector

Figure 24. Uptake and hydrolysis of PEA in HeLa cells expressing FAAH-2. (A) HeLa cells transfected with FAAH, FAAH-2, or mock controls were incubated with 100 nM [^{14}C]PEA for 1 or 5 min and PEA uptake (black bars) and hydrolysis (grey bar) determined. **, $p < 0.01$ and ***, $p < 0.001$ ($n = 3$). (B) Intracellular hydrolysis of [^{14}C]PEA following uptake at 3 sec. *, $p < 0.05$ and **, $p < 0.01$ ($n = 3$).

A

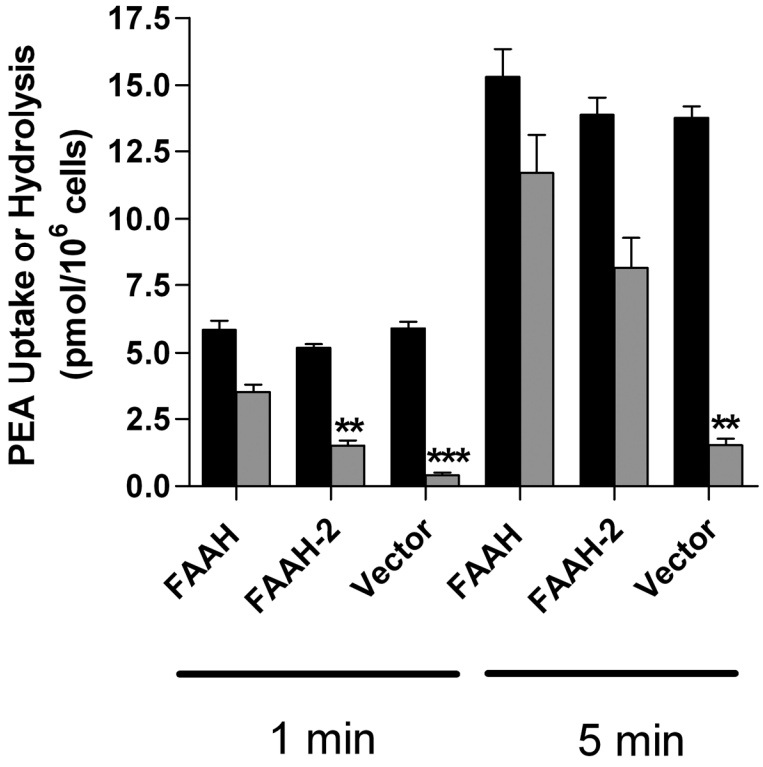
PEA Uptake or Hydrolysis
(pmol/10^6 cells)
17.5
15.0
12.5
10.0
7.5
5.0
2.5
0.0
**
***
**
FAAH
FAAH-2
Vector
FAAH
FAAH-2
Vector
1 min
5 min

B

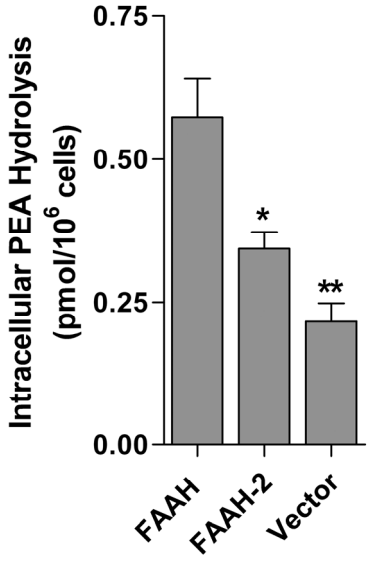
Intracellular PEA Hydrolysis
(pmol/10^6 cells)
0.75
0.50
0.25
0.00
*
**
FAAH
FAAH-2
Vector

Figure 25. Subcellular localization of FAAH2-FLAG in COS-7 and HeLa cells. Cells transfected with FAAH2-FLAG were fixed, permeabilized, and probed with anti-FLAG and anti-calreticulin antibodies. Top panel represents FAAH2-FLAG, middle panel shows calreticulin, and the bottom panel is the merged image.

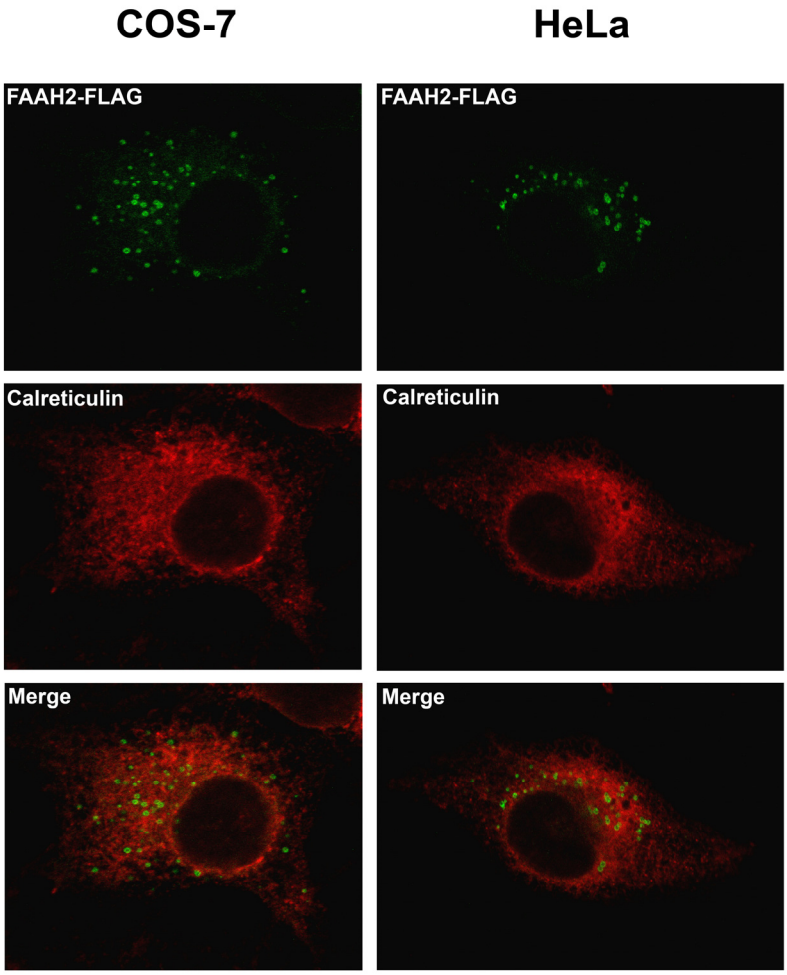
COS-7
HeLa
FAAH2-FLAG
FAAH2-FLAG
Calreticulin
Calreticulin
Merge
Merge

Figure 26. Localization of FAAH-2 to cytoplasmic lipid droplets. (A) Subcellular distribution of FAAH2-FLAG and FAAH2-Myc in COS-7 and HeLa cells. Top panel represents FAAH-2, middle panel shows BODIPY 493/503, and the bottom panel is the merged image. (B) Magnified image of FAAH2-FLAG and BODIPY 493/503 co-localization in HeLa cells.

A

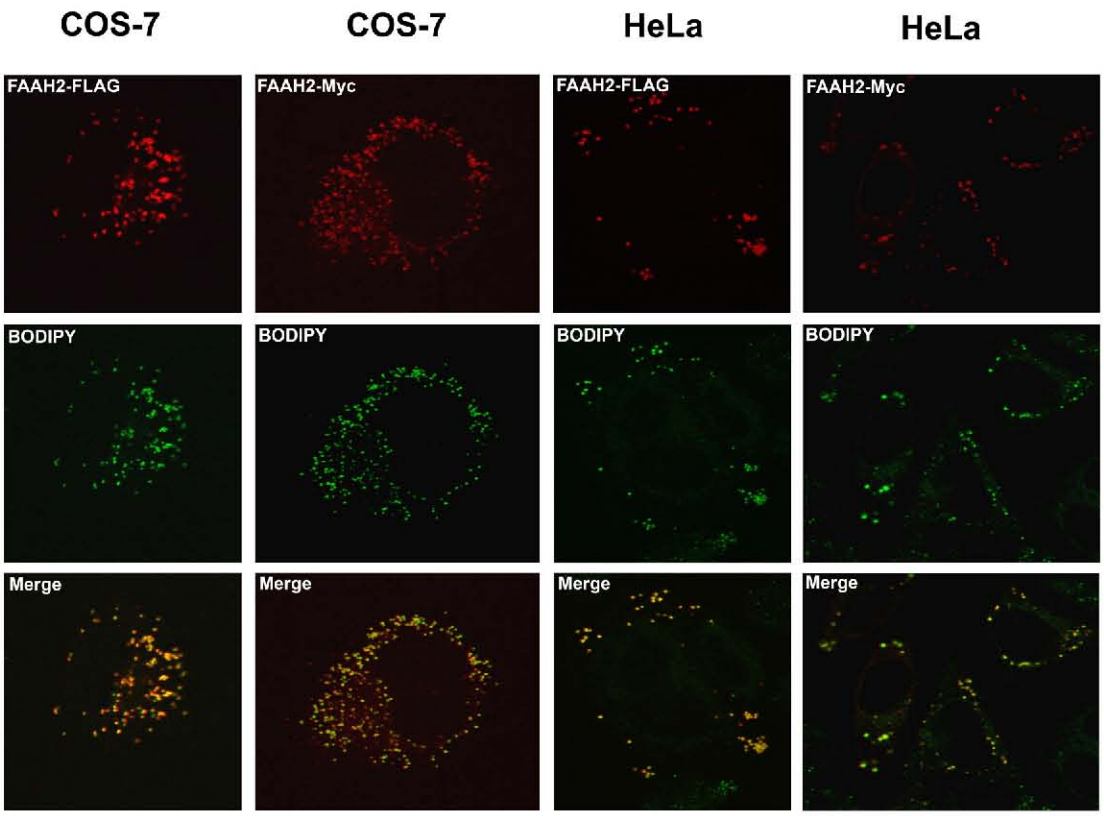
COS-7
COS-7
HeLa
HeLa
FAAH2-FLAG
FAAH2-Myc
FAAH2-FLAG
FAAH2-Myc
BODIPY
BODIPY
BODIPY
BODIPY
Merge
Merge
Merge
Merge

B

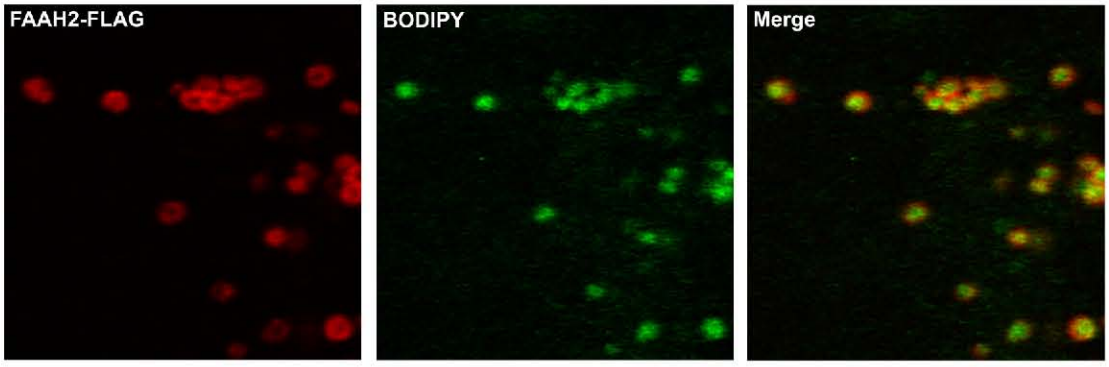
FAAH2-FLAG
BODIPY
Merge

Figure 27. FAAH-FLAG does not reside on lipid droplets. COS-7 or HeLa cells expressing FAAH-FLAG were fixed, permeabilized, and stained with anti-FLAG antibodies and BODIPY 493/503. Top panel shows FAAH-FLAG, middle panel BODIPY 493/503, and the bottom panel the merged image.

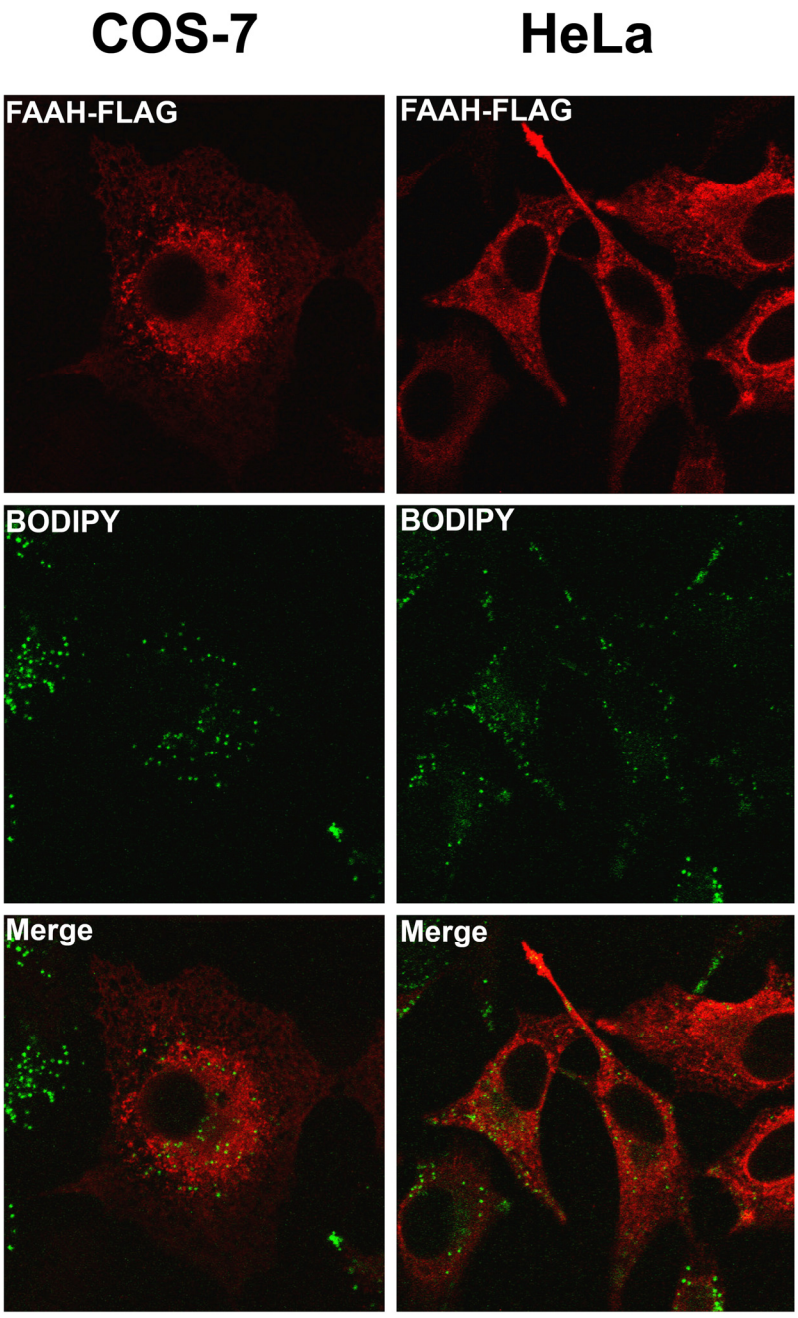
COS-7
HeLa
FAAH-FLAG
FAAH-FLAG
BODIPY
BODIPY
Merge
Merge

Figure 28. SDS-PAGE analysis of FAAH-FLAG, FAAH2-FLAG, and FAAH2(N)-rΔTMFAAH-FLAG localization after subcellular fractionation. HeLa cells were co-transfected with the indicated plasmids and ADRP, and grown overnight in media supplemented 400 μM oleic acid. The cells were harvested and the post-nuclear supernatants subjected to ultracentrifugation. Fractions were collected from the top with fraction 1 corresponding to the floating lipid droplet fraction, P representing the pellet, and S the unfractionated post-nuclear supernatant. The fractions were subsequently acetone precipitated, resolved by SDS-PAGE and probed with anti-FLAG, anti-calnexin, or anti-ADRP antibodies.

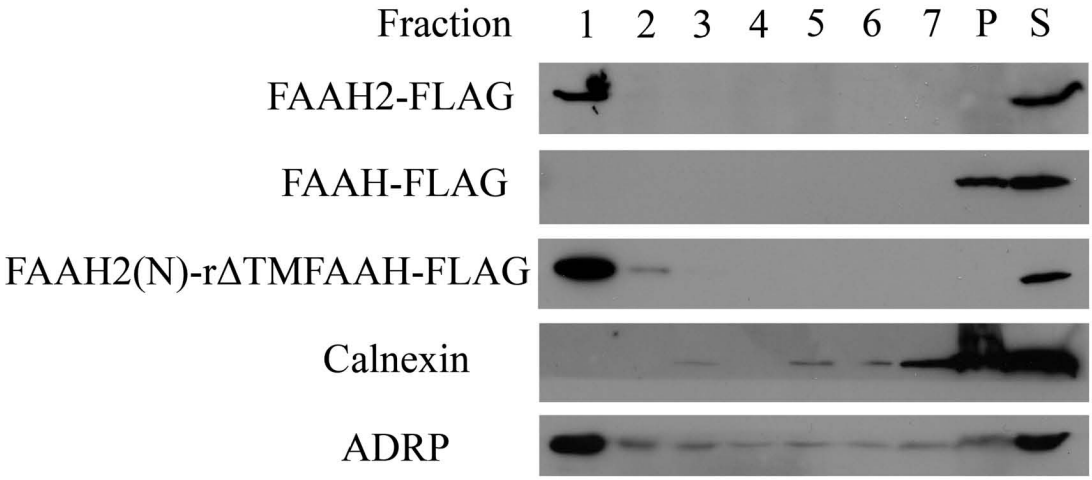
Fraction 1 2 3 4 5 6 7 P S
FAAH2-FLAG
FAAH-FLAG
FAAH2(N)-rΔTMFAAH-FLAG
Calnexin
ADRP

Figure 29. FAAH-2 does not undergo N-linked glycosylation. Post-nuclear supernatants of HeLa cell homogenates expressing the indicated proteins were treated with PNGase F for 1 hr at 37^{o}C, or left untreated. The samples were subsequently resolved by SDS-PAGE and probed with anti-FLAG or anti-β actin antibodies. The luminally oriented CAL-ΔTMFAAH-FLAG serves as a positive control.

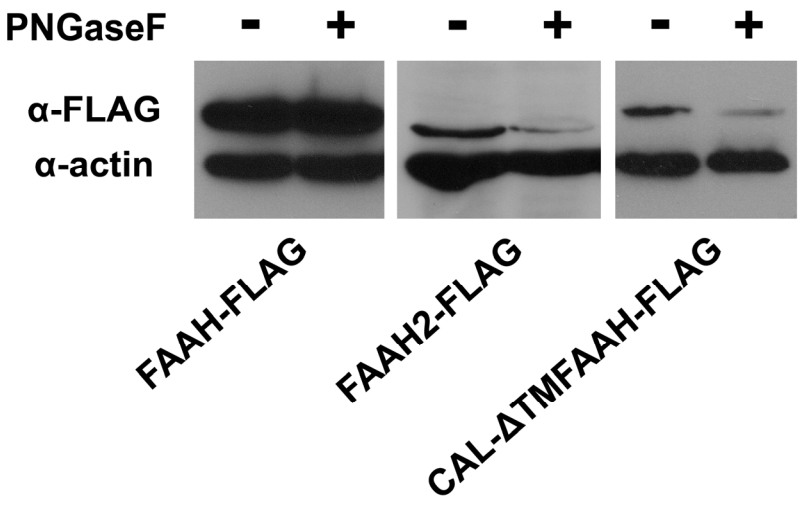
PNGaseF
-
+
-
+
-
+
α-FLAG
α-actin
FAAH-FLAG
FAAH2-FLAG
CAL-ΔTMFAAH-FLAG

Figure 30. Protease protection analysis of FAAH, FAAH-2, and their cytoplasmically- and luminally-oriented variants. Membrane fractions of COS-7 cells transfected with the indicated proteins were reacted with 500 μg/ml proteinase K in the presence or absence of 1% Triton X-100. Control samples were left untreated. The samples were resolved by SDS-PAGE and probed with FLAG and calreticulin antibodies.

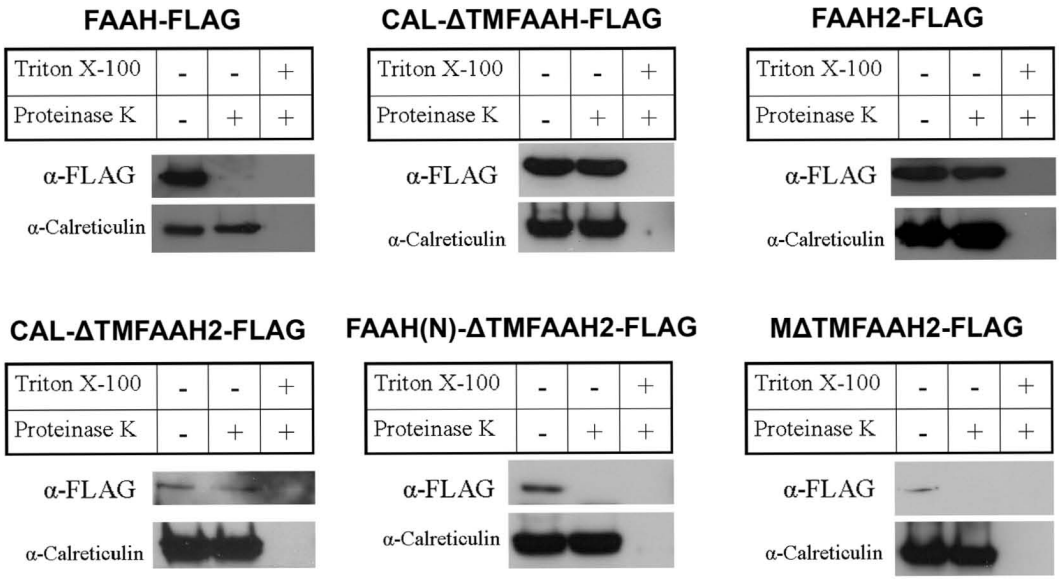
FAAH-FLAG
Triton X-100 - - +
Proteinase K - + +
α-FLAG
α-Calreticulin
CAL-ΔTMFAAH-FLAG
Triton X-100 - - +
Proteinase K - + +
α-FLAG
α-Calreticulin
FAAH2-FLAG
Triton X-100 - - +
Proteinase K - + +
α-FLAG
α-Calreticulin
CAL-ΔTMFAAH2-FLAG
Triton X-100 - - +
Proteinase K - + +
α-FLAG
α-Calreticulin
FAAH(N)-ΔTMFAAH2-FLAG
Triton X-100 - - +
Proteinase K - + +
α-FLAG
α-Calreticulin
MΔTMFAAH2-FLAG
Triton X-100 - - +
Proteinase K - + +
α-FLAG
α-Calreticulin

Figure 31. Expression and activity of cytoplasmically- and luminally-facing FAAH and FAAH-2 variants. (A) Relative expression of FAAH-FLAG, FAAH2-FLAG, and cytoplasmically- and luminally-facing FAAH and FAAH-2 variants were determined by western blotting using anti-FLAG and anti-β actin antibodies. (B) Enzymatic activities of the aforementioned proteins. Activity of CAL-ΔTMFAAH-FLAG was compared to FAAH-FLAG. For the rest of the proteins, activities were compared to FAAH-2. **, $p < 0.01$ and ***, $p < 0.001$. (n = 4-6). (C) Expression of CAL-ΔTMFAAH2(2-532)-FLAG in HeLa cells.

A

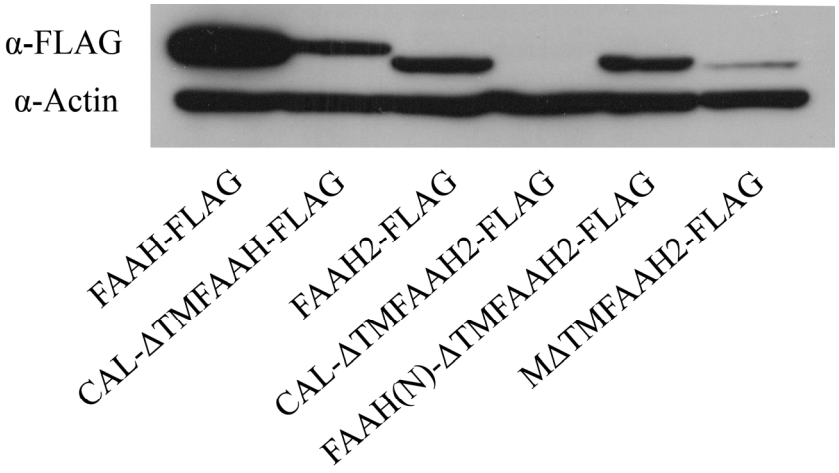
α-FLAG
α-Actin
FAAH-FLAG
CAL-ΔTMFAAH-FLAG
FAAH2-FLAG
CAL-ΔTMFAAH2-FLAG
FAAH(N)-ΔTMFAAH2-FLAG
MΔTMFAAH2-FLAG

B

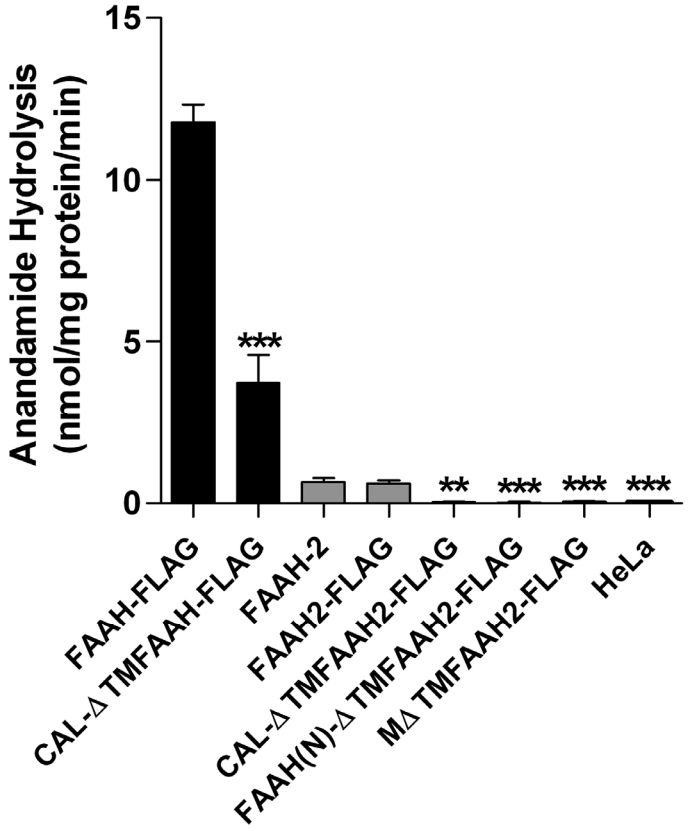
Anandamide Hydrolysis
(nmol/mg protein/min)
15
10
5
0
***
**
***
***
***
FAAH-FLAG
CAL-ΔTMFAAH-FLAG
FAAH-2
FAAH2-FLAG
CAL-ΔTMFAAH2-FLAG
FAAH(N)-ΔTMFAAH2-FLAG
MΔTMFAAH2-FLAG
HeLa

C

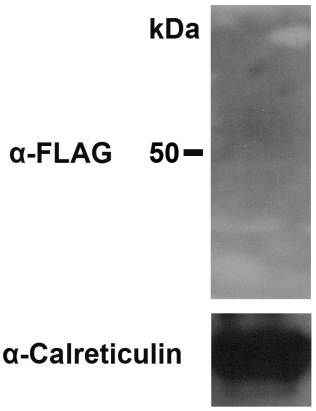
kDa
α-FLAG
50
α-Calreticulin

Figure 32. FAAH-2 is not secreted by cells. Twenty four hours after transfection, COS-7 cells were incubated for 12 hrs in serum-free Opti-MEM media. Media (M) were collected and cell homogenates (C) generated, acetone precipitated, and analyzed by western blotting using anti-FLAG and anti-β actin antibodies. (A) Expression of a secretable form of FABP3 in media and cell homogenates of COS-7 cells. (B) Expressing of FAAH2-FLAG, CAL-ΔTMFAAH-FLAG, or CAL-ΔTMFAAH2-FLAG in media and cell homogenates of COS-7 cells. The residual β-actin signal in the media likely reflects actin released from broken cells.

A

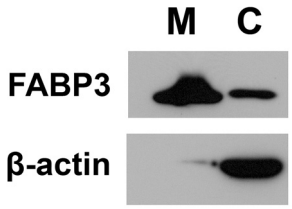
M C
FABP3
β-actin

B

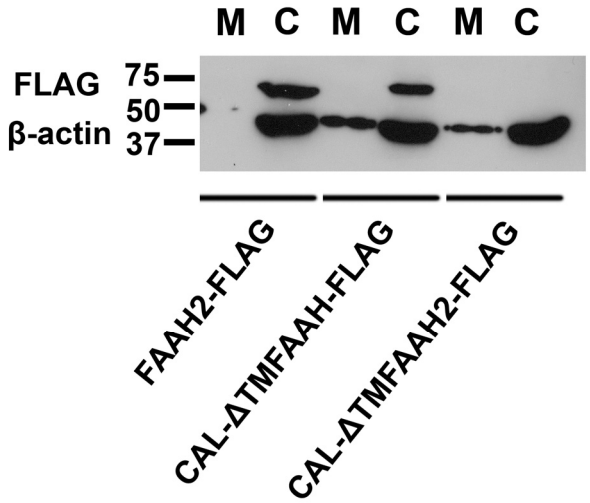
M C M C M C
FLAG
β-actin
75
50
37
FAAH2-FLAG
CAL-ΔTMFAAH-FLAG
CAL-ΔTMFAAH2-FLAG

Figure 33. Immunolocalization of luminally- and cytoplasmically-facing FAAH and FAAH-2 proteins. CAL-ΔTMFAAH2-FLAG, CAL-ΔTMFAAH-FLAG, or FAAH(N)-ΔTMFAAH2-FLAG were expressed in COS-7 cells and visualized using anti-FLAG antibodies and stained with BODIPY 493/503. Top panel represents the proteins of interest, the middle panel shows BODIPY 493/503, and the bottom panel the merged images.

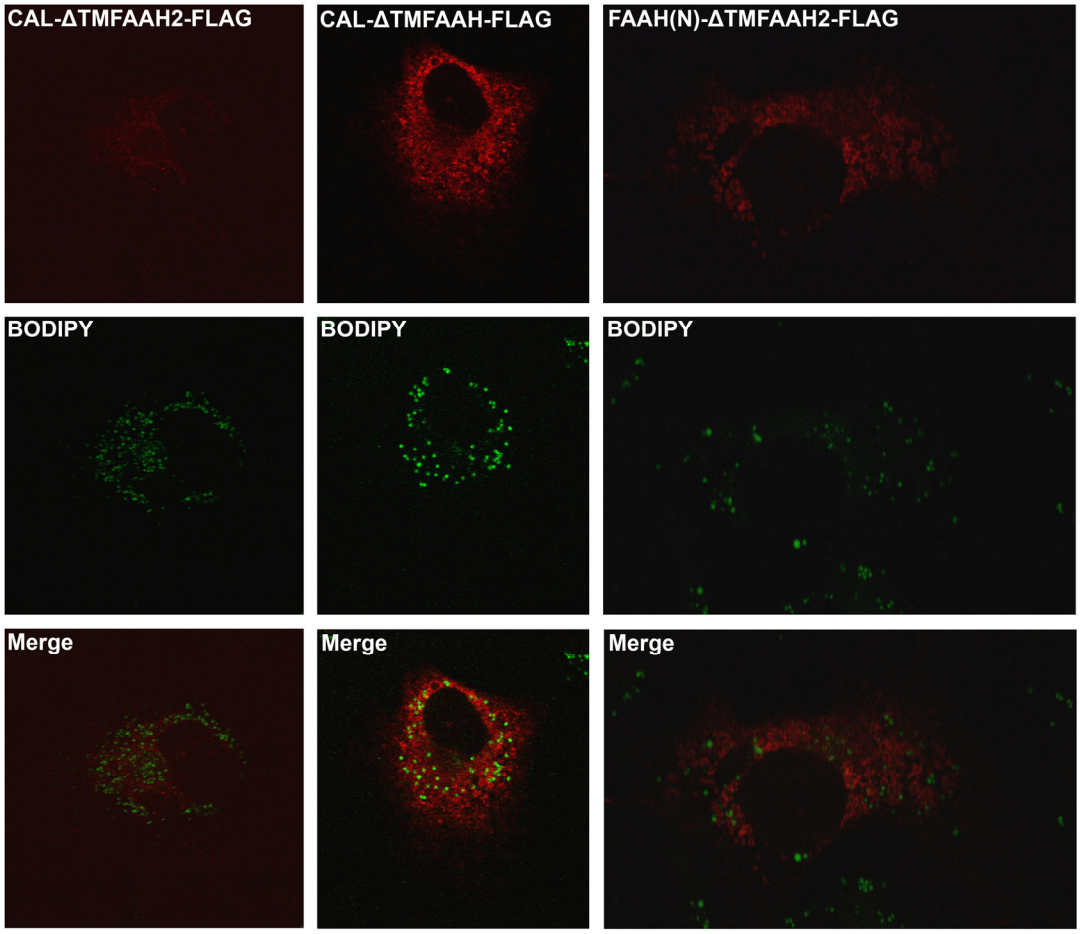
CAL-ΔTMFAAH2-FLAG
CAL-ΔTMFAAH-FLAG
FAAH(N)-ΔTMFAAH2-FLAG
BODIPY
BODIPY
BODIPY
Merge
Merge
Merge

Figure 34. The N-terminus of FAAH-2 mediates lipid droplet targeting. (A) Localization of RFP and FAAH2(N)-RFP in COS-7 cells stained with BODIPY493/503. (B) Co-localization of FAAH2(N)-rΔTMFAAH-FLAG with BODIPY493/503 in COS-7 and HeLa cells. Top panels represent the protein of interest, middle panels the BODIPY 493/503 dye, and bottom panels the merged images.

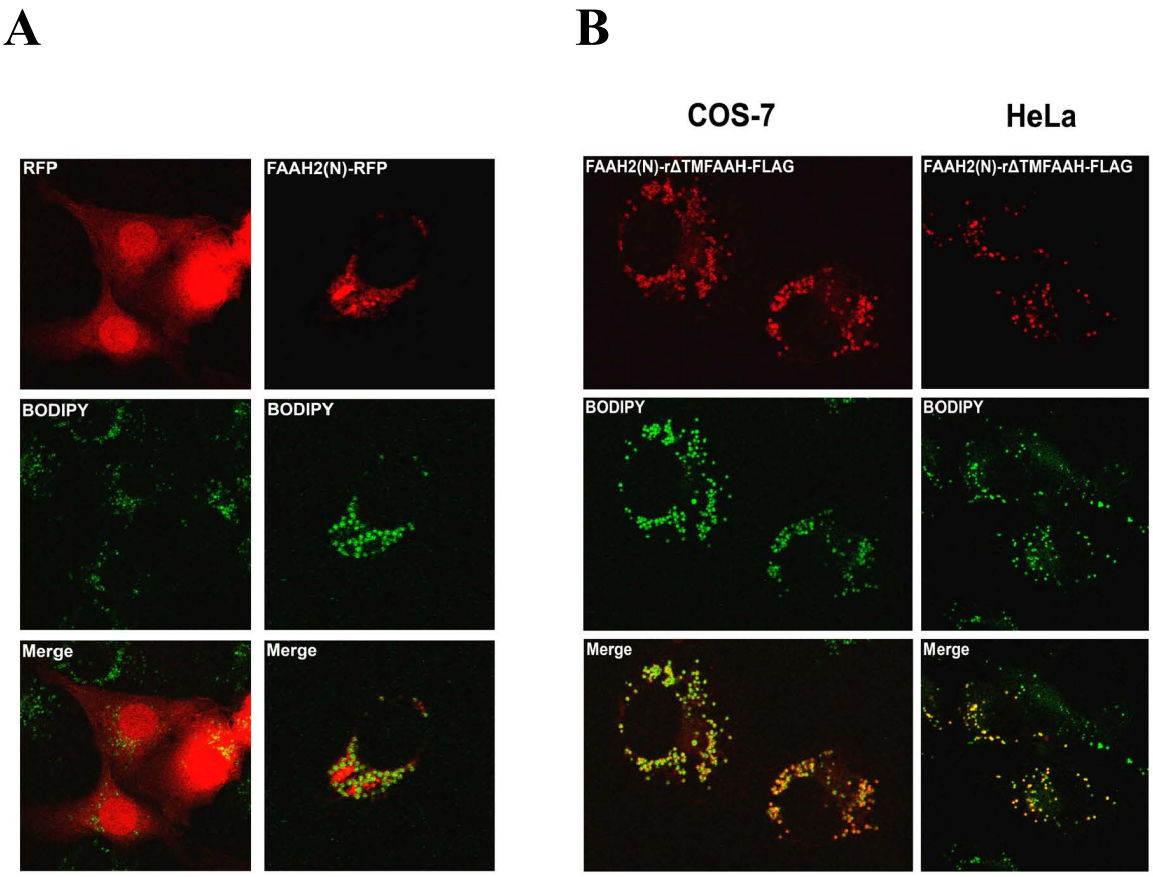
A
B
COS-7
HeLa
RFP
FAAH2(N)-RFP
FAAH2(N)-rΔTMFAAH-FLAG
FAAH2(N)-rΔTMFAAH-FLAG
BODIPY
BODIPY
BODIPY
BODIPY
Merge
Merge
Merge
Merge

Figure 35. Protease protection analysis of FAAH2(N)-rΔTMFAAH-FLAG. Membranes of COS-7 cells expressing FAAH2(N)-rΔTMFAAH-FLAG were treated with 500 μg/ml proteinase K in the presence or absence of 1% Triton X-100. Control samples were left untreated. The samples were resolved by SDS-PAGE and probed with anti-FLAG and anti-calreticulin antibodies.

Triton X-100	-	-	+
Proteinase K	-	+	+

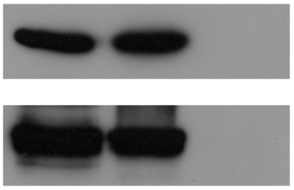

Figure 36. Expression and activities of FAAH2(N)-rΔTMFAAH-FLAG and rFAAH-FLAG(low). (A) Western blot analysis of rFAAH-FLAG, FAAH2(N)-rΔTMFAAH-FLAG, rFAAH-FLAG(low), and FAAH2-FLAG expression in HeLa cells. Blots were probed with anti-FLAG and anti-β actin antibodies. (B) Similar rates ($p > 0.05$) of [^{14}C]anandamide hydrolysis in homogenates of HeLa cells expressing rFAAH-FLAG(low) and FAAH2(N)-rΔTMFAAH-FLAG ($n = 3$).

A

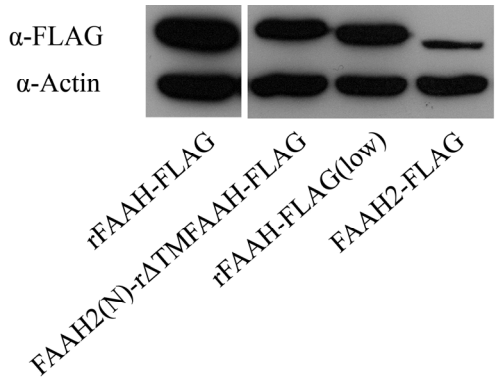
α-FLAG
α-Actin
rFAAH-FLAG
FAAH2(N)-rΔTMFAAH-FLAG
rFAAH-FLAG(low)
FAAH2-FLAG

B

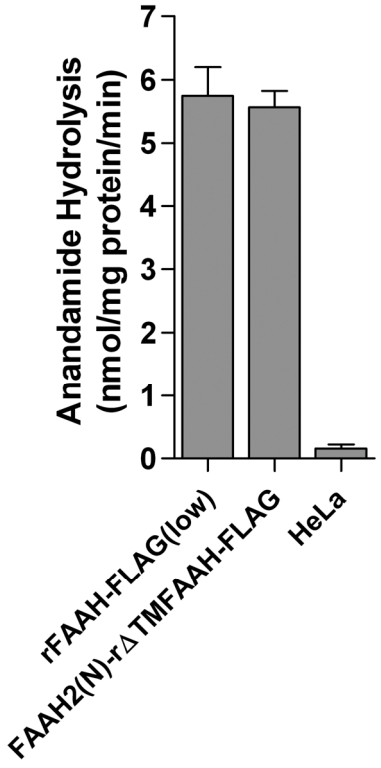
Anandamide Hydrolysis
(nmol/mg protein/min)
0
1
2
3
4
5
6
7
rFAAH-FLAG(low)
FAAH2(N)-rΔTMFAAH-FLAG
HeLa

Figure 37. Anandamide uptake and hydrolysis in HeLa cells expressing rFAAH-FLAG(low), FAAH2(N)-rΔTMFAAH-FLAG, or FAAH2-FLAG. (A) HeLa cells transfected with rFAAH-FLAG(low), FAAH2(N)-rΔTMFAAH-FLAG, FAAH2-FLAG, or vector controls were incubated with 100 nM [^{14}C]anandamide for 1 or 5 min and uptake (black bars) and hydrolysis (grey bars) determined**.** *, $p < 0.05$; **, $p < 0.01$; ***, $p < 0.001$ ($n = 5$). (B) Intracellular hydrolysis of [^{14}C]anandamide following uptake at 3 sec in cells expressing the indicated proteins. **, $p < 0.01$ and ***, $p < 0.001$ ($n = 5$).

A

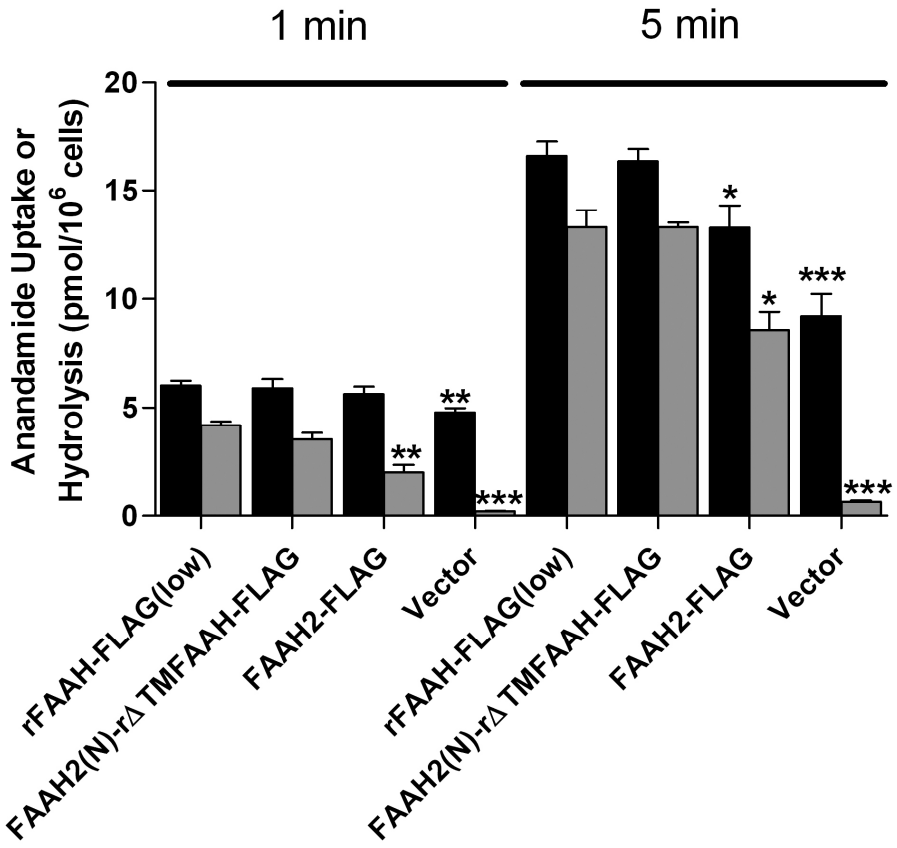
1 min
5 min
Anandamide Uptake or Hydrolysis (pmol/10^6 cells)
20
15
10
5
0
**
**
***
*
*
***
***
rFAAH-FLAG(low)
FAAH2(N)-rΔTMFAAH-FLAG
FAAH2-FLAG
Vector
rFAAH-FLAG(low)
FAAH2(N)-rΔTMFAAH-FLAG
FAAH2-FLAG
Vector

B

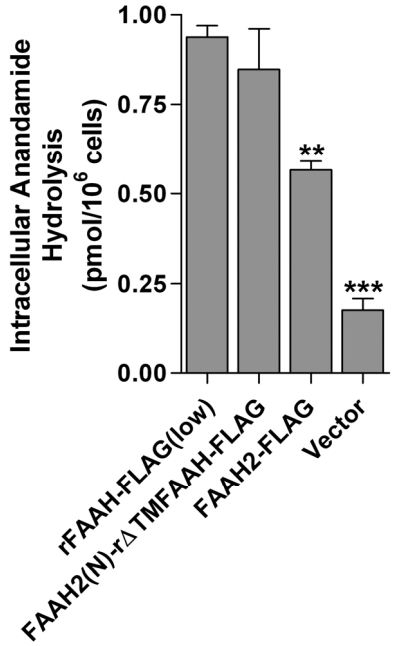
Intracellular Anandamide Hydrolysis (pmol/10^6 cells)
1.00
0.75
0.50
0.25
0.00
**
***
rFAAH-FLAG(low)
FAAH2(N)-rΔTMFAAH-FLAG
FAAH2-FLAG
Vector

DISCUSSION

Regulation of cellular NAE pools requires a coordinated set of synthetic and catabolic enzymes. FAAH is the principal enzyme that degrades NAEs in mice (Cravatt*, et al.*, 2001, Cravatt*, et al.*, 2004). In addition to FAAH, the acid amidase NAAA hydrolyzes PEA, though its role in PEA degradation is restricted to macrophages (Sun*, et al.*, 2005, Tsuboi*, et al.*, 2005). Recently, FAAH-2 was identified as a second FAAH enzyme capable of hydrolyzing NAEs *in vitro* (Wei*, et al.*, 2006). FAAH-2 is found in the genomes of higher mammals but not in mice and rats. The enzyme was reported to be a non-glycosylated luminal membrane protein (Wei*, et al.*, 2006). The current study focused upon unraveling the role of FAAH-2 in NAE inactivation in intact cells and exploring its subcellular localization.

The *in vitro* activity profile of FAAH-2 in the current study is in agreement with the findings of Wei et al. (Wei*, et al.*, 2006), and suggests that FAAH-2 hydrolyzes NAEs with rates ten to thirty times lower than FAAH. In contrast, in the current work FAAH-2 metabolized anandamide and PEA in intact cells with rates approximately one third that of FAAH (Figures 23, 24, and 31A). This suggests that *in vitro* activities do not reveal the true capacity of these enzymes to inactivate NAEs in cells. Therefore, it is likely that FAAH and FAAH-2 may coordinate NAE inactivation *in vivo*, especially in tissues with similar expression of these enzymes such as the kidney, liver, lung and prostate (Wei*, et al.*, 2006). In heart and ovary, which lack significant FAAH expression, FAAH-2 may constitute the primary NAE catabolizing enzyme.

Immunofluorescence and biochemical analyses revealed that FAAH-2 localizes to cytoplasmic lipid droplets. Lipid droplets/adiposomes serve as intracellular storage

depots for triacylglycerides and cholesteryl esters (Bartz*, et al.*, 2007, Brown, 2001, Olofsson*, et al.*, 2008, Olofsson*, et al.*, 2008, Thiele and Spandl, 2008, Zehmer*, et al.*, 2009). Lipid droplets are composed of a neutral lipid core surrounded by a phospholipid monolayer (Tauchi-Sato*, et al.*, 2002, Thiele and Spandl, 2008). Three classes of proteins localize to lipid droplets: lipid anchored proteins such as RAB18, amphipathic-helix containing proteins such as the perilipin, adipophilin, Tip47 family of proteins, and monotopic membrane proteins (Thiele and Spandl, 2008, Zehmer*, et al.*, 2009). FAAH-2 belongs to the latter category of monotopic membrane proteins. In contrast to FAAH-2, FAAH did not localize to lipid droplets. Instead, FAAH localization was restricted to ER membranes, in agreement with previous studies (Arreaza and Deutsch, 1999, Glaser*, et al.*, 2003, Gulyas*, et al.*, 2004, Oddi*, et al.*, 2005, Patricelli*, et al.*, 1998). However, it was recently proposed that a small pool of FAAH may localize to lipid droplets (Oddi*, et al.*, 2008).

The finding that FAAH-2 localizes to cytoplasmic lipid droplets contrasts the predicted localization of the enzyme to the ER lumen (Wei*, et al.*, 2006). This prediction was based upon inaccessibility of proteases towards FAAH-2 in membrane fractions of COS-7 cells following ultracentrifugation (this fraction lacks lipid droplets). In the current study, only a small pool of ER-localized FAAH-2 was detected. The presence of FAAH-2 in the ER lumen may reflect a translocation intermediate for FAAH-2 before reaching lipid droplets. Overrepresentation of this ER-localized pool of FAAH-2 in COS-7 cells may reflect inefficient adiposome targeting due to overexpression of the enzyme.

In the current study, active FAAH-2 enzymes were found on cytoplasmic lipid droplets while a FAAH-2 chimera localizing to the cytoplasmic face of ER membranes

was inactive. Active FAAH-2 was also observed in luminal membrane compartments (Wei*, et al.*, 2006), suggesting that the ER lumen may represent a site of putative post-translational modifications required to generate a catalytically active enzyme. It is noteworthy that most lipid droplet associated proteins exist in the cytoplasm prior to engaging the lipid droplet surface (Zehmer*, et al.*, 2009). However, it was recently shown that apolipoprotein A-V, a protein possessing a cleavable signal sequence and destined to the ER lumen, ultimately localized to lipid droplets (Shu*, et al.*, 2008). The mechanism responsible for translocating apolipoprotein A-V (and FAAH-2) from the ER lumen to lipid droplets is currently not known. However, this unusual translocation process resulting in escape of these proteins from the secretory pathway may be explained by a model in which nascent lipid droplets formed from ER membranes are selectively engaged by luminal ER membrane proteins bearing high affinity lipid droplet targeting sequences (Shu*, et al.*, 2008).

The N-terminus of FAAH-2 was subsequently identified as a lipid droplets targeting sequence. FAAH-2 variants lacking the N-terminus localized to perinuclear membranes and did not co-localize with the lipid droplet marker BODIPY 493/503. Transfer of the N-terminal sequence to RFP and FAAH re-localized both proteins to lipid droplets, suggesting that it is necessary and sufficient for adiposome targeting. The N-terminus of FAAH-2 bears striking similarity to the N-terminal lipid droplet localization sequence of methyltransferase-like 7B (Zehmer*, et al.*, 2008). Both peptides are hydrophobic with the sequence of FAAH-2 possessing interspersed charged residues. Curiously, the N-terminus of FAAH-2 contains several alpha helix disrupting glycines

and prolines (Figure 20), a common feature in lipid droplet localization sequences (Thiele and Spandl, 2008).

Since lipid droplets represent novel intracellular sites of NAE catabolism, it was not clear whether NAEs were efficiently delivered to adiposomes. This possibility was examined in cells expressing a lipid droplet localized variant of FAAH. The rate of anandamide hydrolysis was similar between cells expressing lipid droplet and ER localized FAAH proteins, suggesting that intracellular transport of anandamide (and probably other NAEs) is rapid and organelle non-specific, supporting the FABP model of anandamide trafficking. These data are in agreement with the recent finding that anandamide partitions to lipid droplets in cells (Oddi*, et al.*, 2008).

Collectively, this study establishes FAAH-2 as a bone fide endocannabinoid (and NAE) inactivating enzyme. FAAH-2 localized to cytoplasmic lipid droplets with the N-terminus of FAAH-2 serving as a lipid droplet localization sequence that was required for expression of functional enzyme. FAAH-2 efficiently hydrolyzed anandamide and PEA in intact cells, suggesting that the enzyme may serve as an efficient NAE inactivating enzyme *in vivo*. From a therapeutic perspective, it is noteworthy that ablation of FAAH promotes analgesic, anti-inflammatory and cardioprotective effects (Ahn*, et al.*, 2008, Batkai*, et al.*, 2007), suggesting that targeting FAAH and/or FAAH-2 may be therapeutically useful.

REFERENCES

Ahn K, McKinney MK, & Cravatt BF (2008) Enzymatic pathways that regulate endocannabinoid signaling in the nervous system. *Chem Rev* 108:1687-1707.

Alexander JP & Cravatt BF (2006) The putative endocannabinoid transport blocker LY2183240 is a potent inhibitor of FAAH and several other brain serine hydrolases. *J Am Chem Soc* 128:9699-9704.

Arreaza G & Deutsch DG (1999) Deletion of a proline-rich region and a transmembrane domain in fatty acid amide hydrolase. *FEBS Lett* 454:57-60.

Balali-Mood K, Bond P, & Sansom M (2009) The Interaction of Monotopic Membrane Enzymes with a Lipid Bilayer: A Coarse-Grained MD Simulation Study. *Biochemistry*.

Barr FA, Puype M, Vandekerckhove J, & Warren G (1997) GRASP65, a protein involved in the stacking of Golgi cisternae. *Cell* 91:253-262.

Bartz R, Li WH, Venables B, Zehmer JK, Roth MR, et al. (2007) Lipidomics reveals that adiposomes store ether lipids and mediate phospholipid traffic. *J Lipid Res* 48:837-847.

Batkai S, Rajesh M, Mukhopadhyay P, Hasko G, Liaudet L, et al. (2007) Decreased age-related cardiac dysfunction, myocardial nitrative stress, inflammatory gene expression, and apoptosis in mice lacking fatty acid amide hydrolase. *Am J Physiol Heart Circ Physiol* 293:H909-918.

Beltramo M, Stella N, Calignano A, Lin SY, Makriyannis A, et al. (1997) Functional role of high-affinity anandamide transport, as revealed by selective inhibition. *Science* 277:1094-1097.

Bisogno T, Maurelli S, Melck D, De Petrocellis L, & Di Marzo V (1997) Biosynthesis, uptake, and degradation of anandamide and palmitoylethanolamide in leukocytes. *J Biol Chem* 272:3315-3323.

Bisogno T & Di Marzo V (2007) Short- and long-term plasticity of the endocannabinoid system in neuropsychiatric and neurological disorders. *Pharmacol Res* 56:428-442.

Bojesen IN & Hansen HS (2005) Membrane transport of anandamide through resealed human red blood cell membranes. *J Lipid Res* 46:1652-1659.

Bouaboula M, Hilairet S, Marchand J, Fajas L, Le Fur G, et al. (2005) Anandamide induced PPARgamma transcriptional activation and 3T3-L1 preadipocyte differentiation. *Eur J Pharmacol* 517:174-181.

Bracey MH, Hanson MA, Masuda KR, Stevens RC, & Cravatt BF (2002) Structural adaptations in a membrane enzyme that terminates endocannabinoid signaling. *Science* 298:1793-1796.

Bracey MH, Cravatt BF, & Stevens RC (2004) Structural commonalities among integral membrane enzymes. *FEBS Lett* 567:159-165.

Brown DA (2001) Lipid droplets: proteins floating on a pool of fat. *Curr Biol* 11:R446-449.

Burstein SH, Huang SM, Petros TJ, Rossetti RG, Walker JM, et al. (2002) Regulation of anandamide tissue levels by N-arachidonylglycine. *Biochem Pharmacol* 64:1147-1150.

Cabral GA & Marciano-Cabral F (2005) Cannabinoid receptors in microglia of the central nervous system: immune functional relevance. *J Leukoc Biol* 78:1192-1197.

Cabral GA, Raborn ES, Griffin L, Dennis J, & Marciano-Cabral F (2008) CB2 receptors in the brain: role in central immune function. *Br J Pharmacol* 153:240-251.

Carlisle SJ, Marciano-Cabral F, Staab A, Ludwick C, & Cabral GA (2002) Differential expression of the CB2 cannabinoid receptor by rodent macrophages and macrophage-like cells in relation to cell activation. *Int Immunopharmacol* 2:69-82.

Chebrou H, Bigey F, Arnaud A, & Galzy P (1996) Study of the amidase signature group. *Biochim Biophys Acta* 1298:285-293.

Cravatt BF, Giang DK, Mayfield SP, Boger DL, Lerner RA, et al. (1996) Molecular characterization of an enzyme that degrades neuromodulatory fatty-acid amides. *Nature* 384:83-87.

Cravatt BF, Demarest K, Patricelli MP, Bracey MH, Giang DK, et al. (2001) Supersensitivity to anandamide and enhanced endogenous cannabinoid signaling in mice lacking fatty acid amide hydrolase. *Proc Natl Acad Sci U S A* 98:9371-9376.

Cravatt BF, Saghatelian A, Hawkins EG, Clement AB, Bracey MH, et al. (2004) Functional disassociation of the central and peripheral fatty acid amide signaling systems. *Proc Natl Acad Sci U S A* 101:10821-10826.

Davis JB, Gray J, Gunthorpe MJ, Hatcher JP, Davey PT, et al. (2000) Vanilloid receptor-1 is essential for inflammatory thermal hyperalgesia. *Nature* 405:183-187.

Day TA, Rakhshan F, Deutsch DG, & Barker EL (2001) Role of fatty acid amide hydrolase in the transport of the endogenous cannabinoid anandamide. *Mol Pharmacol* 59:1369-1375.

de Lago E, Fernandez-Ruiz J, Ortega-Gutierrez S, Viso A, Lopez-Rodriguez ML, et al. (2002) UCM707, a potent and selective inhibitor of endocannabinoid uptake, potentiates hypokinetic and antinociceptive effects of anandamide. *Eur J Pharmacol* 449:99-103.

De Petrocellis L, Melck D, Ueda N, Maurelli S, Kurahashi Y, et al. (1997) Novel inhibitors of brain, neuronal, and basophilic anandamide amidohydrolase. *Biochem Biophys Res Commun* 231:82-88.

Deutsch DG & Chin SA (1993) Enzymatic synthesis and degradation of anandamide, a cannabinoid receptor agonist. *Biochem Pharmacol* 46:791-796.

Deutsch DG, Omeir R, Arreaza G, Salehani D, Prestwich GD, et al. (1997) Methyl arachidonyl fluorophosphonate: a potent irreversible inhibitor of anandamide amidase. *Biochem Pharmacol* 53:255-260.

Deutsch DG, Glaser ST, Howell JM, Kunz JS, Puffenbarger RA, et al. (2001) The cellular uptake of anandamide is coupled to its breakdown by fatty-acid amide hydrolase. *J Biol Chem* 276:6967-6973.

Devane WA, Dysarz FA, 3rd, Johnson MR, Melvin LS, & Howlett AC (1988) Determination and characterization of a cannabinoid receptor in rat brain. *Mol Pharmacol* 34:605-613.

Di Marzo V, Fontana A, Cadas H, Schinelli S, Cimino G, et al. (1994) Formation and inactivation of endogenous cannabinoid anandamide in central neurons. *Nature* 372:686-691.

Di Marzo V, De Petrocellis L, & Bisogno T (2005) The biosynthesis, fate and pharmacological properties of endocannabinoids. *Handb Exp Pharmacol*:147-185.

Dickason-Chesterfield AK, Kidd SR, Moore SA, Schaus JM, Liu B, et al. (2006) Pharmacological characterization of endocannabinoid transport and fatty acid amide hydrolase inhibitors. *Cell Mol Neurobiol* 26:407-423.

Egertova M, Giang DK, Cravatt BF, & Elphick MR (1998) A new perspective on cannabinoid signalling: complementary localization of fatty acid amide hydrolase and the CB1 receptor in rat brain. *Proc Biol Sci* 265:2081-2085.

Egertova M, Cravatt BF, & Elphick MR (2003) Comparative analysis of fatty acid amide hydrolase and cb(1) cannabinoid receptor expression in the mouse brain: evidence of a widespread role for fatty acid amide hydrolase in regulation of endocannabinoid signaling. *Neuroscience* 119:481-496.

Egertova M, Simon GM, Cravatt BF, & Elphick MR (2008) Localization of N-acyl phosphatidylethanolamine phospholipase D (NAPE-PLD) expression in mouse brain: A new perspective on N-acylethanolamines as neural signaling molecules. *J Comp Neurol* 506:604-615.

El-Talatini MR, Taylor AH, Elson JC, Brown L, Davidson AC, et al. (2009) Localisation and function of the endocannabinoid system in the human ovary. *PLoS ONE* 4:e4579.

Facchinetti F, Del Giudice E, Furegato S, Passarotto M, & Leon A (2003) Cannabinoids ablate release of TNFalpha in rat microglial cells stimulated with lypopolysaccharide. *Glia* 41:161-168.

Fasia L, Karava V, & Siafaka-Kapadai A (2003) Uptake and metabolism of [3H]anandamide by rabbit platelets. Lack of transporter? *Eur J Biochem* 270:3498-3506.

Fegley D, Kathuria S, Mercier R, Li C, Goutopoulos A, et al. (2004) Anandamide transport is independent of fatty-acid amide hydrolase activity and is blocked by the hydrolysis-resistant inhibitor AM1172. *Proc Natl Acad Sci U S A* 101:8756-8761.

Felder CC, Briley EM, Axelrod J, Simpson JT, Mackie K, et al. (1993) Anandamide, an endogenous cannabimimetic eicosanoid, binds to the cloned human cannabinoid receptor and stimulates receptor-mediated signal transduction. *Proc Natl Acad Sci U S A* 90:7656-7660.

Ferrer-Montiel A, Garcia-Martinez C, Morenilla-Palao C, Garcia-Sanz N, Fernandez-Carvajal A, et al. (2004) Molecular architecture of the vanilloid receptor. Insights for drug design. *Eur J Biochem* 271:1820-1826.

Fezza F, Oddi S, Di Tommaso M, De Simone C, Rapino C, et al. (2008) Characterization of biotin-anandamide, a novel tool for the visualization of anandamide accumulation. *J Lipid Res* 49:1216-1223.

Fliegel L, Burns K, MacLennan DH, Reithmeier RA, & Michalak M (1989) Molecular cloning of the high affinity calcium-binding protein (calreticulin) of skeletal muscle sarcoplasmic reticulum. *J Biol Chem* 264:21522-21528.

Fu J, Gaetani S, Oveisi F, Lo Verme J, Serrano A, et al. (2003) Oleylethanolamide regulates feeding and body weight through activation of the nuclear receptor PPAR-alpha. *Nature* 425:90-93.

Fu J, Oveisi F, Gaetani S, Lin E, & Piomelli D (2005) Oleoylethanolamide, an endogenous PPAR-alpha agonist, lowers body weight and hyperlipidemia in obese rats. *Neuropharmacology* 48:1147-1153.

Fu J, Astarita G, Gaetani S, Kim J, Cravatt BF, et al. (2007) Food intake regulates oleoylethanolamide formation and degradation in the proximal small intestine. *J Biol Chem* 282:1518-1528.

Furuhashi M, Tuncman G, Gorgun CZ, Makowski L, Atsumi G, et al. (2007) Treatment of diabetes and atherosclerosis by inhibiting fatty-acid-binding protein aP2. *Nature* 447:959-965.

Furuhashi M, Fucho R, Gorgun CZ, Tuncman G, Cao H, et al. (2008) Adipocyte/macrophage fatty acid-binding proteins contribute to metabolic deterioration through actions in both macrophages and adipocytes in mice. *J Clin Invest* 118:2640-2650.

Furuhashi M & Hotamisligil GS (2008) Fatty acid-binding proteins: role in metabolic diseases and potential as drug targets. *Nat Rev Drug Discov* 7:489-503.

Garcia-Ovejero D, Arevalo-Martin A, Petrosino S, Docagne F, Hagen C, et al. (2009) The endocannabinoid system is modulated in response to spinal cord injury in rats. *Neurobiol Dis* 33:57-71.

Glaser ST, Abumrad NA, Fatade F, Kaczocha M, Studholme KM, et al. (2003) Evidence against the presence of an anandamide transporter. *Proc Natl Acad Sci U S A* 100:4269-4274.

Glaser ST, Deutsch DG, Studholme KM, Zimov S, & Yazulla S (2005) Endocannabinoids in the intact retina: 3 H-anandamide uptake, fatty acid amide hydrolase immunoreactivity and hydrolysis of anandamide. *Vis Neurosci* 22:693-705.

Glaser ST, Kaczocha M, & Deutsch DG (2005) Anandamide transport: a critical review. *Life Sci* 77:1584-1604.

Goparaju SK, Ueda N, Yamaguchi H, & Yamamoto S (1998) Anandamide amidohydrolase reacting with 2-arachidonoylglycerol, another cannabinoid receptor ligand. *FEBS Lett* 422:69-73.

Gulyas AI, Cravatt BF, Bracey MH, Dinh TP, Piomelli D, et al. (2004) Segregation of two endocannabinoid-hydrolyzing enzymes into pre- and postsynaptic compartments in the rat hippocampus, cerebellum and amygdala. *Eur J Neurosci* 20:441-458.

Hanhoff T, Lucke C, & Spener F (2002) Insights into binding of fatty acids by fatty acid binding proteins. *Mol Cell Biochem* 239:45-54.

Hashimotodani Y, Ohno-Shosaku T, Tsubokawa H, Ogata H, Emoto K, et al. (2005) Phospholipase Cbeta serves as a coincidence detector through its Ca2+ dependency for triggering retrograde endocannabinoid signal. *Neuron* 45:257-268.

Hashimotodani Y, Ohno-Shosaku T, & Kano M (2007) Endocannabinoids and synaptic function in the CNS. *Neuroscientist* 13:127-137.

Herkenham M, Lynn AB, Johnson MR, Melvin LS, de Costa BR, et al. (1991) Characterization and localization of cannabinoid receptors in rat brain: a quantitative in vitro autoradiographic study. *J Neurosci* 11:563-583.

Hillard CJ, Edgemond WS, Jarrahian A, & Campbell WB (1997) Accumulation of N-arachidonoylethanolamine (anandamide) into cerebellar granule cells occurs via facilitated diffusion. *J Neurochem* 69:631-638.

Hillard CJ & Jarrahian A (2000) The movement of N-arachidonoylethanolamine (anandamide) across cellular membranes. *Chem Phys Lipids* 108:123-134.

Hillard CJ & Jarrahian A (2003) Cellular accumulation of anandamide: consensus and controversy. *Br J Pharmacol* 140:802-808.

Hohmann AG, Martin WJ, Tsou K, & Walker JM (1995) Inhibition of noxious stimulus-evoked activity of spinal cord dorsal horn neurons by the cannabinoid WIN 55,212-2. *Life Sci* 56:2111-2118.

Hotamisligil GS, Johnson RS, Distel RJ, Ellis R, Papaioannou VE, et al. (1996) Uncoupling of obesity from insulin resistance through a targeted mutation in aP2, the adipocyte fatty acid binding protein. *Science* 274:1377-1379.

Howlett AC (1985) Cannabinoid inhibition of adenylate cyclase. Biochemistry of the response in neuroblastoma cell membranes. *Mol Pharmacol* 27:429-436.

Howlett AC, Barth F, Bonner TI, Cabral G, Casellas P, et al. (2002) International Union of Pharmacology. XXVII. Classification of cannabinoid receptors. *Pharmacol Rev* 54:161-202.

Huang SM, Bisogno T, Trevisani M, Al-Hayani A, De Petrocellis L, et al. (2002) An endogenous capsaicin-like substance with high potency at recombinant and native vanilloid VR1 receptors. *Proc Natl Acad Sci U S A* 99:8400-8405.

Jacobsson SO & Fowler CJ (2001) Characterization of palmitoylethanolamide transport in mouse Neuro-2a neuroblastoma and rat RBL-2H3 basophilic leukaemia cells: comparison with anandamide. *Br J Pharmacol* 132:1743-1754.

Jeong WI, Osei-Hyiaman D, Park O, Liu J, Batkai S, et al. (2008) Paracrine activation of hepatic CB1 receptors by stellate cell-derived endocannabinoids mediates alcoholic fatty liver. *Cell Metab* 7:227-235.

Kaczocha M, Hermann A, Glaser ST, Bojesen IN, & Deutsch DG (2006) Anandamide uptake is consistent with rate-limited diffusion and is regulated by the degree of its hydrolysis by fatty acid amide hydrolase. *J Biol Chem* 281:9066-9075.

Kanaji S, Iwahashi J, Kida Y, Sakaguchi M, & Mihara K (2000) Characterization of the signal that directs Tom20 to the mitochondrial outer membrane. *J Cell Biol* 151:277-288.

Katona I, Sperlagh B, Sik A, Kafalvi A, Vizi ES, et al. (1999) Presynaptically located CB1 cannabinoid receptors regulate GABA release from axon terminals of specific hippocampal interneurons. *J Neurosci* 19:4544-4558.

Koutek B, Prestwich GD, Howlett AC, Chin SA, Salehani D, et al. (1994) Inhibitors of arachidonoyl ethanolamide hydrolysis. *J Biol Chem* 269:22937-22940.

Lambert DM & Fowler CJ (2005) The endocannabinoid system: drug targets, lead compounds, and potential therapeutic applications. *J Med Chem* 48:5059-5087.

Lichtman AH, Shelton CC, Advani T, & Cravatt BF (2004) Mice lacking fatty acid amide hydrolase exhibit a cannabinoid receptor-mediated phenotypic hypoalgesia. *Pain* 109:319-327.

Listenberger LL, Ostermeyer-Fay AG, Goldberg EB, Brown WJ, & Brown DA (2007) Adipocyte differentiation-related protein reduces the lipid droplet association of adipose triglyceride lipase and slows triacylglycerol turnover. *J Lipid Res* 48:2751-2761.

Liu J, Wang L, Harvey-White J, Osei-Hyiaman D, Razdan R, et al. (2006) A biosynthetic pathway for anandamide. *Proc Natl Acad Sci U S A* 103:13345-13350.

Liu RZ, Li X, & Godbout R (2008) A novel fatty acid-binding protein (FABP) gene resulting from tandem gene duplication in mammals: transcription in rat retina and testis. *Genomics* 92:436-445.

Lo Verme J, Fu J, Astarita G, La Rana G, Russo R, et al. (2005) The nuclear receptor peroxisome proliferator-activated receptor-alpha mediates the anti-inflammatory actions of palmitoylethanolamide. *Mol Pharmacol* 67:15-19.

Maccarrone M, Fiorucci L, Erba F, Bari M, Finazzi-Agro A, et al. (2000) Human mast cells take up and hydrolyze anandamide under the control of 5-lipoxygenase and do not express cannabinoid receptors. *FEBS Lett* 468:176-180.

Mackie K & Hille B (1992) Cannabinoids inhibit N-type calcium channels in neuroblastoma-glioma cells. *Proc Natl Acad Sci U S A* 89:3825-3829.

Mackie K, Devane WA, & Hille B (1993) Anandamide, an endogenous cannabinoid, inhibits calcium currents as a partial agonist in N18 neuroblastoma cells. *Mol Pharmacol* 44:498-503.

Mackie K, Lai Y, Westenbroek R, & Mitchell R (1995) Cannabinoids activate an inwardly rectifying potassium conductance and inhibit Q-type calcium currents in AtT20 cells transfected with rat brain cannabinoid receptor. *J Neurosci* 15:6552-6561.

Maeda K, Cao H, Kono K, Gorgun CZ, Furuhashi M, et al. (2005) Adipocyte/macrophage fatty acid binding proteins control integrated metabolic responses in obesity and diabetes. *Cell Metab* 1:107-119.

Man WC, Miyazaki M, Chu K, & Ntambi JM (2006) Membrane topology of mouse stearoyl-CoA desaturase 1. *J Biol Chem* 281:1251-1260.

Matsuda LA, Lolait SJ, Brownstein MJ, Young AC, & Bonner TI (1990) Structure of a cannabinoid receptor and functional expression of the cloned cDNA. *Nature* 346:561-564.

Maurelli S, Bisogno T, De Petrocellis L, Di Luccia A, Marino G, et al. (1995) Two novel classes of neuroactive fatty acid amides are substrates for mouse neuroblastoma 'anandamide amidohydrolase'. *FEBS Lett* 377:82-86.

McFarland MJ & Barker EL (2004) Anandamide transport. *Pharmacol Ther* 104:117-135.

McKinney MK & Cravatt BF (2005) Structure and function of fatty acid amide hydrolase. *Annu Rev Biochem* 74:411-432.

Munro S, Thomas KL, & Abu-Shaar M (1993) Molecular characterization of a peripheral receptor for cannabinoids. *Nature* 365:61-65.

Murphy EJ, Barcelo-Coblijn G, Binas B, & Glatz JF (2004) Heart fatty acid uptake is decreased in heart fatty acid-binding protein gene-ablated mice. *J Biol Chem* 279:34481-34488.

Murphy EJ, Owada Y, Kitanaka N, Kondo H, & Glatz JF (2005) Brain arachidonic acid incorporation is decreased in heart fatty acid binding protein gene-ablated mice. *Biochemistry* 44:6350-6360.

Oddi S, Bari M, Battista N, Barsacchi D, Cozzani I, et al. (2005) Confocal microscopy and biochemical analysis reveal spatial and functional separation between anandamide uptake and hydrolysis in human keratinocytes. *Cell Mol Life Sci* 62:386-395.

Oddi S, Fezza F, Pasquariello N, De Simone C, Rapino C, et al. (2008) Evidence for the intracellular accumulation of anandamide in adiposomes. *Cell Mol Life Sci* 65:840-850.

Ohno-Shosaku T, Maejima T, & Kano M (2001) Endogenous cannabinoids mediate retrograde signals from depolarized postsynaptic neurons to presynaptic terminals. *Neuron* 29:729-738.

Okamoto Y, Morishita J, Tsuboi K, Tonai T, & Ueda N (2004) Molecular characterization of a phospholipase D generating anandamide and its congeners. *J Biol Chem* 279:5298-5305.

Olofsson SO, Bostrom P, Andersson L, Rutberg M, Levin M, et al. (2008) Triglyceride containing lipid droplets and lipid droplet-associated proteins. *Curr Opin Lipidol* 19:441-447.

Olofsson SO, Bostrom P, Andersson L, Rutberg M, Perman J, et al. (2008) Lipid droplets as dynamic organelles connecting storage and efflux of lipids. *Biochim Biophys Acta*.

Omeir RL, Arreaza G, & Deutsch DG (1999) Identification of two serine residues involved in catalysis by fatty acid amide hydrolase. *Biochem Biophys Res Commun* 264:316-320.

Oropeza VC, Mackie K, & Van Bockstaele EJ (2007) Cannabinoid receptors are localized to noradrenergic axon terminals in the rat frontal cortex. *Brain Res* 1127:36-44.

Ortar G, Ligresti A, De Petrocellis L, Morera E, & Di Marzo V (2003) Novel selective and metabolically stable inhibitors of anandamide cellular uptake. *Biochem Pharmacol* 65:1473-1481.

Ortega-Gutierrez S, Hawkins EG, Viso A, Lopez-Rodriguez ML, & Cravatt BF (2004) Comparison of anandamide transport in FAAH wild-type and knockout neurons: evidence for contributions by both FAAH and the CB1 receptor to anandamide uptake. *Biochemistry* 43:8184-8190.

Owada Y, Yoshimoto T, & Kondo H (1996) Spatio-temporally differential expression of genes for three members of fatty acid binding proteins in developing and mature rat brains. *J Chem Neuroanat* 12:113-122.

Owada Y, Suzuki I, Noda T, & Kondo H (2002) Analysis on the phenotype of E-FABP-gene knockout mice. *Mol Cell Biochem* 239:83-86.

Owada Y, Suzuki R, Iwasa H, Spener F, & Kondo H (2002) Localization of epidermal-type fatty acid binding protein in the thymic epithelial cells of mice. *Histochem Cell Biol* 117:55-60.

Owada Y, Takano H, Yamanaka H, Kobayashi H, Sugitani Y, et al. (2002) Altered water barrier function in epidermal-type fatty acid binding protein-deficient mice. *J Invest Dermatol* 118:430-435.

Owada Y, Abdelwahab SA, Kitanaka N, Sakagami H, Takano H, et al. (2006) Altered emotional behavioral responses in mice lacking brain-type fatty acid-binding protein gene. *Eur J Neurosci* 24:175-187.

Owada Y (2008) Fatty acid binding protein: localization and functional significance in the brain. *Tohoku J Exp Med* 214:213-220.

Patricelli MP, Lashuel HA, Giang DK, Kelly JW, & Cravatt BF (1998) Comparative characterization of a wild type and transmembrane domain-deleted fatty acid amide hydrolase: identification of the transmembrane domain as a site for oligomerization. *Biochemistry* 37:15177-15187.

Patricelli MP & Cravatt BF (1999) Fatty acid amide hydrolase competitively degrades bioactive amides and esters through a nonconventional catalytic mechanism. *Biochemistry* 38:14125-14130.

Patricelli MP & Cravatt BF (2001) Proteins regulating the biosynthesis and inactivation of neuromodulatory fatty acid amides. *Vitam Horm* 62:95-131.

Pelsers MM, Hanhoff T, Van der Voort D, Arts B, Peters M, et al. (2004) Brain- and heart-type fatty acid-binding proteins in the brain: tissue distribution and clinical utility. *Clin Chem* 50:1568-1575.

Regard JB, Sato IT, & Coughlin SR (2008) Anatomical profiling of G protein-coupled receptor expression. *Cell* 135:561-571.

Richieri GV, Ogata RT, Zimmerman AW, Veerkamp JH, & Kleinfeld AM (2000) Fatty acid binding proteins from different tissues show distinct patterns of fatty acid interactions. *Biochemistry* 39:7197-7204.

Rimmerman N, Bradshaw HB, Hughes HV, Chen JS, Hu SS, et al. (2008) N-palmitoyl glycine, a novel endogenous lipid that acts as a modulator of calcium influx and nitric oxide production in sensory neurons. *Mol Pharmacol* 74:213-224.

Rockwell CE, Snider NT, Thompson JT, Vanden Heuvel JP, & Kaminski NE (2006) Interleukin-2 suppression by 2-arachidonyl glycerol is mediated through peroxisome proliferator-activated receptor gamma independently of cannabinoid receptors 1 and 2. *Mol Pharmacol* 70:101-111.

Saghatelian A, Trauger SA, Want EJ, Hawkins EG, Siuzdak G, et al. (2004) Assignment of endogenous substrates to enzymes by global metabolite profiling. *Biochemistry* 43:14332-14339.

Sarker KP, Biswas KK, Yamakuchi M, Lee KY, Hahiguchi T, et al. (2003) ASK1-p38 MAPK/JNK signaling cascade mediates anandamide-induced PC12 cell death. *J Neurochem* 85:50-61.

Schroeder F, Atshaves BP, McIntosh AL, Gallegos AM, Storey SM, et al. (2007) Sterol carrier protein-2: new roles in regulating lipid rafts and signaling. *Biochim Biophys Acta* 1771:700-718.

Schug TT, Berry DC, Shaw NS, Travis SN, & Noy N (2007) Opposing effects of retinoic acid on cell growth result from alternate activation of two different nuclear receptors. *Cell* 129:723-733.

Sessler RJ & Noy N (2005) A ligand-activated nuclear localization signal in cellular retinoic acid binding protein-II. *Mol Cell* 18:343-353.

Shiratsuchi A, Watanabe I, Yoshida H, & Nakanishi Y (2008) Involvement of cannabinoid receptor CB2 in dectin-1-mediated macrophage phagocytosis. *Immunol Cell Biol* 86:179-184.

Shu X, Ryan RO, & Forte TM (2008) Intracellular lipid droplet targeting by apolipoprotein A-V requires the carboxyl-terminal segment. *J Lipid Res* 49:1670-1676.

Simon GM & Cravatt BF (2006) Endocannabinoid biosynthesis proceeding through glycerophospho-N-acyl ethanolamine and a role for alpha/beta-hydrolase 4 in this pathway. *J Biol Chem* 281:26465-26472.

Simon GM & Cravatt BF (2008) Anandamide biosynthesis catalyzed by the phosphodiesterase GDE1 and detection of glycerophospho-N-acyl ethanolamine precursors in mouse brain. *J Biol Chem* 283:9341-9349.

Smirnova E, Goldberg EB, Makarova KS, Lin L, Brown WJ, et al. (2006) ATGL has a key role in lipid droplet/adiposome degradation in mammalian cells. *EMBO Rep* 7:106-113.

Snider NT, Kornilov AM, Kent UM, & Hollenberg PF (2007) Anandamide metabolism by human liver and kidney microsomal cytochrome p450 enzymes to form hydroxyeicosatetraenoic and epoxyeicosatrienoic acid ethanolamides. *J Pharmacol Exp Ther* 321:590-597.

Snider NT, Sikora MJ, Sridar C, Feuerstein TJ, Rae JM, et al. (2008) The endocannabinoid anandamide is a substrate for the human polymorphic cytochrome P450 2D6. *J Pharmacol Exp Ther* 327:538-545.

Stark K, Dostalek M, & Guengerich FP (2008) Expression and purification of orphan cytochrome P450 4X1 and oxidation of anandamide. *FEBS J* 275:3706-3717.

Starowicz K, Nigam S, & Di Marzo V (2007) Biochemistry and pharmacology of endovanilloids. *Pharmacol Ther* 114:13-33.

Starowicz KM, Cristino L, Matias I, Capasso R, Racioppi A, et al. (2008) Endocannabinoid dysregulation in the pancreas and adipose tissue of mice fed with a high-fat diet. *Obesity (Silver Spring)* 16:553-565.

Stremmel W, Pohl L, Ring A, & Herrmann T (2001) A new concept of cellular uptake and intracellular trafficking of long-chain fatty acids. *Lipids* 36:981-989.

Sulsky R, Magnin DR, Huang Y, Simpkins L, Taunk P, et al. (2007) Potent and selective biphenyl azole inhibitors of adipocyte fatty acid binding protein (aFABP). *Bioorg Med Chem Lett* 17:3511-3515.

Sun Y, Alexander SPH, Kendall DA, & Bennett AJ (2008) Involvement of fatty acid binding proteins in the transport of endocannabinoids to peroxisome proliferator activated receptors. *International Cannabinoid Research Society, Burlington, Vermont*:17.

Sun YX, Tsuboi K, Zhao LY, Okamoto Y, Lambert DM, et al. (2005) Involvement of N-acylethanolamine-hydrolyzing acid amidase in the degradation of anandamide and other N-acylethanolamines in macrophages. *Biochim Biophys Acta* 1736:211-220.

Tauchi-Sato K, Ozeki S, Houjou T, Taguchi R, & Fujimoto T (2002) The surface of lipid droplets is a phospholipid monolayer with a unique Fatty Acid composition. *J Biol Chem* 277:44507-44512.

Thiele C & Spandl J (2008) Cell biology of lipid droplets. *Curr Opin Cell Biol* 20:378-385.

Tsuboi K, Sun YX, Okamoto Y, Araki N, Tonai T, et al. (2005) Molecular characterization of N-acylethanolamine-hydrolyzing acid amidase, a novel member of the choloylglycine hydrolase family with structural and functional similarity to acid ceramidase. *J Biol Chem* 280:11082-11092.

van der Stelt M, Trevisani M, Vellani V, De Petrocellis L, Schiano Moriello A, et al. (2005) Anandamide acts as an intracellular messenger amplifying Ca2+ influx via TRPV1 channels. *EMBO J* 24:3026-3037.

Van Sickle MD, Duncan M, Kingsley PJ, Mouihate A, Urbani P, et al. (2005) Identification and functional characterization of brainstem cannabinoid CB2 receptors. *Science* 310:329-332.

Webb M, Luo L, Ma JY, & Tham CS (2008) Genetic deletion of Fatty Acid Amide Hydrolase results in improved long-term outcome in chronic autoimmune encephalitis. *Neurosci Lett* 439:106-110.

Wei BQ, Mikkelsen TS, McKinney MK, Lander ES, & Cravatt BF (2006) A second fatty acid amide hydrolase with variable distribution among placental mammals. *J Biol Chem* 281:36569-36578.

Wilson RI, Kunos G, & Nicoll RA (2001) Presynaptic specificity of endocannabinoid signaling in the hippocampus. *Neuron* 31:453-462.

Wilson RI & Nicoll RA (2001) Endogenous cannabinoids mediate retrograde signalling at hippocampal synapses. *Nature* 410:588-592.

Xu LZ, Sanchez R, Sali A, & Heintz N (1996) Ligand specificity of brain lipid-binding protein. *J Biol Chem* 271:24711-24719.

Yazulla S, Studholme KM, McIntosh HH, & Deutsch DG (1999) Immunocytochemical localization of cannabinoid CB1 receptor and fatty acid amide hydrolase in rat retina. *J Comp Neurol* 415:80-90.

Yu M, Ives D, & Ramesha CS (1997) Synthesis of prostaglandin E2 ethanolamide from anandamide by cyclooxygenase-2. *J Biol Chem* 272:21181-21186.

Zehmer JK, Bartz R, Liu P, & Anderson RG (2008) Identification of a novel N-terminal hydrophobic sequence that targets proteins to lipid droplets. *J Cell Sci* 121:1852-1860.

Zehmer JK, Huang Y, Peng G, Pu J, Anderson RG, et al. (2009) A role for lipid droplets in inter-membrane lipid traffic. *Proteomics* 9:914-921.

Zimmerman AW, van Moerkerk HT, & Veerkamp JH (2001) Ligand specificity and conformational stability of human fatty acid-binding proteins. *Int J Biochem Cell Biol* 33:865-876.

Zygmunt PM, Petersson J, Andersson DA, Chuang H, Sorgard M, et al. (1999) Vanilloid receptors on sensory nerves mediate the vasodilator action of anandamide. *Nature* 400:452-457.

Appendix

Constructs used in chapter 2. N(TM) represents the N-terminal transmembrane region of either FAAH or FAAH-2. CAL represents the signal sequence from calreticulin. In MΔTMFAAH2-FLAG, M represents the N-terminal methionine that was added to provide a translation start site. FAAH(N) and FAAH2(N) represent the N-terminal transmembrane regions of either enzyme. Black represents human FAAH, brown represents rat FAAH, blue shows FAAH-2, grey shows the FLAG tag, dark blue is the Myc tag, green is CAL, light blue is a methionine, and red is RFP.